Ageing, Grey Matter Loss and Resting-State Effective Connectivity

Max Korbmacher

MAPSYK360 Master's in Psychology:

Behavioural Neuroscience

at

UNIVERSITY OF BERGEN

FACULTY OF PSYCHOLOGY

Autumn, 2021

Author Note

Max Korbmacher ⓘ https://orcid.org/0000-0002-8113-2560

Correspondence concerning this dissertation should be addressed to

max.korbmacher@gmail.com.

Supervisor Information

Supervisor 1: Prof. Karsten Specht ⓘ https://orcid.org/0000-0002-9946-3704

Department of Biological and Medical Psychology, University of Bergen

Supervisor 2: Liucija Vaišvilaitė

Department of Biological and Medical Psychology, University of Bergen

Word Count: 15,615

Abstract

Ageing affects the human body in different ways. Healthy ageing is accompanied by an asymmetrical grey matter thinning, which affects the naturally thicker hemisphere stronger (Roe et al., 2021). How these structural changes relate to intrinsic activation patterns measured by resting state functional Magnetic Resonance Imaging (fMRI) remains unclear. Hence, in the current study, the relationship between grey matter probability values (GMPV) and effective connectivity (EC) was investigated. We used data from the BETULA longitudinal project ($N = 227$) from the collection waves T_5 and T_6. Canonical Correlation Analysis suggested patterns of relationships between EC and GMPVs within the Default Mode Network and the Central Executive Network, which were specified using generalized additive models predicting EC by GMPVs. EC changed over time in connections from left dorsal Prefrontal Cortex to right medial Temporal Gyrus and right Prefrontal Cortex to left Precuneus and could be better predicted by GMPVs than chronological age. There was a weak relationship between structural and functional lateralisation. Overall, the results support the expected ageing structure-function relationships.

Keywords: ageing, grey matter, effective connectivity, resting state, fMRI

Sammendrag

Aldring påvirker kroppen på forskjellige måter. Ikke-patologisk aldring karakteriseres av asymmetrisk tap av grå materie, som påvirker den tjukkere hemisfæren sterkere (Roe et al., 2021). Det er ukjent hvordan disse strukturelle forandringene kan relateres til intrinsisk aktivitet som måles med «resting state» funksjonell magnetresonanstomografi (fMRI). Derfor undersøkte vi sammenhengen mellom sannsynlighetsverdier for grå materie (GMPV) og effektiv konnektivet (EC). De observerte dataene inneholder to tidspunkter, T_5 og T_6, fra det longitudinelle BETULA prosjektet ($N = 227$). Canonical Correlation Analysis indikerer relasjoner mellom EC og GMPV innom Default Mode Network og Central Executive Network. Sammenhengen mellom EC og GMPV ble spesifisert ved hjelp av generalized additive models. I tillegg fant vi forskjeller i EC mellom T_5 og T_6, fra venstre dorsal Prefrontal Cortex til høyre medial Temporal Gyrus og høyre Prefrontal Cortex til venstre Precuneus. Videre predikerte GMPV EC bedre enn kronologisk alder. Sammenhengen mellom strukturell og funksjonell lateralisering i de aktuelle dataene var svak. Det ble funnet markører for sammenhengen mellom hjernestruktur og -funksjon.

Nøkkelord: aldring, grå materie, effektiv konnektivitet, resting state, fMRI

Acknowledgements

I want to thank everybody who accompanied me on this journey towards this dissertation. First and foremost, the most important are often those who are not visible from the outside. In that sense, my partner Amanda Alvinstedt Bogefors and my family have played a major role behind the scenes and helping me to realise this project.

When it comes to 'the visibles' the two key figures were my supervisors Liucija Vaišvilaitė and Karsten Specht who were always available and supportive. Only their feedback made the dissertation in its current form possible and gave me important perspectives and insights into the field and its methods along the way.

Thirdly, I want to thank James Roe, who inspired this dissertation by giving a talk at the university of Bergen. Afterwards, James was of incredible help to me explaining his findings in detail, providing additional information, discussing implications, and helping to inform our analyses by some additional computations he did for me. Without him, this dissertation would not have been possible in its present form.

A fourth invaluable mention are the entire Re:State Group and the Bergen fMRI Group, which made me feel at home as they function much like a 'research family' at the University of Bergen. When there was help needed, I had different people with different expertise to speak to and never felt left alone - even in times of a worldwide pandemic.

Finally, I want to thank the team behind the BETULA longitudinal project who were so kind to allow us access to their data. Their hard work collecting data from hundreds of participants allows the neuroscience community of today to retrieve extremely interesting and valuable information.

Remembering my colleague and friend Tania Martínez Montero who went from us too early.

Abbreviations

BOLD signal	–	blood oxygen level dependent signal
CEN	–	central executive network
CSD	–	cross spectral density
CSD-DCM	–	cross spectral density dynamic causal modelling
DAN	–	dorsal attention network
DCM	–	dynamic causal modelling
DMN	–	default mode network
EC	–	effective connectivity
ECI	–	echo-planar imaging
FC	–	functional connectivity
fMRI	–	functional Magnetic Resonance Imaging
GAM	–	generalized additive model
GLM	–	generalized linear model
GMPV	–	grey matter probability value
rs-fMRI	–	resting-state fMRI
ldPFC	–	left dorsal Prefrontal Cortex
LI	–	laterality index
lPC	–	left Precuneus
lmTG	–	left medial Temporal Gyrus

lPC2rPC   –   Effective connectivity from left Precuneus to right Precuneus.

(*Note:* the "2" between the brain regions is also being used for other pairs of regions indicating a causal relationship. The first region indicates the origin of the connection and the second the end.)

lPFC   –   left Prefrontal Cortex

VASO method –   vascular space occupancy method

raPFC   –   right anterior Prefrontal Cortex

rmTG   –   right medial Temporal Gyrus

rPC   –   right Precuneus

rPFC   –   right Prefrontal Cortex

rs-FC   –   resting-state functional connectivity

rs-EC   –   resting state effective connectivity

SC   –   structural connectivity

SN   –   salience network

task-fMRI   –   task-based fMRI

Contents

Introduction

Ageing is an essential part of life, affecting the human body in different ways. When researching ageing, the process is differentiated into healthy and pathological ageing. Healthy ageing can be defined as pathology- and diagnosis-free ageing (Peel et al., 2004) or as ageing while maintaining functional abilities and thereby wellbeing (WHO, 2020). However, healthy ageing also includes elements such as natural age-related atrophy or cortical thinning (Peel et al., 2004). Pathological ageing is accompanied by neurodegenerative disorders defined by the progressive, selective, and systematic loss of neurons in different brain regions (Martin, 1999). This leads to the disruption of the particular neurotransmitter systems which can be categorised into specific disorders such Alzheimer's, Parkinson's or Huntington's Diseases (Martin, 1999).

The understanding of the effects of age and ageing on brain function is still limited (Grady, 2012). Neuroimaging modalities such as fMRI are useful tools to observe brain function across ageing (D'Esposito et al., 2003). Most studies use FC to show that brain function changes in both healthy and pathological ageing (D'Esposito et al., 2003). While these studies' findings still need to be replicated, they also only allow limited inference about about how age and ageing affect the quality of the relationships between brain regions, such as their EC (Sala-Llonch et al., 2015).

Only recently, Roe and colleagues (2021) found increased grey matter loss in most asymmetric brain regions to be a unique feature of ageing. How the loss of grey matter in these regions relates to EC is an unanswered question. Overall, the observation of healthy ageing can help establish a baseline understanding of the heterogenous process of ageing.

Therefore, this work will examine the relationship between grey matter and EC in an ageing sample. As fMRI is used in this study, the first chapter gives an overview of the neuroimaging technique fMRI and its history, followed by its different applications. First, an overview of the function of the method is provided. Second, the two main application settings, task and resting state fMRI are being described and compared. In this study, we used rs-fMRI data and further descriptions focus hence on rs-fMRI. Third, analytical approaches of rs-fMRI data are being described, followed by fourth, most recent findings on networks focus on rs-fMRI.

The second chapter presents current literature on cerebral changes during ageing, distinguishing structural and functional changes. First, cortical thinning, and second, grey matter asymmetry (changes) are being discussed in the light of healthy ageing. Third, the state of the literature on age and ageing-dependent signal and connectivity changes are being described. Finally, the interplay of brain structure and function during ageing is being discussed.

The third chapter embeds fMRI research and the current study into the context of the ongoing replication crisis. Pitfalls and potential solutions are being discussed.

The fourth chapter gives an overview of the project. Both research questions and hypotheses are specified.

Magnetic Resonance Imaging

One of the most widely used techniques in neuroimaging is magnetic resonance imaging (MRI). Magnetic resonance scanners create a strong magnetic field B_0, which affects the alignment of the body's protons, with Hydrogen protons (H) being of particular interest which can be found in water molecules (H_2O) (Purves et al., 2013). Gradients send radio frequency pulse frequencies B_1 for a few milliseconds, which changes the naturally running spin and directionality of the protons. After the radio pulse has been sent, the protons re-align along the scanner's main magnetic field (B_0) which can be measured by the coil. The coil amplifies and digitizes the signal to extract information on both frequency and phase. A sequence[1] is used to produce images of the brain in slices (Purves et al., 2013).

Functional Imaging

Functional MRI (fMRI) specifically uses different sequences to capture *changes over time.* The most commonly used fMRI sequences are echo planar imaging (EPI) sequences, as EPI is relatively fast allowing for more data sampling (Kirilina et al., 2016). Changes in voxel intensities gives information about the oxygenation of haemoglobin measured by the

---

[1] Sequences are the 'runs of the scanner', characterised by a frequency or combinations of frequencies used repeatedly for imaging. The characteristics of the frequency influence the output recorded by the head coil. For example, during MRI, T_1-weighted images are obtained when using short repetition (TR) and echo times (TE). T_2-weighted images can be obtained when using both long TR and TE. T_1-weighted images give information about grey-to-white-matter contrasts and T_2-weighted images between cerebral tissue and cerebrospinal fluid (Purves et al., 2013).

blood-oxygen level dependent (BOLD) signal (Purves et al., 2013). Other sequences can provide information about cerebral blood flow, volume or oxygen metabolism (L. Huber et al., 2019).

The underlying principle for BOLD fMRI is biological. When neurons fire, astrocytes, one type of glial cells, signal to the blood vessels to supply more oxygen (which is being carried by the transport protein haemoglobin) and glucose-rich blood to cover the neurons' metabolic demands (Attwell et al., 2010). Importantly, haemoglobin has different magnetic properties when oxygenised compared to deoxygenised, which is then captured by the EPI sequence. The underlying assumption for further inference is that brain areas displaying increased activity will become identifiable by higher oxyhaemoglobin levels carried into these areas by incoming, 'freshly' oxygenised blood, as these areas consume oxygen and glucose. The decrease of the relative concentration of deoxyhaemoglobin during the income of oxyhaemoglobin-rich blood can then be measured at the specific locations across the brain.

The body interprets the astrocytes' signals as a sign to oversupply the firing neurons, potentially anticipating future firing or simply supplying other metabolites from the blood. Within circa 5-6 seconds the fMRI signal peaks and then slowly decreases reaching levels below the baseline, lasting for 20-30 seconds, which has been modelled by the hemodynamic response function (HRF) (Elbau et al., 2018; Lindquist et al., 2009; Tsvetanov, Henson, et al., 2020). Hence, the BOLD signal is an indirect measure of synaptic activity reflected in collective 'firing' or local field potentials, which allows inferences about neuronal activity (Grady, 2012).

Over the years, fMRI has become one of the most popular methods among current neuroimaging techniques with an increasing number of publications every year (Marinsek, 2017). There are several reasons for the popularity of fMRI. Firstly, the technique offers a high spatial resolution compared to other neuroimaging techniques while still maintaining an acceptable temporal resolution. Secondly, fMRI is non-invasive. Thirdly, MRI scanners are widely available in Europe and North America and once installed, they open wide possibilities for new discoveries (Glover, 2011).[2]

Although fMRI is used in clinical studies, to support or monitor therapy, and study the effects of pharmacological interventions (Glover, 2011), its application is still limited and does usually not exceed presurgical planning (Specht, 2020). However, recent findings show that clinical fMRI has the potential to be used for individually tailored applications (Gordon et al., 2017; Gratton et al., 2018; Greene et al., 2020; Poldrack et al., 2015). Furthermore, both highly sampled single subject (Gordon et al., 2017; Gratton et al., 2018) and group-averaged data might help to identify biomarkers and develop diagnostic classifiers for neuropsychological disorders (e.g., Eslami et al., 2019; Thomas et al., 2020). Advances in

---

[2] Additionally, a rather hypothetical reason is the attractiveness of graphical neuroimaging outputs. Some evidence suggests that evaluating information presented with neuroimages tends to appear more trustworthy and scientific in comparison with information presented as plain text or with standard graphs (Baker et al., 2017). The underlying process of this "neuroimaging bias" is yet poorly understood, possibly inapplicable to experts in the field (Baker et al., 2017). However, the increasing provision of funding for fMRI projects, in comparison to other fields', might partly stem from this bias (Frégnac & Laurent, 2014).

establishing diagnostic classifiers are ongoing and adopting different machine-learning techniques provides relatively good diagnostic accuracy (see Šimundić, 2009) using MRI data (Yassin et al., 2020) or combination of fMRI and MRI data (Rakić et al., 2020). All considered, fMRI has a large potential for a range of applications in clinical and research settings (Gratton et al., 2018), even more so with the help of further development of methodology (Thomas et al., 2020).

task-based fMRI

In the approximately first 20 years since fMRI has been discovered by Ogawa and colleagues (1990), paradigm-based or task-based fMRI (task-fMRI) were used as the fMRI design of choice (Specht, 2020). The idea behind task-fMRI is that specific tasks evoke neuronal activity followed by metabolic changes, such as, oxyhaemoglobin-rich blood inflow, measured by BOLD-contrasts. An example of task-fMRI is to show images signalling the participant to tap with their index finger as the experimental condition alternating with a control condition showing only a fixation cross which does not require any movement. An elicited BOLD signal in motor areas, cerebellum and striatum during finger tapping (experimental condition) indicates activity in these regions during motor task execution (Gountouna et al., 2010). Additionally, subtracting the BOLD signal during the resting/control condition's from the task condition informs the relative signal change, which should be statistically significant in the mentioned motor regions (Gountouna et al., 2010).

resting-state fMRI

Resting state fMRI (rs-fMRI) has first been introduced into the field by Biswal and colleagues (1995) in a seminal experiment. In rs-fMRI, the procedure can be seen as opposite

to task-fMRI. Instead of engaging in a particular task, the participant rests either with eyes closed or looking at an empty slide, fixation cross or similar (Poldrack, 2018). Hence, "rest" in rs-fMRI studies is refined as inactive wakefulness, when the participants is awake, but not involved in any particular cognitive task. Rs-fMRI analyses focus on low-frequency BOLD-signal fluctuations, which are often used to map synchronous fluctuations, also called functional connectivity (Lee et al., 2013). Crucially, these patterns are systematic/non-random and show spatiotemporal patterns (Lee et al., 2013).

Ever since its introduction, rs-fMRI has been widely adopted (Snyder, 2016). Some of the main reasons are that: i) rs-fMRI is assumed to reveal unique information about the functional organisation of the brain, ii) the costs are lower than for task-fMRI, as the scanning durations are usually shorter, iii) rs-fMRI is easy to administer as it does not require participants to learn or execute any procedures, therefore constraint free (Canario et al., 2021). This allows to investigate individuals who are not able to execute certain tasks, due to cognitive impairment, motor problems (e.g., Lau et al., 2016; Y. Zhang et al., 2017) and neuropsychological disorders such as Alzheimer's (Sanz-Arigita et al., 2010; Zhiqun Wang et al., 2015; Zhao et al., 2012; Zhou et al., 2013); or Parkinson's Disease (Göttlich et al., 2013; Pan et al., 2017; Sang et al., 2015; Wei et al., 2014). Lately, the focus of the scientific community has been on development of new methods and improving research practices in neuroimaging studies. Several open access databases have been established over the recent years containing rich rs-fMRI data in order to achieve the aforementioned goals (Eickhoff et al., 2016; Harms et al., 2018; Madan, 2017).

Comparison of resting-state vs. task-based fMRI

Task-fMRI is based on the assumption that neurons deplete of oxygen when firing, when the neuronal firing is evoked by a task or stimulus. The oxygen-depletion leads to the HRF-modelled overshoot of oxyhaemoglobin-rich blood. Conversely, the idea of rs-fMRI is based on the fact that, even during awake resting, approximately 20% of the body's energy is consumed by the brain (Clarke & Sokoloff, 1999), which suggest there is high activity during rest (Hyder et al., 2013). This indicates that the brain constantly executes intrinsic processes, measurable by low frequency fluctuations below 0.1Hz (Biswal et al., 1995), which are not yet fully understood. A range of findings indicate an underlying permanent prevalence of top-down, also called intrinsic processes, which do not appear in response to specific sensory inputs (Friston, 2002). It is suggested that these intrinsic networks might exist in order to process information in an efficient and less energy-consuming way (van den Heuvel & Hulshoff Pol, 2010). In this context, it has been hypothesised that the brain uses elements of anticipation or works in a hypothesis-testing fashion, partly to conserve energy as well as to assure survival (Poldrack, 2018). Intrinsic processing seems to play an essential role in such prediction-making and hypothesis-testing.

Moreover, many, if not most, of the major functional task-specific hubs have been mapped out on a macro-scale over the recent decades. The accumulated evidence suggests cognitive processes are dependent on the functioning of large-scale, interconnected networks rather than single regions (Hugdahl, 2018). Accordingly, the majority of fMRI research outputs has recently moved from task- towards rs-fMRI connectivity (Marinsek, 2017).

Critics of rs-fMRI argue that resting-state is just another task "state" (Campbell & Schacter, 2017). Subjects still exhibit activations dependent on a wide range of mental activities they engage in, which is likely to happen at rest (Campbell & Schacter, 2017). Additionally, it is likely that there are cohort-dependent differences in the engaged activates, possibly affecting the reliability of rs-fMRI (Campbell & Schacter, 2017).

However, task-fMRI is not unanimously perceived as more reliable in comparison to rs-fMRI (e.g., C. M. Bennett & Miller, 2013; Elliott et al., 2020). For example, based on the task characteristics and experimental design, task-fMRI datasets often differ strongly from one another (C. M. Bennett & Miller, 2013). Hence, different task-fMRI studies' findings are often difficult to compare with each other aggravating the findings' generalisability.

Briefly, rs-fMRI is set out to explore relationships between intrinsic neural activities in different cerebral regions over time (Poldrack, 2018). Task-fMRI on the other hand is focussed on activations provoked by a task. Therefore, rs-fMRI is preferentially chosen to investigate more general questions about the prevailing functional networks and their dynamics. However, it is not to say that any of the mentioned measures is obsolete – rs-fMRI and task-fMRI are simply different tools to be applied in the right settings. To gain a holistic and detailed understanding of cognitive processes using neuroimaging, the most sensible option is to consider both resting-state and task networks, depending on the aim and hypothesis on hand (e.g., Campbell & Schacter, 2017; Dohmatob et al., 2021).

Analysis of Resting State fMRI Data

When analysing resting state fMRI data, the goal is to identify consistent patterns of spontaneous fluctuations in brain activity (Smith et al., 2013). These patterns of co-

occurring brain activity are also called connectivity and can be mapped out into resting-state

networks (rs-networks) or functional connectome (Smith et al., 2013). There are two major

analytical approaches for inferences about rs-networks: functional connectivity (FC) and

effective connectivity (EC).

FC displays statistical dependencies between measures, using correlation analyses

(Smith et al., 2013; Zeidman, Jafarian, Corbin, et al., 2019). Simultaneously occurring signal

in different regions over time will be linked under the assumption that these co-active

regions cooperate in a network.

EC is a probabilistic measure of the direct causal relationships between brain regions;

their effect on each other and themselves (Zeidman, Jafarian, Corbin, et al., 2019). This adds

the directionality of effects within or between rs-networks (Friston et al., 2003). EC adopts

the Bayesian approached to analyse the imaging data by using Dynamic Causal Modelling

(DCM) to assess the connectivity between selected regions (see for DCM Friston et al., 2003;

Zeidman, Jafarian, Corbin, et al., 2019; Zeidman, Jafarian, Seghier, et al., 2019).

Importantly, as with other Bayesian methods, in DCM, prior assumption of the probability

will together with observed probabilities inform the posterior probabilities. DCM priors are

the qualities of connectivity, such as directionality (Friston et al., 2003).

Commonly, in order to estimate the FC or EC, the main network nodes are selected,

that are functionally distinct brain regions, representing the network's edges/nodes (see

figure 1 in Smith et al., 2013). To establish nodes or regions of interest (ROI), commonly

parcellation is used; the brain is divided into voxels or spheres which serve as network nodes.

Different data or hypothesis driven approaches can be used determine the parcellation of the

brain. First, neighbouring voxels can be clustered based on time-series-dependent similarities (k-nearest neighbour). Second, independent component analysis (ICA) indicates the independent activity pattern of different brain regions. Overlapping node activity maps in a time-series are represented by network edges (Smith et al., 2013). Third, early rs-fMRI studies calculated FC seed-based by selecting a region of the brain, for example an 8mm^3 voxel, and then correlating its time-series with all other voxels' time-series (Smith et al., 2013). Fourth, when testing specific hypotheses regarding the relationship between brain regions, a more recent approach – DCM – is used, examining directional connections within and between specific nodes.

Parcellations with higher dimensionality (more nodes) will result in a finer analysis of the network connectivity by revealing information on within large-scale network connectivity (Lee et al., 2013). A lower dimensionality will inform about between connectivity, however with less detail regarding within large-scale network connectivity. Seed-based approaches are commonly used to test hypotheses on connectivity when prior information is available about the seed region (rather hypothesis-driven). These tests are correlational when using FC and causal when using EC. Data-driven approaches, such as ICA and different types of unsupervised machine-learning algorithms usually are used to explore networks and their qualities by clustering information (Lee et al., 2013).

Recent Analytical Advances: Dynamic Causal Modelling

Recently, Dynamic Causal Modelling (DCM) has become more popular for analysing fMRI data. DCM is an analytical tool implemented in SPM12 developed by Friston and colleagues in (2003) (Friston et al., 2003). DCM relies on Bayesian statistics and allows to

model EC. In comparison to more mainstream analyses, based on frequentist statistics, namely the correlational relationship between voxel-level signal intensities, DCM simulates the bidirectional relationship between and within selected ROIs/nodes using the Bayesian model *inversion* and *comparison* (Zeidman, Jafarian, Corbin, et al., 2019). Initially, DCM has been developed for hypothesis testing in task neuroimaging. The technique is not limited to fMRI and has previously been used in electroencephalography (EEG) and magnetencephalography (MEG). More recently DCM has been applied to rs-fMRI data (Zeidman, Jafarian, Corbin, et al., 2019).

Given the nature of DCM, the analysis requires predefined priors and selected ROIs (Friston et al., 2003). Broadly the DCM procedure can be described in three steps (Zeidman, Jafarian, Corbin, et al., 2019), that are the following: model specification, model estimation, and model comparison. Model specification, also called forward models are specified for the data, and are driven by the hypothesis at hand. Usually, several competing forward models are defined, which then are fitted to the dataset, i.e., estimating the model accuracy. Model estimation or model inversion assesses the probability of observing the data under the previously specified models and is defined as model evidence. Finally, model comparison, as suggested by its name, is used to compare the predefined and fitted models on a group level (Zeidman, Jafarian, Corbin, et al., 2019). For the model comparison at the group level, Bayesian approaches, such as Parametric Empirical Bayes (PEB), or frequentist approaches, such as ANCOVA, can be used (Zeidman, Jafarian, Seghier, et al., 2019).

DCM for cross spectral densities (CSD) is the latest development for resting-state DCM. CSD is modelled by between-nodes/ROIs correlations of BOLD-signal frequency

distributions (Friston et al., 2014; Zeidman, Jafarian, Corbin, et al., 2019). Thereby, time course-dependent signal changes of one region are modelled as dependency of another region, representing EC (Friston et al., 2014; Zeidman, Jafarian, Corbin, et al., 2019). CSD-DCM is useful to model rs-fMRI, as it focusses on frequency instead of time, where large timepoint-dependent changes are not expected, as it would be in task-fMRI. This allows CSD-DCM to model statistical dependencies among timeseries. Different from other DCMs (e.g., applied to task-fMRI data), connection strength between nodes is assumed to be constant in CSD-DCM. In other words, no time-dependent fluctuations are being modelled, allowing for more efficient calculation as it requires less computational power than other DCMs and is more sensitive to inter-individual differences (Zeidman, Jafarian, Corbin, et al., 2019).

Resting-State Networks

Evidence from electroencephalography (EEG), positron emission tomography (PET) and fMRI provides evidence for the existence of a range of intrinsic resting-state networks across cortical as well as subcortical structures (Allen et al., 2011; Damoiseaux et al., 2006; Hacker et al., 2013; Mantini et al., 2007; Raichle et al., 2001). Three of these networks have been labelled to be core neurocognitive networks: default mode network (DMN), salience network (SN) and central executive network (CEN), and are suggested to be incremental for healthy cerebral functioning and cognition (Bagarinao et al., 2019; Bressler & Menon, 2010; Tsvetanov et al., 2016).

Default Mode Network

The DMN was the first intrinsic network discovered (Biswal et al., 1995). Before its discovery it was thought to be merely de-activations during the resting blocks in task fMRI

studies (see Shulman et al., 1997). Today, the DMN has been observed in other mammals as well such as monkeys, cats and mice (Raichle, 2015). In humans, three major DMN nodes have been defined: i) the ventral medial (VMPFC), ii) dorsal medial prefrontal cortex (DMPFC), and iii) the posterior cingulate cortex and adjacent precuneus including the lateral parietal cortex, approximate Brodmann area 39 (Raichle, 2015; Tsvetanov et al., 2016). Although the role of the DMN remains unclear, certain functions have been attributed to the network and its subunits, such as self-referential thought (DMPFC), emotion processing (VMPFC), and recollection of experiences (posterior elements) (Raichle, 2015). Moreover, studies suggest that atypical DMN functioning and its connectivity with CEN and SN are associated with disease and disorders of the brain (A. C. Chen et al., 2013; Raichle, 2015). Dysregulation of connectivity between the DMN nodes within and between other networks has been linked to depression (increased within-DMN connectivity; Kaiser et al., 2016), bipolar II disorder (decreased DMN-cerebellum and within DMN connectivity; Gong et al., 2019; X. Luo et al., 2018), schizophrenia (evidence of direction of network alterations is yet unclear), attention-deficit/hyperactivity disorder (reduced within DMN connectivity), and neurodegenerative disorders such as Alzheimer's Disease (reduced within DMN connectivity; Greicius, 2008).

Central Executive Network

CEN, also called cognitive control network or cognitive executive network has two main nodes: the dorsolateral prefrontal cortex (DLPFC) and posterior parietal cortex (PPC). CEN has been attributed to functions such as higher order cognition and attention regulation (Bressler & Menon, 2010; Tsvetanov et al., 2016). Cognitive or executive control

is an umbrella term for family of top-down cognitive functions necessary to cognitively control behaviour, such as inhibition, allowing for self-control; interference control, allowing for selective attention and cognitive inhibition; and working memory as well as cognitive flexibility, allowing for flexible, adaptive and creative real-time information processing (Diamond, 2013), finally initiation, vigilance and planning (Niendam et al., 2012). A number of studies has linked the mentioned functions with CEN (e.g., Niendam et al., 2012; Reineberg et al., 2018) as well as the connectivity between CEN, DMN and SN (e.g., Beaty et al., 2015). Interestingly, negative mood seems to decrease efficiency of information transfer within CEN (Provenzano et al., 2019). A range of neuropsychological disorders have been associated with CEN dysregulation, such as altered DMN-CEN connectivity in major depression (Mulders et al., 2015), decreased FC between CEN and cerebellum in bipolar II disorder (X. Luo et al., 2018), increased within CEN connectivity in obsessive compulsive disorder (OCD) (Y. Chen et al., 2016), decreased within CEN FC in borderline personality disorder (Doll et al., 2013), increased FC between CEN-DMN in schizophrenia (Manoliu et al., 2014).

Salience Network

SN main nodes are the anterior insula (AI) and anterior cingulate cortex (ACC) (Bressler & Menon, 2010; Tsvetanov et al., 2016). The name of this network stems from the functions of insula, i.e. detecting salient events/stimuli and allocating executive and sensorimotor resources to them (Goulden et al., 2014). SN and its subregions have also been suggested to be responsible for switching between DMN and CEN (Chand & Dhamala, 2017; Goulden et al., 2014; Sridharan et al., 2008; Uddin, 2015). This modulating function of SN

seems especially disrupted in pathological ageing, such as age-related mild cognitive

impairment (Chand et al., 2017) or Alzheimer's Disease (He et al., 2014; Joo et al., 2016).

Additionally, in posttraumatic stress disorder (PTSD) (Abdallah et al., 2019) and

unmedicated bipolar II disorder (Gong et al., 2019) within SN FC has been found to be

increased. Interestingly, opposite to CEN, negative mood seems to increase the efficiency of

information transfer within the SN (Provenzano et al., 2019).

Cerebral Changes During Healthy Ageing

Aging is an essential part of life. Throughout the lifespan, the brain reorganises continuously adapting to the everchanging environment and 'challenges at hand' (Y. Chang, 2014; Poldrack, 2018; Poldrack et al., 2015). Ageing can be quantified in different ways, for example, by looking at behavioural patterns, chronological or biological age. Grey matter properties, including cortical thinning and grey matter asymmetries are an example for biomarkers of ageing (e.g., Aycheh et al., 2018; Goh, 2011; Grady, 2012; N. Luo et al., 2020; Pur et al., 2019; Shaw et al., 2016). Additionally, functional properties, such as BOLD signal changes, can serve as biomarkers of ageing (Garrett et al., 2017; Gaut et al., 2019; Grady & Garrett, 2014; Kumral et al., 2020; Z. Li et al., 2017; Nomi et al., 2017; Tsvetanov et al., 2015).

In this section, an overview of the current state of the literature is being given. Firstly, structural changes during ageing are being described, namely, the well-documented phenomenon of cortical/grey matter thinning and its lateralisation. Thereafter, age-dependent changes in cerebrovascular signals are discussed, and finally, bringing both brain structure and function together, the relationship between grey matter loss and functional connectivity.

Cortical Thinning

Over the recent years an extensive amount of research has linked chronological age to cortical thinning (e.g., Aycheh et al., 2018; Goh, 2011; Grady, 2012; N. Luo et al., 2020; Pur et al., 2019; Shaw et al., 2016). Hence, cortical thickness has been frequently treated as one of several indicators of biological age during healthy and pathological ageing (Aycheh et al.,

2018; Corps & Rekik, 2019; Dafflon et al., 2020; Khundrakpam et al., 2015). Cortical

thickness has also been classified as a biomarker of different ageing-related diseases, such as

Alzheimer's Disease (AD) (Dickerson & Wolk, 2012). Recent evidence suggests that cortical

thickness in the frontal areas is most susceptible to thinning during the process of healthy

ageing (Lemaitre et al., 2012; Roe et al., 2021).

Given the existing evidence, it is suggested that cortical thickness among other

structural data obtained from T_1-weighted MR, can be used to predict chronological age

(Aycheh et al., 2018; Bashyam et al., 2020; Cole, 2020; Madan & Kensinger, 2018; J. Wang

et al., 2014). Chronological age can be defined as individual physical age value, whereas

biological age can be derived from different biomarkers of interest, such as grey matter

properties. Using two different databases (IXI and INDI), Wang and colleagues (2014) found

that cortical thickness combined with curvatures – modelling sulci and gyri shapes with

vectors, that predicted chronological age with high accuracy and sensitivity; with deviations

of 4.57 and 1.38 years for the different datasets. In a large-scale cohort study, Aycheh and

colleagues (2018) reported that cortical thickness is a reliable predictor of chronological age

with a mean absolute error of 4 years (Aycheh et al., 2018). Another regression model

presented by Madan and Kensinger (2018) compared different data modalities to determine

which of them can serve as the best predictor of age. Their results suggest cortical thickness,

when used as predictors together with fractal dimensionality - a measure of complexity of

cortical and subcortical structures - served most accurately for chronological age-prediction

with a median error of 6–7 years. Finally, a total of thirty-four neuroimaging measures were

informative predictors of chronological age according to Cole and colleagues (2020). Of these,

grey matter volume and white matter hyperintensities were found to be the most informative

predictors in a regression model predicting chronological age. Given all the above, it can be

assumed that cortical thinning is not only a part of healthy ageing but can also be used as

an estimate for chronological and biological age, and consequently be related to brain

function.

Cortical Thickness Asymmetry Changes

A wide range of evidence shows that the brain is both structurally and functionally

asymmetric (Agcaoglu et al., 2015; Chiarello et al., 2016; Hugdahl, 2005; Karolis et al., 2019;

Kong et al., 2018; Toga & Thompson, 2003). These asymmetries are affected by the process

of healthy ageing (Roe et al., 2021; N. Zuo et al., 2020). Recent research revealed that

chronological age is negatively associated with asymmetries in cortical thickness (Agcaoglu et

al., 2015; Roe et al., 2021). The strongest asymmetries in cortical thickness occur in the late

20s, predominantly in frontal lobe, higher order cortical regions (Roe et al., 2021). The

asymmetries decline continuously, because of decreases in thickness of the thicker

hemisphere, during the following years in both healthy ageing and AD patients, with a

notable acceleration in AD (Roe et al., 2021; N. Zuo et al., 2020). Changes in cortical

thickness asymmetries are an important, however often overlooked feature of healthy ageing

(Roe et al., 2021). Advancing the knowledge of structural changes during the lifespan will

consequently advance inferences about pathological and healthy ageing. Moreover, improving

the understanding of age-related structural changes offers the potential to link such to age-

related functional and behavioural changes in both healthy individuals and patients.

Cerebrovascular Signals

The ageing of the body influences both neuronal and vascular systems (D'Esposito et al., 2003; Tsvetanov et al., 2019; West et al., 2019). In turn, the hemodynamic responses change in healthy ageing due to the effects on the vascular systems, such as cerebral blood volume and flow, cerebral metabolic rate of oxygen and venous oxygenation (Lu et al., 2013).

This results in additional noise in fMRI data (T. T. Liu, 2016). The magnitude of these noise components is often bigger than the signal of interest, making de-noising and noise reduction procedures crucial. Moreover, the signal-to-noise-ratio has been used as a metric of acquisition performance. Noise can be non-BOLD and BOLD-related. Examples for non-BOLD-related noise are motor activity, inter-scan, inter-subject, and inter-site variability and BOLD-related can originate from cardiac pulsation and respiration (T. T. Liu, 2016).

Different MR sequences provide diverse information about the ageing brain. An example of such would be the vascular space occupancy (VASO) technique, also used as an indirect measurement of neuronal activity (L. Huber et al., 2014, 2017). VASO offers higher spatial specificity, which can add further detail to fMRI data, especially when used with higher magnetic field strength of 7T (L. Huber et al., 2014, 2017). Since VASO is solely focussed on cerebral blood flow, the signal is less susceptible to other physiological noise (Lu et al., 2013). VASO can additionally provide details about factors contributing to the BOLD signal, for example, how cerebral blood flow contributes to the BOLD signal (Lu et al., 2013). However, a considerable amount of research is still focussed on validating VASO as a

valid method (Donahue et al., 2006; Hua et al., 2009; L. Huber, Finn, et al., 2020; L. Huber, Poser, et al., 2020; Jin & Kim, 2008; Scouten & Constable, 2007; Uh et al., 2011; Wu et al., 2010). Currently, BOLD fMRI remains the leading technique (Lu et al., 2013). Nonetheless, variations in sequences artifact susceptibilities are dependent on the observed brain region (Lu et al., 2013). It is hence useful to observe either VASO or BOLD signal selectively dependent on the observed ROI, or both signals together (Lu et al., 2013). In the following the more researched BOLD signal changes during healthy ageing described in the literature will be summarized, followed by ageing-dependent connectivity changes.

BOLD Signal Changes in Healthy Ageing

It has been established, that the shape and temporal properties of the HRF vary between age groups: the time to reach the peak amplitude increases with older age, where the peak amplitudes are overall smaller (Abdelkarim et al., 2019; D'Esposito et al., 1999; Tsvetanov, Henson, et al., 2020; West et al., 2019). Additionally, the HRF is much more variable in older adults, from the mid-50s, potentially due to stronger differences in overall health and activity levels compared to younger adults (18-30 years) (West et al., 2019).

Given the above, neurovascular coupling is affected with increasing age, in turn influencing the BOLD signal (D'Esposito et al., 2003). The literature indicates, that healthy ageing leads to a global decrease of BOLD signal variability (Garrett et al., 2017; Gaut et al., 2019; Grady & Garrett, 2014; Kumral et al., 2020; Z. Li et al., 2017; Nomi et al., 2017; Tsvetanov et al., 2015), where some evidence suggests a positive association between BOLD signal and ageing (Garrett et al., 2010). Nevertheless, more or increased task-induced signal does not mean "better" (e.g., Grady, 2012). Depending on the brain region and task, an

increased BOLD response does not have to lead to better task performance, but can also signify worse task performance (Grady, 2012). This is due to the interplay of excitatory and inhibitory firing, and the use of single brain regions for multiple functions (Hugdahl, 2018).

Connectivity Changes

Age-dependent physiological changes as summarized in the previous sections lead to changes in FC (Bethlehem et al., 2020; Sala-Llonch et al., 2015; Stumme et al., 2020). For example, older adults seem to have a higher global flexibility compared to younger adults, indicating that nodes switch more often between modules over time (Malagurski et al., 2020). Additionally, there is significantly higher variability in network organisation in older adults (Malagurski et al., 2020). Such age-related FC changes have previously been labelled as disruptions in large-scale networks characterised by decreased strength and organisation of the connections (Andrews-Hanna et al., 2007; Goh, 2011) at the same time affecting the networks' efficiency in transferring information (Bagarinao et al., 2020). Specifically, the age-related cortical thickness asymmetry decrease in frontal and attentional networks (see Roe et al., 2021) might influence FC in the same areas (for comparison: Agcaoglu et al., 2015; Grady, 2012; Salami et al., 2014; Spreng et al., 2016).

Neuroimaging research on healthy ageing has mainly focussed on FC and BOLD signal variability, with only few studies reporting EC changes during ageing (see review by Sala-Llonch et al., 2015). Studies on ageing reporting EC suggest that both within and between large-scale network EC contribute to explaining the variations in ageing as EC differs between age groups (Tsvetanov et al., 2015). Further literature indicates decreased EC in motor areas during motor imagery (imagined/mentalised movement, see L. Wang et

al., 2019), or stronger fronto-medio-temporal EC during an emotional memory task in comparison with younger adults (Waring et al., 2013). Finally, ageing influences EC when processing positive but not negatively loaded information, possibly leading to an age-related "positivity effect" (Addis et al., 2010). Interestingly, results from Addis and colleagues (2010) study on EC during healthy ageing suggests that only processing positive information is changed in comparison to negatively loaded information, likely leading to an age-related "positivity effect" (Addis et al., 2010). In the aforementioned study, EC of between the two groups, i.e., young vs. old individuals was compared when participants were exposed to images which were previously rated negatively and associated with high arousal, and to positively rated, low-arousal images. No age effects were discovered for the encoding of the negative images, but there were age differences discovered when encoding the positive images.

A range of studies has shown that older adults show decreased FC in caudal brain regions including occipital, parietal and medio-temporal lobes (Goh, 2011). It has been suggested that this is due to a dedifferentiation of processing specificity (Goh, 2011). For example, studies comparing groups with mean ages of 20.9 and 60.9 (Park et al., 2004), or 67.36 (ranging from 59–80) and 25.73 years (ranging from 20–35) respectively (Voss et al., 2008) revealed that the visual cortex BOLD contrast in younger adults is more distinct for different visual stimuli than in older adults. On the other hand, age-related atrophy can lead to inaccuracies in co-registrations and hence makes BOLD-responses appear lower in older ($M_{age} = 64.9$, $SD = 2.8$ years) compared to younger individuals ($M_{age} = 26.1$, $SD = 2.2$) (X. Liu et al., 2017).

Within Network Functional Connectivity. Generally, chronological age has

been associated negatively with whole brain FC (Farras-Permanyer et al., 2019), as well as

within large-scale network resting-state functional connectivity[3] (rs-FC) (Bagarinao et al.,

2019, 2020; Varangis et al., 2019). Chronological age has also been negatively associated with

EC stability of neuronal activity within these networks (Tsvetanov et al., 2016). The same

applies to FC in DMN, dorsal attention network (DAN)[4], CEN and SN (Campbell &

Schacter, 2017; Damoiseaux et al., 2008; Ferreira & Busatto, 2013; Grady, 2012; Mak et al.,

2017; Salami et al., 2014; Skouras & Scharnowski, 2019; Spreng et al., 2016; Tsvetanov et al.,

2016; Varangis et al., 2019; Voss et al., 2010). Additionally, recent evidence suggests that

ageing affects DMN and CEN connectivity stronger than traumatic brain injury

(Bittencourt-Villalpando et al., 2021).

However, there are specific within resting-state network differences (e.g.,

Damoiseaux, 2017). For example within the DMN (Boraxbekk et al., 2016; Mak et al., 2017;

Salami et al., 2014), Voss et al. (2010) found age-related decreases in posterior DMN FC,

both for local and distributed connections. Similarly, Salami, Pudas and Nyberg (2014)

showed that FC decreases in most parts of the DMN with increasing age. An exception

seems to be the angular gyrus which showed a weaker negative relationship between

---

[3] See for a definition of functional connectivity the chapter "Analysis of Resting-State fMRI Data".

[4] The dorsal attention network has also been labelled the task-positive network as it is positively correlated to

different tasks, as opposed to the DMN (Esposito et al., 2018). Both dorsal and ventral rs-fMRI attention

networks resemble the attention networks identified during task-fMRI neuroanatomically (Fox et al., 2006).

chronological age and FC than other DMN parts (Salami et al., 2014), consistent with previous findings (Allen et al., 2011; Biswal et al., 2010). In addition to an increased number of connections to the inferior parietal lobes, Tsvetanov and colleagues (2016) found that the connectivity in the right anterior insula increased with age. Even though, the major trend shows a decrease of DMN FC with higher age during both healthy and pathology related ageing, it is not a simple gradual decrease. The relationship between DMN FC strength and age has been suggested to be modelled as inverted U-shape (age on the x-axis, FC on the y-axis) (Mak et al., 2017).

The age-related FC changes in SN as well as CEN seem to be similar to those in the DMN (He et al., 2013; Joo et al., 2016; Onoda et al., 2012). However, it has been suggested that those can be counteracted by cognitive training (Cao et al., 2016; M. Xu et al., 2020). Moreover, compared to younger adults, older healthy adults seem to engage SN and DMN less often (Marstaller et al., 2015). Similarly, FC within the anterior cingulate cortex was found to increase with higher age (Cao et al., 2014). The key nodes of SN and CEN appear to be negatively related with both healthy and pathological ageing (He et al., 2013, 2014; Joo et al., 2016). On the contrary, FC within DAN is suggested to be reduced with increasing age (Spreng et al., 2016), providing a possible explanation of the well-known age-related deterioration of attention processes (Tomasi & Volkow, 2012). Although it could be assumed that there is an overall trend of decrease in connectivity within large-scale networks during healthy ageing, bidirectional region-dependent patterns of age-related within network connectivity changes make it difficult to conclude with such all-or-nothing statement.

Between Network Functional Connectivity. In contrast to within large-scale network FC decreases, the between large-scale network FC has been positively associated with increasing age, which is also referred to as de-differentiation (Damoiseaux, 2017; Goh, 2011; Grady et al., 2016; Hughes et al., 2020; Stumme et al., 2020). Simultaneously, Bagarinao et al. (2019) concluded that the core neurocognitive networks (DMN, SN, CEN) and basal ganglia networks showed relatively preserved connectivity between networks. Furthermore, Spreng and colleagues' (2016) suggested that DAN-DMN FC was higher for healthy older adults compared to younger adults. Other networks, such as the hippocampal system were found to show increased connectivity with frontal networks, which has been associated with lower memory processing (Salami et al., 2014). The literature suggests that the FC is increased in visuospatial and precuneus networks with other networks in older individuals (Bagarinao et al., 2019). Additionally, there has been a range of reports of increased DMN-FPN FC (Campbell & Schacter, 2017). Opposingly, there is evidence for decreased FPN-DAN FC (Campbell & Schacter, 2017), DMN-SN FC (Cao et al., 2014), and CEN-DMN connectivity (He et al., 2013). Moreover, the anterior cingulate cortex, a region of the SN, has been reported to exhibit a decrease in FC to other regions such as hippocampus and thalamus during the process of healthy ageing (Cao et al., 2014). Hence, the connectivity between networks and directionality of age-related changes of such cannot be generalized for the entire brain.

There have been estimates of chronological age accounting for circa 10% of the individual differences in FC (Boraxbekk et al., 2016). Furthermore, Tsvetanov and colleagues (2016) found, that EC between SN, DMN, and DAN could explain up to 20% of

the variance of age. Further, Tsvetanov et al. (2019) showed that the relationship between age and FC could be explained by the neurovascular and cardiovascular factors. Unfortunately, the overall understanding of how structural and functional changes interact throughout healthy ageing is still limited (Carp et al., 2011; Fjell et al., 2017; Kalpouzos et al., 2012).

In conclusion, age-related physiological changes lead to differences in BOLD signal variability. Since FC is calculated based on the BOLD signal, these changes are directly related to the BOLD signal variability. On the one hand, the academic literature suggests that there are age-related trends of within network FC decreases and between network FC increases. On the other hand, there are age-dependent regional FC changes not following these trends, dependent on a variety of factors, which may as well be structural (e.g., Damoiseaux & Greicius, 2009). It is therefore reasonable to investigate the relationship between structural and functional parameters to achieve a better understanding of the ageing brain. To our knowledge, there are no studies addressing the relationship between grey matter properties and EC. Hence, the next section will focus on the relationship between grey matter and FC, another estimate of connectivity.

Relationship between Grey Matter and Functional Connectivity

Recent literature on ageing suggests a relationship between cortical thickness and FC in humans (Huntenburg et al., 2017; Tsvetanov, Gazzina, et al., 2020) and non-human primates (Beul et al., 2017). One example in humans are grey matter and FC differences between left and right handers, which can be linked to behaviour (M. Li et al., 2015). However, in a study by Huntenburg and colleagues (2017) the relationship between cortical

thickness and FC did not persist when controlling for shared cortical thickness variance and T_1 parameters. Furthermore, the relationship between cortical thickness and FC were not found by Mueller and colleagues (2013), albeit the authors report a positive correlation ($r = 0.30$, $p < 0.0001$) between sulcal depth variability and FC variability. More recent evidence by Vieira and colleagues (2020) revealed a relationship between FC and cortical thickness throughout the ageing process. Additionally, age-related cortical thinning was related to changes in white matter diffusion parameters (Pinto et al., 2020), fractal dimension, and cortical surface changes (King et al., 2009; Reishofer et al., 2018), but also FC, specifically in the DMN (Fjell et al., 2017; Romero-Garcia et al., 2014). However, this relationship between cortical thickness and FC in DMN does not seem to be strong (Fjell et al., 2017).

Given all the above, the relationship between structural and functional connectivity is still unclear (Fjell et al., 2017; N. Luo et al., 2020; Zimmermann et al., 2016). The evidence from several studies do suggest a structural-functional-connectivity-relationship is present (Levakov et al., 2021; Rosenthal et al., 2018; Ystad et al., 2011), other studies challenge these findings, proposing that the relationship is non-existent (e.g., Tsang et al., 2017). Conversely, FC was found to be a predictor of cortical thickness in pathological development, such as Parkinson's Disease progression (Yau et al., 2018). Recent evidence suggests, it can be concluded that age affects structural and functional parameters differentially as well as task performance based on both individual differences and type of task (Rieck et al., 2021). Although there is a body of literature indicating some association between cortical thickness and FC in humans, understanding the relationship between FC,

cortical thinning, and other structural parameters requires further investigation, especially

considering the process of healthy ageing.

fMRI Reliability

It is often unclear where uncertainty in fMRI findings originates, as there are many different sources of error, which lowers generalizability. Particularly multivariate phenomena such as ageing become difficult to explain when error is added from additional sources outside the phenomena's parameter space, for example, via analytic and/or inferential errors (Nieuwenhuis et al., 2011; Poldrack, 2011; Yarkoni, 2019), questionable research practices (Gelman & Loken, 2013; Lilienfeld, 2017; Simmons et al., 2011; Wicherts et al., 2016) or a biased literature which fails to report null findings (Francis, 2013; Friese & Frankenbach, 2020; Wicherts, 2017). The term replication crisis refers to low reliability and replicability, which has recently thematised particularly in psychology and biomedical sciences (e.g., De Boeck & Jeon, 2018; Gelman & Loken, 2013; Ioannidis, 2018; Loken & Gelman, 2017; Nuzzo, 2015; Pashler & Harris, 2012). Neuroimaging has "its own replication crisis" (Boekel et al., 2015; Dinga et al., 2019; D. E. Huber et al., 2019), as indicated by a notable trend of failed attempts to replicate previously published fMRI studies (Boekel et al., 2015; Dinga et al., 2019). In addition, publication bias aggravates fMRI meta-analyses (Müller et al., 2018), and the usage of QRPs might be common (Poldrack et al., 2017). Overall, replicability depends on a multitude of study-specific factors, such as pre-processing, statistical procedures and their power, study design, and the strength of the observed effect (for more detail on fMRI reliability and replicability issues see Appendix H). This section will however focus on how to improve fMRI reliability and replicability, which is crucial to all aspects of fMRI research, including ageing research, as this can be directly related to present executed research.

Different practices have continuously been developed and improved, considering the

replication crisis and how to tackle it in neuroscience (Gorgolewski & Poldrack, 2016;

Nichols et al., 2017). Major themes include making data, code, and much information as

possible around the final papers openly accessibly, in order to avoid QRPs (Gorgolewski &

Poldrack, 2016). Additional initiatives include a) to constantly revise fMRI data processing

and analysis choices and their influence on statistical inference (Botvinik-Nezer et al., 2020;

Poldrack et al., 2017) and b) to collect, gather and curate large open access

datasets/databases to establish reusable data and coordinated collaborations (DuPre et al.,

2020; Eickhoff et al., 2016; W. Liu et al., 2017; Madan, 2017; Poldrack & Gorgolewski, 2014;

Tardif et al., 2016; Van Horn & Gazzaniga, 2013). Such large datasets help to increase study

samples and thereby power, which helps detecting true effects while avoiding false positives

(see for more on statistical power: Cohen, 1992). Power can also be increased with the help

of higher data quality and increased recording times – for example, to up to 20-30 mins,

combining different measures when calculating connectivity (X. N. Zuo et al., 2019), or more

recent sampling approaches such as multi-echo sequences (Lynch et al., 2020). If new data

are to be collected, a sensible step to calculate and justify sample sizes is a priori power

analysis, which has only recently been adapted to neuroscience (Poldrack et al., 2017). After

the results are known, reporting both corrected and uncorrected values supports

transparency and balances type 1 and 2 error rates (Poldrack et al., 2017). A type 1 error,

also false positive, refers to the rejection of the null hypothesis although it is true. Type 2

errors, or false negatives, refer to the wrongful claim that the null hypothesis is true

although it is not. The choice of α- and β-levels influence type 1 and 2 error rates,

respectively.

Additionally, recommended practices for achieving a more reliable neuroimaging

findings include avoiding or at least minimizing the following; i) noise induced by weak

experimental design and data processing methods (X. N. Zuo & Xing, 2014), ii) the usage of

specific error-prone analytical methods (Eklund et al., 2016) and variations of analytical

choices (Botvinik-Nezer et al., 2020). In that sense, it has been expressed that rs-fMRI needs

better de-noising and analysis techniques (O'Connor & Zeffiro, 2019). Finally, iii) QRPs

(Poldrack et al., 2017), and iv) a lack of control for error and multiple comparison should be

avoided (C. Bennett et al., 2009; Eklund et al., 2016; Loring et al., 2002; Woo et al., 2014).

v) Using such techniques, code, and reporting in a standardised fashion would increase

reliability (Botvinik-Nezer et al., 2020; Nichols et al., 2017; Poldrack et al., 2017).

While there seems to be a good understanding on how to improve fMRI reliability at

different frontiers, as outlined above, the contribution of individual differences to BOLD

signal fluctuations are unclear. It is established that a large number of exogenous and

endogenous factors affect both within- and between-subjects BOLD signal variability

(Appendix I) Some studies suggest only small within-subject rs-FC fluctuations when

scanning the same individual(s) repeatedly (Gordon et al., 2017; Poldrack et al., 2015).

Moreover, individual differences from group-level network organisation or "network variants"

seem to be constant, suggesting to be trait-like characteristics of rs-FC (Seitzman et al.,

2019). However, there are still many influential factors to be discovered. This urges further

investigation, not only by asking which factors influence the BOLD signal, but also under

which conditions (Specht, 2020).

Although at different pace across countries, world population is experiencing an

ongoing longevity revolution, meaning that the share of older adults across societies is

increasing (United Nations, 2019). Ageing and individual differences connected to it is a

universal phenomenon pressing the importance to understand underlying mechanisms of the

brain in healthy and pathological ageing. Ageing leads to structural cerebral changes, but

how these relate to functional variability remains unclear. Hence, this study will explore

effects of age-related structural cerebral changes on EC in a well-powered study. To ensure

the use of the findings for the broader scientific community, all materials, data, and code are

openly available at https://osf.io/9bax3/ to maximise reproducibility and replicability.

Project Overview

This project set out to answer the questions: 'what are general associations between cortical thickness, chronological age and effective connectivity?', and 'how does grey matter lateralisation influence effective connectivity during healthy ageing?'. Answering these questions helps to provide a range of insights into whether cortical thickness and chronological age, as well as lateralisation are important to consider when drawing inferences about effective connectivity and other forms of BOLD-signal derived data from resting-state fMRI in healthy ageing. The relationship between structural measures such as cortical thickness and measures of connectivity can help modelling healthy ageing and explain age-related cognitive changes and decline. Moreover, as ageing is a human universal, it is a factor which cannot be circumvented when testing participants. A better understanding and control of ageing effects can help to improve data processing and interpretability. In accordance with previous findings, we formulated the following preregistered[5] hypotheses:

- **H$_1$** Regional cortical thickness is positively associated with regional effective connectivity.

- **H$_{2a}$** Older subjects have a lower within large-scale network effective connectivity than younger subjects.

---

[5] Find the preregistration at https://osf.io/mysrp.

- **H₂ᵦ** Older subjects have a higher between large-scale network (DMN and CEN) effective connectivity than younger subjects.

- **H₃** cortical thickness is over time a better predictor of effective connectivity than chronological age.

- **H₄** Individuals' cortical thickness lateralisation and chronological age predict effective connectivity lateralisation.

    - **H₄ₐ** Left-lateralised cortical thickness predicts left-lateralised effective connectivity

    - **H₄ᵦ** Right-lateralised cortical thickness predicts right-lateralised effective connectivity

The analyses focus on DMN and CEN as those networks have not only been found to be influenced by ageing, and have been connected to different ageing-related behavioural changes (such as cognitive decline), but are also likely influenced by the mainly frontal grey matter de-assymetrisation, which represent major parts of both DMN and CEN (Roe et al., 2021). If cortical thickness and/or chronological age are reliable predictors in a model explaining effective connectivity, they should be considered in future fMRI studies to increase the findings' robustness and reliability when observing individuals of different age groups. In case a strong predictor for EC can be identified, it might serve as biomarker for both healthy and pathological ageing. Furthermore, the results help to interpret ageing-dependent changes in cortical thickness asymmetries and extend previous findings on the asymmetric ageing brain by Roe and colleagues (2021). Evidence on the relationship between cortical thickness and effective connectivity is still sparse, and this study will

advance the literature with novel insights from a large-scale longitudinal sample.

Finally, this research will help to better understand general dynamics of the healthily ageing

brain.

Methods

Participants

For the original data collection in Umeå, the BETULA Project received local IRB approval. Data for the current project were provided by the BETULA project team after an ethics approval was obtained from the BETULA steering committee. The BETULA Project is a longitudinal study focussed on healthy ageing, memory and dementia in Sweden lead by Prof. Nyberg from Umeå University (Nilsson et al., 1997, 2004). For the purposes of this project, the data from T_5 (2008-2010) and T_6 (2013-2014) were used.

There were 375 participants at T_5, and 233 at T_6. Due to technical errors and/or severe motion during scanning, corrupted data or not coming back for the re-test led to the reduced participant number at T_6. Participants with more than 5% of missing resting-state fMRI data were excluded from the analysis.

The final sample resulted in 227 participants with functional and structural MRI scans from two independent occasions with approximately 4 years in between. At the first point of data collection, participants were at least 25 years old and Swedish native speakers. Information on age was available as cohort membership, with each cohort spanning 5 years. Based on this information, the age ranged from 25 to 80 years ($M = 46.7$, $Mdn = 45$, $SD= 9.71$). Additionally, the age ranged from 25 to 80 years ($M = 46.7$, $Mdn = 45$, $SD= 9.72$) at T_5 and from 25 to 80 years ($M = 46.7$, $Mdn = 45$, $SD= 9.72$) at T_6. For the purpose of this study, participants were divided into two age group via a median split ($Mdn = 45$ years). That resulted in a younger group with $n = 122$ ($M = 39.47$, $SD = 5.51$, $Mdn =40$, $min = 25$,

$max = 45$ years) and an older group with $n = 105$ ($M = 55.1$, $SD = 6.11$, $Mdn = 55$, $min = 50$, $max = 80$ years).

Procedure

Full procedure of the BETULA study can be found in Salami et al (2014). Importantly for this study, participants were screened for neurological pathology, dementia, and auditory or visual impairment, and excluded when any of the mentioned were present. Rs-fMRI were acquired as part of several scans. All participants' rs-fMRI were acquired over a 6-minutes period during which participants were asked to look at a fixation cross after acquiring structural MRI (Salami et al., 2014).

Data Acquisition

Images were acquired at Umeå University, Sweden with a 3-T General Electric scanner equipped with a 32-channel head coil (Salami et al., 2014). A gradient echo-planar imaging (ECI) sequence (37 transaxial slices, thickness: $3.4 \, \text{mm}$, gap $= 0.5 \, \text{mm}$, TR $= 2000 \, \text{ms}$, TE $= 30 \, \text{ms}$, flip angle: $80°$, field of view: $25 \times 25 \, \text{cm}$, 170 volumes) was used for rs-fMRI acquisition (Gorbach et al., 2020). Ten dummy scans were collected and discarded before experimental image acquisition (Salami et al., 2014). High-resolution T_1-weighted structural images were collected with a 3D fast spoiled gradient EPI sequence (180 slices; thickness $= 1 \, \text{mm}$; TR $= 8.2 \, \text{ms}$; TE $= 3.2 \, \text{ms}$; flip angle $= 12°$; field of view: $25 \times 25 \, \text{cm}$) (Salami et al., 2014).

Image Processing

Data were pre-processed in the MATLAB package SPM12. First, the slice-timing correction was applied, using the temporal middle slice (number 2) as reference image. Data

were then realigned and un-warped and the additionally estimated mean images across the

time series served as reference image for the co-registration with the structural T1 image. In

the following step, this co-registered structural image was segmented and subsequently all

volumes were normalised into MNI space using deformation fields, which was estimated

during the segmentation procedure (probability maps for grey matter, white matter,

cerebrospinal fluid, and other organics). The images were smoothed using a Gaussian kernel

of 6x6x6 mm^3 and finally two Generalized Linear Models applied regressing out the effects of

movement, white matter and cerebrospinal fluid.

Research Design

A repeated measures design was used to investigate the relationship between cortical

thickness and effective connectivity. A 2 x 2 mixed design was used to look at differences in

EC between younger and older adults and their cortical thickness comparing T_5 and T_6. The

same mixed designs were used to investigate whether biological age (estimated as grey

matter probabilities) or chronological age are better predictors of EC changes, and whether

there are differences in EC between people with either primarily left-, right, or bi-laterally

leaning grey matter probabilities. Observed variables were grey matter probability values for

each ROI (8 in total), chronological age (recorded as cohort membership), effective

connectivity values for each node and between nodes (64 in total), as well as the

lateralization of grey matter probability values calculated by the Laterality Index

[LI = (L - R) / (L + R]. For the Laterality index, L has been specified as volume of the

specified left region and R as the volume of the specified right region (e.g., Esteves et al.,

2017). Here, we used grey matter probability instead of volume. A negative LI indicates a

higher probability in the right hemisphere, and a positive LI indicates a higher probability in

the left hemisphere in the specific ROI. When applying the LI formula, we defined the

specific region, for example Left Dorsolateral Prefrontal Cortex of the CEN as Left and the

right counterpart, Right Anterior Prefrontal Cortex of the CEN, as Right (see Table 1).

Cortical thickness and chronological age could be read out directly as a numeric value from

the BETULA database. EC was extracted using DCM, and the grey matter probability

values were calculated from the segmented T1-weighted images.

Selection of Regions of Interest

ROIs were selected based on the surface areas which are mostly affected by

asymmetric grey matter loss as reported by Roe and colleagues (2021) for their BETULA

sample (Figure 1A). These regions focus largely on frontal regions making the examination of

DMN and CEN particularly promising (e.g., as reported in Yeo et al, 2011; Figure 1B), as

those share main nodes with the most affected areas by grey matter loss reported by Roe et

al. (2021). Additionally, DMN and CEN connectivity have previously been reported to be

affected by ageing (e.g., Bittencourt-Villalpando et al., 2021).

Establishing statistically informed ROIs required combining the grey matter

thickness-informed, structural regions identified by Roe et al.'s (2021) with functional

mapping of intrinsic networks. An established atlas has been provided by Yeo et al. (2011)

and was applied here as a mask on the surface maps developed by Roe et al.'s (2021).

Freesurfer (Fischl, 2012) was used to identify the regions, as depicted in Figure 1C and 1D.

From these, the largest symmetric clusters for anterior and posterior DMN and CEN were

selected (see appendices A to D for full overview of clusters by regions and hemisphere),

resulting in 8 ROIs for DCM (Table 1).

Table 1. Regions of Interest for the Dynamic Causal Modelling selected by cluster size

Node Position	Region	Cluster Size (mm²)	MNI Coordinates		
			x	y	z
Anterior DMN	Left Dorsolateral Prefrontal Cortex (ldPFC)	233.32	-40.2	47.2	3.7
Anterior DMN	Right Anterior Prefrontal Cortex (raPFC)	210.73	40.1	46	5.7
Posterior DMN	Left Precuneus (lPC)	87.11	-42.9	-54.5	36.5
Posterior DMN	Right Precuneus (rPC)	85.06	41.4	-51.9	40.8
Anterior CEN	Left Prefrontal Cortex (lPFC)	1742.43	-7.1	54.2	30.3
Anterior CEN	Right Prefrontal Cortex (rPFC)	1678.16	6.8	52.2	31.6
Posterior CEN	Left Medial Temporal Gyrus (lmTG)	961.66	-64	-17.7	-16.8
Posterior CEN	Right Medial Temporal Gyrus (rmTG)	857.31	62.4	-16.3	-15.4

Figure 1. Identification of Regions of Interest by Combing Surface with Connectivity Maps
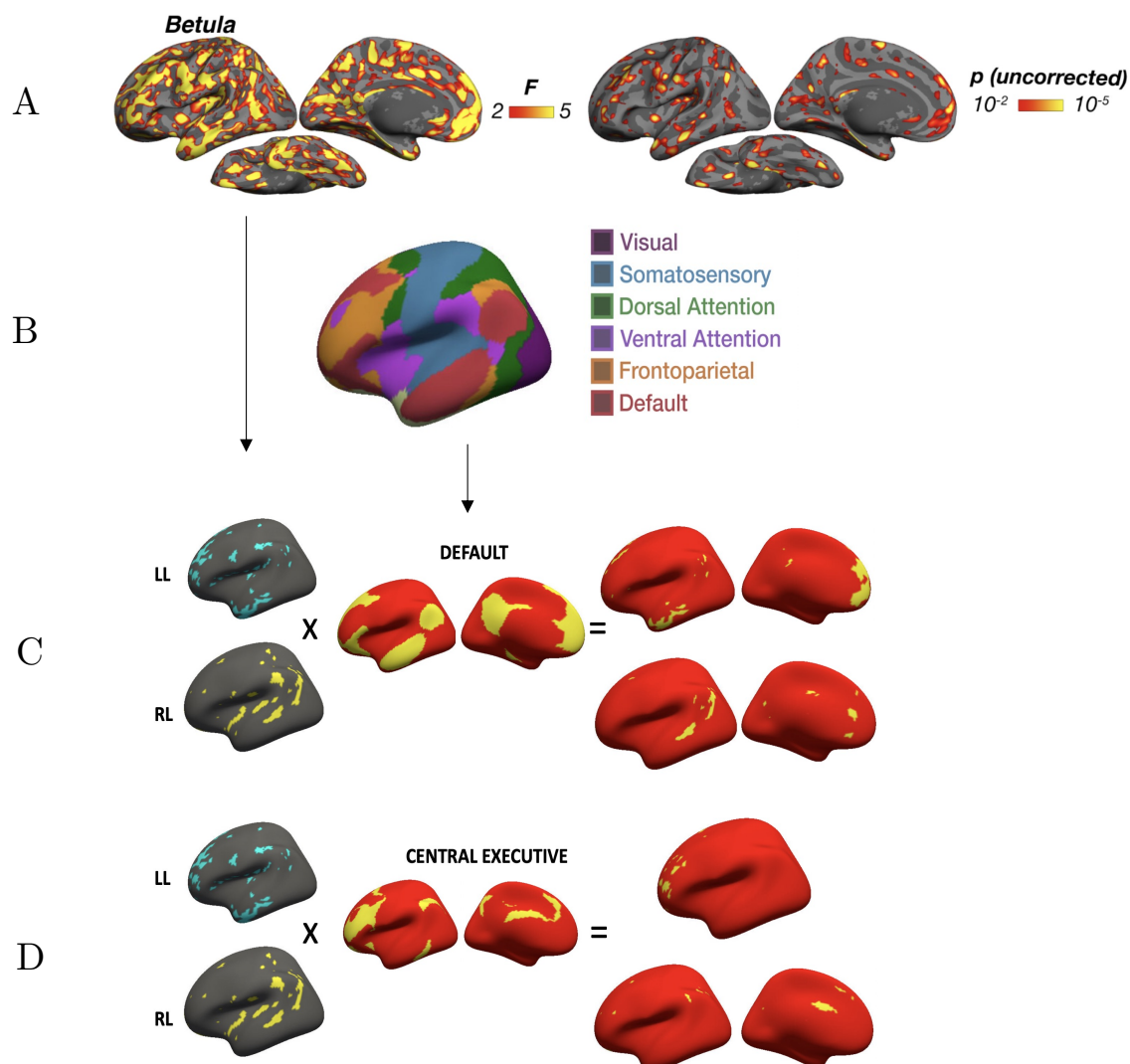
LL-leftwards grey matter loss. RL-rightwards grey matter loss. Default: Default Mode Network, Central Executive: Central Executive Network. A) Age-dependent grey matter asymmetry changes conjunction maps identified by Roe et al. (2021) - supplementary Fig. 6). B) Seven intrinsic network parcellation by Yeo et al. (2011). C) Overlaying Roe et al.'s (2021) surface maps with the Yeo et al.'s (2011) locations of the Default Mode Network. D) Overlaying Roe et al.'s (2021) surface maps with the Yeo et al.'s (2011) locations of the Central Executive Network.

Analyses

A first-level analysis was conducted using the SPM package (v2018) in MATLAB.

Namely, CSD-DCM was used, with the inverse Fourier transformation to calculate EC for all

possible connections within and between the ROIs (Zeidman, Jafarian, Corbin, et al., 2019).

ROIs are defined as DMN and CEN for each individual, with four central nodes for each of

the two networks, resulting in a total of eight nodes (Table 1). Hence, a total of sixty-four

possible connections were assumed as priors for the DCM, which used the data from 454

fMRI acquisitions, representing two scanning occasions for each of the participants. The

outputs were sixty-four EC values for each of the $n = 227$ participants.

Departing from the preregistration, instead of voxel-based morphometry (VBM)

giving information about cortical thickness, Grey Matter Probability Values (GMPV) were

used to assess grey matter differences in two separate age groups (young versus old).

GMPVs are based on the probability of each voxel within the ROI being grey matter, based

on the signal intensity. Across voxels, this gives a representation of grey matter relative to

all other types of tissue (Narr et al., 2005). GMPVs were extracted for each ROI with the

MarsBaR toolbox for SPM12 (MATLAB) using the segmented voxels.

For group-level analyses, *first*, a Canonical Correlation Analysis (CCA) was used to

relate GMPVs to EC to examine whether local grey matter changes influence EC (H_1).

Executing bivariate correlations would result in 64 x 8 = 512 possible correlations, which

would be difficult to interpret. A suitable alternative is CCA, which is used to examine

relationships between two sets of variables (Hotelling, 1936). CCA allows to some extent to

reduce data dimensionality while keeping interpretability by forming latent

factors/dimensions from cross-covariance matrices (Hotelling, 1936). *Second,* mixed semi-parametric MANOVAs were conducted to test age differences in EC in five models: two for self-inhibitory and two for between nodes EC in DMN and CEN, and one for the connections between DMN and CEN (H_2). Models were organised in this way to allow network-specific inference while distinguishing self-inhibitory from between node EC and within from between network connections, allowing to answer H_{2a} and H_{2b}. *Third*, for each of the sixty-four EC values four GAMs were compared against each other examining whether biological age would be a better predictor of EC than chronological age (H_3). *Fourth*, Repeated Measures Correlations and GAMs were used to explore to which extend lateralised GMPVs (calculated with the help of the Laterality Index) could predict lateralised EC.

Additionally, different descriptive and explorative analyses are reported in the appendix to give a better understanding of the observed data supporting the interpretability of the results relevant to answering the hypotheses. Those include, *firstly*, a 2 (age group) x 2 (timepoint) mixed semi-parametric MANOVA on GMPVs testing whether there was atrophy of grey matter in the ROIs over time and differences between age groups. *Secondly*, Intraclass Correlations (ICC) were used to estimate test-retest reliability of EC values. *Thirdly*, repeated measures correlations between the eight GMPVs and *fourthly*, bilateral correlations of GMPV and EC at the eight nodes were used to describe grey matter across the brain and how GMPV and EC relate cross-hemispherically. Finally, exploratory GAMs were used to quantify how combined lateralised GMPVs could predict regular and lateralised EC values, which served to extend on the planned analyses, allowing for deeper insights. All

statistical analyses on SPM outputs were carried out with R v3.6 (R Core Team, 2017). All

code is available at https://osf.io/9bax3/.

Results

Grey Matter Probability Values (GMPV) and Effective Connectivity (EC) in Hz were calculated for each of the 8 ROIs (4 in the DMN and 4 in the CEN) at two timepoints (T_5 and T_6) in DCM. Additionally, DCM provided EC between the 8 nodes, accounting for 8 x 8 = 64 connections in total. While more positive self-inhibitory EC values indicate increased self-inhibition, negative between network EC values indicate inhibitory connections and positive excitatory connections, respectively (Zeidman, Jafarian, Corbin, et al., 2019). No data were missing.

For the factorial design, participants' chronological age, here defined as Cohort membership with 5-year range recorded at T_5 (see Figure 2), was used to establish a younger and older group establishing the between-subjects factor, and timepoint (T_5 and T_6) the within-subjects factor[6], respectively.

Figure 2. Participants' Age Distribution Based on Cohorts Defined at T_5

---
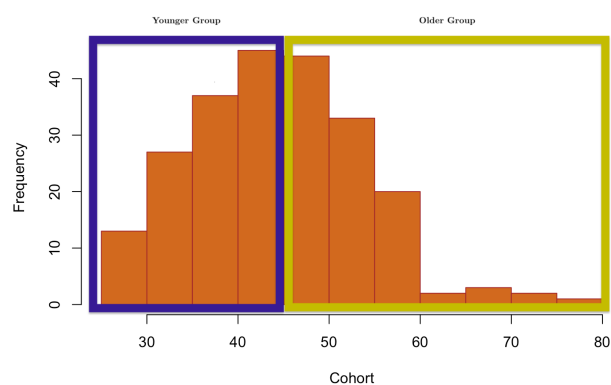
[6] For descriptive statistics of GMPVs and self-inhibitory EC at T_5 and T_6 see Appendix J. For exploratory repeated measures correlations of GMPVs see Appendix E.

Sensitivity Analyses

Using the pwr package in R (Champely et al., 2020), a sensitivity analysis using the smallest sample size of $n = 105$ defining the older group of adults aged older than 45, with α $= .05$ and $\beta = .80$ (power) revealed that the smallest detectable effects to be $r = 0.27$ for correlations, $d = 0.37$ for t-tests (with $n_1 = 122$, $n_2 = 105$ after median-split comparing the older and younger groups). An $n = 227$ with the same parameters results in $f^2 = 0.07$ for Generalized Linear Models (GLM) with 8 predictors, and $f^2 = 0.13$ for One-way ANOVAs.

When aiming for $\beta = .95$ and keeping the other parameters as described above, the minimal detectable effects are $r = 0.34$ for correlations, $d = 0.48$ for t-tests (with $n_1 = 122$, $n_2 = 105$ after median-split), $f^2 = 0.1$ for GLMs with 8 predictors, and $f^2 = 0.13$ for One-way ANOVAs. The power curve for a 2x2 ANOVA indicates that at $\alpha = .05$, with the current smallest group size of $n = 105$, the minimal detectable effect size is at $f^2 = 0.09$ when aiming for $\beta = 80\%$ power (Figure 3; see Appendix G for additional power simulations).

Figure 3. Power Curve for 2 x 2 ANOVA with the Smallest Group Being $n = 105$
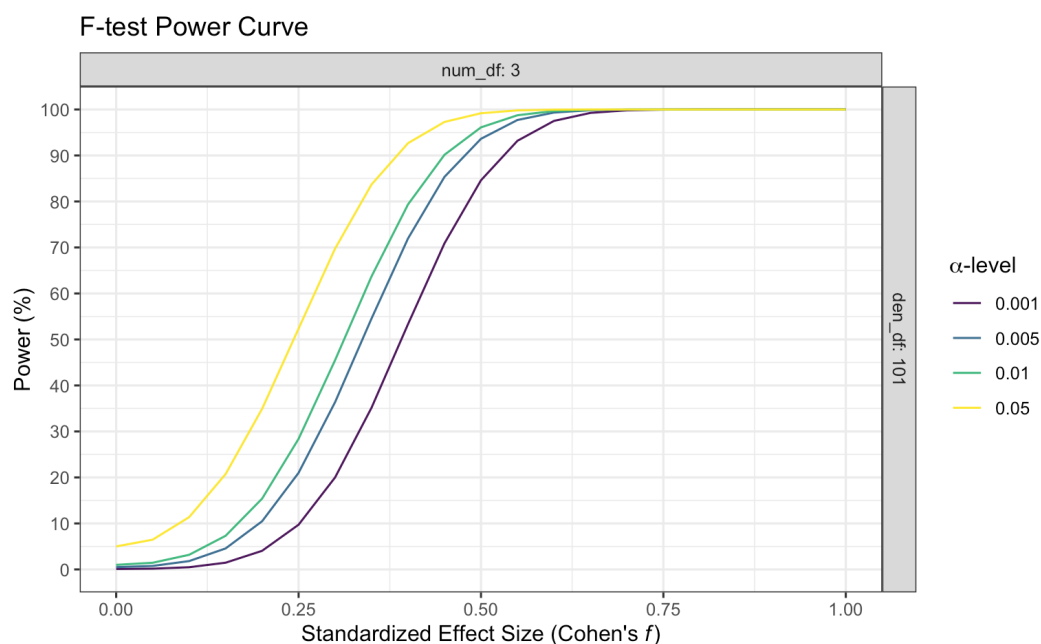
H_1: The Relationship between Grey Matter Probability Values (GMPV) and Effective Connectivity (EC)

Table 2. Test of Canonical Dimensions for Grey Matter Probability, Effective Connectivity, Timepoint and Cohort

Dimension	Canonical Multiple Correlation r	F	df1	df2	p value
1	0.79	1.33	585	3414.79	$<.0001$
2	0.71	1.21	567	3045.29	.002

To test the relationship between GMPVs and EC, CCA was used on all data. This included GMPVs, all (self-inhibitory and between-nodes) EC values, timepoint and cohort membership, resulting in two statistically significant dimensions (see Table 2).

Table 3. Grey Matter Probability and Self-Inhibitory Effective Connectivity Values as Standardized Canonical Coefficients on the Two Canonical Dimensions

CEN	Dimension		DMN	Dimension	
	1	2		1	2
lPFC GMPV	-0.48	-0.17	ldPFC GMPV	-0.42	0.57
rPFC GMPV	0.22	-0.16	raPFC GMPV	0.29	0.43
lmTG GMPV	0.56	-0.54	lPC GMPV	0.11	-0.45
rmTG GMPV	-0.03	-0.04	rPC GMPV	-0.69	-0.03
lPFC EC	0.05	-0.45	ldPFC EC	-0.27	0.00
rPFC EC	-0.29	0.37	raPFC EC	0.02	-0.21
lmTG EC	-0.22	-0.10	lPC EC	0.23	0.17
rmTG EC	0.24	0.04	rPC EC	0.27	-0.09

Note: Not all CCA coefficients are included in this table; only GMPVs and self-inhibitory EC values. For a full overview of all coefficients see Appendix F: grouped by connections within the DMN (Appendix F.1), within the CEN (Appendix F.2), and between DMN and CEN (Appendix F.3).

Suggested by the loadings of the GMPVs on the two dimensions (Table 3), these two dimensions can for example be interpreted as reflecting CEN (dimension 1) and DMN

(dimension 2). However, the standardised coefficients reflect the clustering onto the CEN and DMN dimensions only partly. Therefore, the relationship between EC and GMPV and H_1 cannot be rejected.

H_2: Effective Connectivity in Younger Compared to Older Subjects

To test whether younger subjects differ from older subjects in their EC (H_2), five mixed 2 (age group: younger vs older sub-sample) x 2 (timepoint: T_5 vs T_6) semi-parametric or modified MANOVA-type models were run. Model 1 tested self-inhibitory connections within CEN. Model 2 tested self-inhibitory connections within DMN. Model 3 tested between-node connections within CEN, model 4 between-node connections within DMN, and model 5 between CEN and DMN. See Figure 4 for an overview of EC connections which differed significantly from zero in each of the four cells. Model 1 observing self-inhibitory CEN EC at the network's four nodes (lPFC, rPFC, lmTG, rmTG) showed a significant effect of age $F(4, 227) = 10.97$, $p = .037$, but not of timepoint $p = .11$ or the timepoint-age interaction $p = .70$. For model 2 observing self-inhibitory DMN EC at the network's four nodes (ldPFC, raPFC, lPC, rPC) there were no significant effects of age ($p = .99$), timepoint ($p = .12$), or age-timepoint interactions ($p = .10$). Model 3 observing CEN EC at all of the network's possible twelve between node connections, showed a significant effect of timepoint $F(12, 227) = 33.71$, $p = .005$, but no effect of age ($p = .61$), or the time-age interaction ($p = .25$). Model 4 observing DMN EC at all of the possible twelve between node connections, showed no significant effects of timepoint ($p = .31$), age ($p = .06$), or their interaction ($p = .89$), and model 5 observing DMN-CEN EC showed a significant main effect of timepoint

$F(32, 227) = 63.25$, $p = .006$, but not for age ($p = .32$), or the age-timepoint interaction ($p = .83$).

Bonferroni-corrected univariate Mann Whitney post-hoc comparisons for age-group differences in EC found a significant difference in lPFC EC between the younger ($Mdn = -0.09$) and older ($Mdn = -0.007$) subsamples, $U = 21994$, $p = .036$, $r = 0.12$, 95% CI [0.03, 0.21]. No other post-hoc comparisons for age-effects were significant.

Figure 4. Effective Connectivity by Age Group and Timepoint Different from Zero
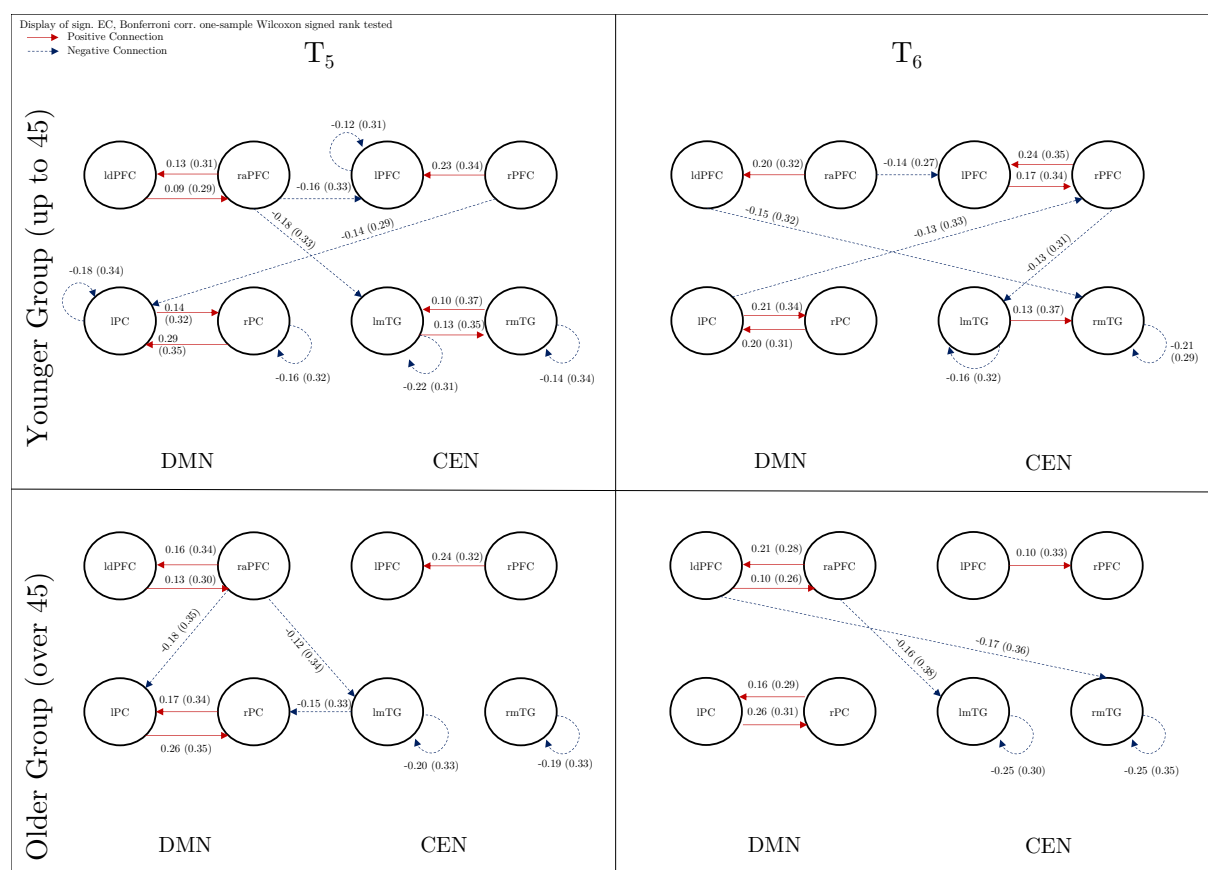
Results of 228 Bonferroni-corrected Wilcoxon one-sample signed rank tests, leaving out non-significant EC values. Negative between-node EC values indicate inhibitory connections, positive values excitatory connections. Self-inhibitory connections show increased inhibition for more positive values.

Note: This is a descriptive figure to visualise data not used to test any hypothesis.

Bonferroni-corrected univariate Mann Whitney post-hoc comparisons for timepoint differences in EC revealed a significant increase in inhibitory EC in the ldPFC to rmTG connection from T_5 (Mdn = -0.032) to T_6 (Mdn = -0.138), $U = 16343$, $p = .026$, $r = 0.23$, 95% CI [0.10, 0.35], and a significant change in EC in the rPFC to lPC connection from inhibitory EC at T_5 (Mdn = -0.091) to excitatory EC at T_6 (Mdn = 0.008), $U = 9400$, $p = .016$, $r = 0.24$, 95% CI [0.11, 0.36]. No other post-hoc comparisons for age-effects were significant. The age-group difference in lPFC EC was as predicted by H_{2a}, yet the effect size was below the detectable range (see Sensitivity Analysis section) and can be labelled a false positive. No other differences were observed and H_{2a} could be rejected. Timepoint/ageing effects in ldPFC to rmTG and rPFC to lPC connections were as predicted by H_{2b} (and correlation tests sufficiently powered: for $n = 227$, $\alpha = .05$, $\beta = .80$, $r_{min} = .185$), supporting H_{2b} for the ldPFC to rmTG connection, but not rPFC to lPC EC, which does overall not allow to answer H_{2b} conclusively.

H_3: Grey Matter Probability Values and Age as Predictors of Effective Connectivity

GMPVs were used as a proxy for biological age (for more detail on group differences in GMPV see Appendix J) and age-cohort membership for chronological age, serving both as predictors for Effective Connectivity (EC). As the data were non-normal, indicated by Shapiro-Wilk's tests and QQ-Plots, linear models were selected only for control purposes. Instead generalized additive models (GAM) were used to predict EC from GMPVs and age in five different models for each of the possible sixty-four connections, allowing models which better fit the data. The first model was the null model containing only timepoint (T) as a

$$\text{Model 0: EC} = \beta_0 + T + \varepsilon,\ \varepsilon \sim N(0,\ \sigma^2) \tag{1}$$

$$\text{Model 1: EC} = \beta_0 + T + f(age) + \varepsilon,\ \varepsilon \sim N(0,\ \sigma^2) \tag{2}$$

$$\text{Model 2: EC} = \beta_0 + T + f(GM_1) + \ldots + f(GM_8) + f(age) + \varepsilon,\ \varepsilon \sim N(0,\ \sigma^2) \tag{3}$$

$$\text{Model 3: EC} = \beta_0 + T + f(GM_1) + \ldots + f(GM_8) + \varepsilon,\ \varepsilon \sim N(0,\ \sigma^2) \tag{4}$$

$$\text{Model 4: EC} = \beta_0 + T + (GM_1)\beta_1 + \ldots + (GM_8)\beta_8 + (age)\beta_9 + \varepsilon,\ \varepsilon \sim N(0,\ \sigma^2) \tag{5}$$

T: timepoint, GM: grey matter probability values, age: cohort membership

predictor (Equation 1). In model 1, age was added as a predictor (Equation 2), and model 2 GMPVs, respectively, forming the full model (Equation 3). In model 3 age was subtracted from the full model (Equation 4). Finally, model 4 was a linear equivalent to the full GAM, used to control whether a linear model was the better fit (Equation 5). The difference between models 0-3 and 4 (Equations 1-5 below) are the smoothing functions f(x), which allow for to fit the model to non-linear data/trends. As H_3 predicted biological age to be a better predictor of EC, model 1 only contained GMPVs and model 4 only age as predictors. GAM smoothing parameters were determined using unbiased risk estimation (UBRE) based on the mean square error. Analyses of Deviance (AoD) were used to test the GAMs against each other and the Akaike Information Criterion (AIC) and R^2_{adj} to compare model fit across all models.

The null model's (Equation 1) *Mdn R^2_{adj}* = -0.001 % of the variance in the between-nodes EC values and *Mdn R^2_{adj}* = .70% of the variance in self-inhibitory nodes. Model 1 (Equation 2) including chronological age and timepoint explained *Mdn R^2_{adj}* = 3.03% of the variance in the between-nodes EC values and *Mdn R^2_{adj}* = 1.73% of the variance in self-inhibitory nodes. The full model (Equation 3) explained *Mdn R^2_{adj}* = 4.31% of the variance in the between-nodes EC values and *Mdn R^2_{adj}* = 4.77% of the variance in self-inhibitory

nodes. Yet, when comparing the models, most of the best fitting models were the grey-matter-only models (Equation 4), which explained $Mdn\ R^2_{adj} = 3.97\%$ of the variance in the

Figure 5. Box and Violin Plots of R^2_{adj} Values for the Five Models Explaining EC Across

Between-Nodes and Self-Inhibitory Connections from Timepoint, Age, and GMPVs
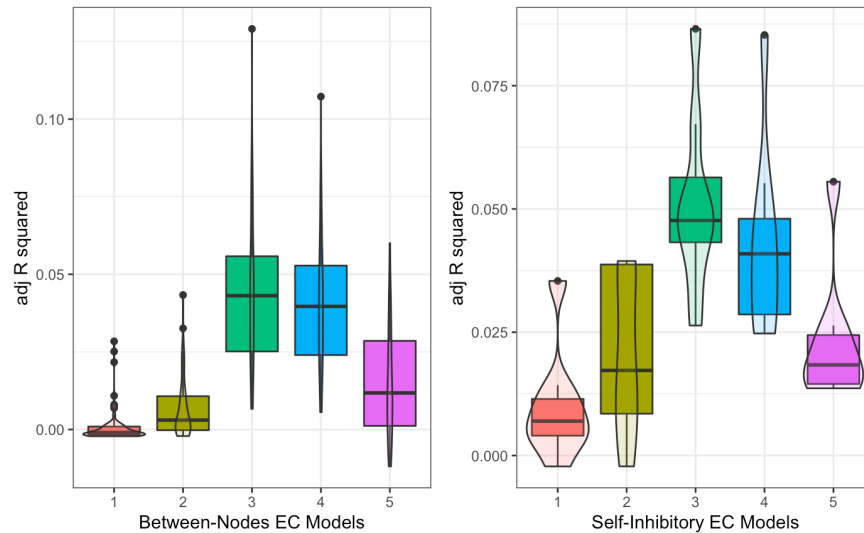
between-nodes EC values and $Mdn\ R^2_{adj} = 4.09\%$ of the variance in self-inhibitory nodes.

Finally, generally, the linear control models (Equation 5) explained less of the variance in

the between-nodes EC values $Mdn\ R^2_{adj} = 1.18\%$ and in self-inhibitory nodes $Mdn\ R^2_{adj} = 1.84\%$ than models 2 and 3. Full information on model comparisons and predictors can be

found in Appendix M. The data support H_3 that biological age is a better predictor of EC

than chronological age.

H_4: Lateralised Grey Matter Probability and Effective Connectivity

The GMPV Laterality Index (LI) was calculated to establish anterior and posterior

lateralised GMPVs for CEN and DMN using the eight GMPV values, and twenty-four

monohemispheric between-nodes values as well as eight self-inhibitory EC values. To avoid

confounded results from negative denominators, we adapted the LI formula as suggested

by Seghier (2008) to LI = (L-R)/(|L|+|R|), with L and R indicating the values for the respective hemispheres. A total of four lateralised GMPVs and sixteen lateralised EC resulted which were related to each other in 4x16 repeated measures correlations. After Bonferroni correction for multiple testing ($\alpha/64$), the correlation between lateralized anterior DMN GMPVs and the connection between lateralized EC from DMN PFC to CEN mTG was marginally significant r_{rm} = -0.22, 95% CI [-0.34, -0.09], p = .058; and significant between lateralized posterior DMN GMPVs and Precuneus to CEN PFC lateralised EC, r_{rm} = 0.23, 95% CI [0.10, 0.35], p = .039. No other correlations were significant. These results do not allow for final conclusions about H_4.[7]

---

[7] Different exploratory follow-up analyses can be found in the appendices: Appendix K for exploratory Spearman's correlations between bilateral pairs of GMPVs and ECs; Appendix N for exploratory GAMs of the sixty-four ECs modelled by lateralized GMPVs; Appendix P for GAMs explaining lateralized EC from the lateralized GMPVs.

Discussion

The aim of this study was to investigate the influence of grey matter loss on effective connectivity in an ageing sample. Canonical correlations indicated that there was a meaningful relationship between EC and GMPVs explained by two dimensions, which can be interpreted as the observed networks, CEN and DMN. When grouping participants into older and younger groups, an effect of age-group was found for self-inhibitory CEN EC and an effect of ageing for within CEN and between DMN and CEN EC. Yet, univariate tests showed this effect to be limited to between DMN and CEN EC: ldPFC to rmTG and rPFC to lPC. Moreover, GMPVs were shown to be better predictors of EC than chronological age. Modelling GMPV lateralisation effects on the lateralisation of EC via repeated measures correlations, using the Laterality Index, resulted in two significant correlations. First, a negative relationship was found between lateralized anterior DMN GMPVs and the lateralized EC connection from DMN PFC to CEN mTG. Second, a positive relationship was revealed between lateralized posterior DMN GMPVs and Precuneus to CEN PFC lateralised EC. The results' implications are discussed by firstly revising the GMPV-EC relationship and secondly, the relationship between age, ageing, GMPV lateralisation and EC. Thirdly, limitations are discussed with a focus on EC reliability and study design. Finally, future directions for follow-up and extension studies are being provided.

The Relationship Between Grey Matter and Effective Connectivity

Several studies suggest there is a relationship between grey matter properties, such as thickness, and FC (Huntenburg et al., 2017; Tsvetanov, Gazzina, et al., 2020), and that ageing has an effect on this relationship (Fjell et al., 2017; Romero-Garcia et al., 2014).

However, the dynamics of the interplay between structure and function during ageing are yet unclear (Fjell et al., 2017; N. Luo et al., 2020; Zimmermann et al., 2016). In some cases, no connection between specific grey matter properties and connectivity could be found, for example, for grey matter thickness and FC (Tsang et al., 2017). Moreover, FC-SC relationships cannot be generalized to EC and the evidence on the EC-grey matter relationship is limited. There is a general consensus that the brain can be described with the help of interacting structural and functional networks (Batista-García-Ramó & Fernández-Verdecia, 2018), making the inclusion of SC into DCMs useful (Hahn et al., 2019; Sokolov et al., 2018). Yet, there are, to my knowledge, no studies on the relationship between EC and GMPVs or other grey matter measures for DMN and CEN.

In this study, a CCA showed that EC and GMPV data can be arranged in two dimensions, which can be interpreted as the two networks observed here, namely CEN and DMN. These networks have previously been defined as the main resting state networks and can be used to differentiate between task-active (CEN) and inactive (DMN) networks (Hugdahl et al., 2015) or default and extrinsic mode networks (Riemer et al., 2020). Interestingly, bivariate correlations of GMPVs and EC did not yield any significant relationships, suggesting multivariate dependencies. Hence, only when the contribution of grouped GMPVs is considered when explaining EC, the relationship between GMPVs and EC becomes visible, likely due to large intra-individual variations (Lo et al., 1995). GAMs showed that GMPVs could explain a small, yet significant proportion of EC variability across ECs. Additionally, GMPVs seemed to explain self-inhibitory EC better than between-node EC, which indicates local dependencies. Local dependencies seem also to be supported

by lateralized GMPVs explaining only a small proportion of the variance of lateralized EC, with single predictors responsible for most of the variance explained by models superior to the null model (Appendix O). One way of interpreting these results is that GMPVs are related to EC, but that there are mediators of this relationship which explain EC better, such as white matter tracts, which can be used to model SC (Zhijiang Wang et al., 2014). Most recent efforts investigating how structural features explain functional features of the brain focussed on white matter fibre tracts (see Jamalabadi et al., 2021). However, recent evidence shows that in addition to white matter tracts also grey matter density at the network nodes plays a role for SC (Jamalabadi et al., 2021). Moreover, different characteristics of grey matter can be related to white-matter-tract-based structural connectivity (Jamalabadi et al., 2021; Zhijiang Wang et al., 2014), which in turn can be related to EC (Furl, 2015) and FC (Damoiseaux & Greicius, 2009; Honey et al., 2009; Messé et al., 2015). While Jamalabadi and colleagues (2021) suggest that grey matter and white matter properties improve SC modelling, more research is needed to relate such models to EC or FC. Additionally, the combination of different structural and functional features serves better in predicting behaviour and disease than functional features on their own, forming another reason to further investigate structure-function relationships (Yao et al., 2021).

Age, Grey Matter Lateralisation and Effective Connectivity

In line with the current theory, that brain age is represented more accurately by biological properties than chronological age, we found that GMPVs predicted self-inhibitory EC better than chronological age (Cole et al., 2019). Dedifferentiation has been put forward

as a possible explanatory mechanism of ageing-specific changes in brain function (Goh, 2011). This has been specified by previous evidence for decreasing within network FC (Bagarinao et al., 2019, 2020; Varangis et al., 2019) but increasing between network FC (Damoiseaux, 2017; Goh, 2011; Grady et al., 2016; Hughes et al., 2020; Stumme et al., 2020). The detected lower within-network EC of the older compared to the younger group can be classified as a statistical artifact (type 1 error), based on the standard assumptions of minimal power being 80% and alpha = 0.05. Significant aging/timepoint-differences between network EC from ldPFC to rmTG and from rPFC to lPC provided mixed evidence for the assumption of increased between network connectivity. While the ldPFC to rmTG became more inhibitory, the rPFC to lPC connection was inhibitory at T_5 and became slightly excitatory at T_6 (yet statistically not different from 0). The reason for this mixed evidence might be, the lack of GMPV decrease over time. With a significant decrease of GMPVs over time, for example, when choosing longer inter-test intervals, also more EC changes might be expected. Another reason for the lack of observed effects might be that the MANOVAs on EC were underpowered. Power simulations based on randomly selected EC values indicated power below 80% (Appendix G). However, these simulations cannot be directly applied to the tests run, as different EC values were combined in the MANOVA models.

Focussing on lateralisation effects, the presented results are not conclusive. It is important to keep in mind that functional and grey matter asymmetries are not necessarily congruent with each other within the DMN (Saenger et al., 2012). Moreover, lateralised EC values are difficult to interpret. For example, a positive lateralised EC value can indicate more excitatory EC in the left compared to the right hemisphere, but also that there is more

inhibitory activity in the left compared to the right hemisphere. This is a function and problem of the laterality index equation (Seghier, 2008).

Only *one* positive repeated measures correlation was found indicating parallel lateralisation of grey matter and EC, namely between lateralized posterior DMN GMPVs and Precuneus to CEN PFC lateralised EC values. Considering that GMPVs did not significantly decrease over time, this finding is not necessarily surprising. However, opposing to the predictions in H_4, the second meaningful correlation, based on the correlation strength and approaching significance, indicated the opposite relationship. Such effect could be interpreted as the more "left lateralised" GMPVs, the more "right lateralised" EC. This provides rather no congruent evidence for bivariate relationship between local lateralised grey matter and lateralised EC (as proposed by Saenger et al., 2012). When further exploring multivariate relationships (Appendix O), by modelling lateralised EC from lateralised GMPVs and chronological age, in nearly all models there was one lateralised GMPV which explained a small proportion, but most of the variance within the models in lateralised EC, and none of the lateralised GMPVs served to predict CEN self-inhibitory lateralised EC. This indicates that this relationship depends to a certain extent on specific GMPV changes. Potentially, analysing larger GMPV volumes would help describing this relationship better. However, only a small proportion of variance in lateralised EC could be explained by lateralised GMPVs.

Furthermore, there were differences between CEN and DMN in self-inhibitory nodes and, for which it is likely, that the lateralized GMPVs lack explanatory power because the two networks differ in how they are functionally affected by structural changes during

healthy ageing (Appendix O). The academic literature suggests, that lateralization changes in resting state networks, such as the DMN (Banks et al., 2018). Additionally, lateralization of both DMN and CEN during ageing are influenced by further factors such as cognitive training (C. Luo et al., 2016). However, only recently a comprehensive taxonomy on functional lateralisation has been published (Karolis et al., 2019), and accordingly, a deeper understanding of the interplay between structural and functional lateralisation during healthy ageing is still lacking and requires further investigation.

Although GMPVs were generally the better predictors of EC than age, age was a still a significant predictor of EC in several of the GAMs. However, directionality of the influence of either age or GMPVs could not be generalized from the model predictors as there were no uniform trends. Ageing effects have been identified in the literature as global signal decrease (Garrett et al., 2017; Gaut et al., 2019; Grady & Garrett, 2014; Kumral et al., 2020; Z. Li et al., 2017; Nomi et al., 2017; Tsvetanov et al., 2015), and within network FC decrease (Bagarinao et al., 2019, 2020; Varangis et al., 2019) and between network FC increase (Damoiseaux, 2017; Goh, 2011; Grady et al., 2016; Hughes et al., 2020; Stumme et al., 2020). Here, we articulated the hypotheses following such trends in the literature in addition to grey matter loss could as a possible explanation of EC changes. Yet, we did not find any EC differences between age groups, however EC changes over time indicating ageing effects. Simultaneously, we found that GMPVs could explain a proportion of the variance in the different EC values, which indicates differential influence of regional GMPV on specific functional connections. Further research is needed unveiling the relationship of grey matter and other markers of brain structure and EC during healthy ageing.

Limitations

Low Effective Connectivity Reliability

Intra-class correlations values of EC were extremely low (ICC < .12, Appendix L), indicating that most of the variance was explained by within-individual effects (Noble et al., 2019). This is not the only example of low ICCs for EC values using DCM. Another study observed low cross-session correlations of EC in both Parkinson's patients and healthy controls during an action selection task is Rowe et al. (2010). As a comparison, global regression DCM, using the Human Connectome Project resting state data, EC ICCs were considerably lower (mean ICC = .24, 95% CI [-0.18 0.59]) than for the social cognition task (mean ICC = .42, 95% CI [-0.07 0.75]) (Frässle & Stephan, 2021). Such global estimates are higher than the local estimates provided in this study. The listed EC ICCs are coherent with test-retest calculations for FC from both rs-fMRI (Noble et al., 2019) and task-fMRI, which suggests a considerably small test-retest reliability (Elliott et al., 2020). Based on this, it is not surprising that group-level analyses of the presented EC data show diffuse patterns over time, are difficult to be clustered into meaningful dimensions, as attempted with CCAs, correlated with GMCVs (or other variables), or compared in single to multi-factorial design in any meaningful way. Specifically individual differences in ageing might contribute to decreased ICCs, given the trend of decreased EC stability at older ages (Tsvetanov et al., 2016). This explains in part why the presented models have only considerably small explanatory power (e.g., indicated by low R^2_{adj} values) for EC, and timepoint-dependent changes are problematic to trace (as test-retest reliability is low), making the interpretation of the results difficult.

Study Design

The inter-scanning interval might be crucial to reliably detect EC as well as EC changes. While a recent study has shown global rs-fMRI EC ICC to be poor with mean ICC = .24 with an unspecified inter-session, but below 4 years (Frässle & Stephan, 2021), the inter-session period of this study extends to 4 years. Short-term test-retests rs-fMRI studies showed higher ICCs, for example in children with and without attention-deficit/hyperactivity disorder (Somandepalli et al., 2015). Hence, the long time between scanning session might have led to low ICCs. Opposingly, reducing the time between scans might increase ICC values. Moreover, the presented low ICCs might indicate that resting state networks are not stable on a local level, even at key-network nodes, while global networks are kept relatively stable intra-individually (Poldrack et al., 2015).

On the other hand, one might also argue for longer inter-scan intervals. Diffuse and potentially non-linear relationships over time between grey matter volume and FC have also been found in pathological samples, such as Alzheimer's Disease (Serra et al., 2016). It is possible that longitudinal data needs to be sampled over longer periods than done here (potentially decades) for the full effects of grey-matter atrophy on brain function to become detectable (Serra et al., 2016). Here, we found a main effect of age-group but not of time-point or their interaction on GMPVs (Appendix J). This might indicate that the inter-sampling period was too short to detect grey matter loss and consequential EC changes. Another explanation could be that functional plasticity compensates for structural changes (Greenwood, 2007). In that case, even when increasing the inter-scan interval, no ageing-effects would be detected.

Additionally, the current DCM framework was limited to eight 6mm^3 spheres, which were defined based on the grey matter de-asymmetrisation hubs defined in Roe et al. (2021) and their overlay with the DMN and CEN defined by Yeo el al (2011). It is possible that these spheres were too small or numerically insufficient to model the respective networks appropriately. The selected spheres are only parts of the greater network regions (e.g., Precuneus in DMN), which might have exhibited excitatory or inhibitory activity at other locations within the same network which were not considered in the current analysis. In other words, the scale of observation is important and a good trade-off between local and global specificity (network vs whole brain) needs to be established on a study-to-study basis to allow for a well-fitting yet generalizable model (Hawkins, 2004).

Increasing the complexity of the current resting state network models by including more nodes and connections between nodes would increase the computations needed, potentially also the models' representativeness of multiconnected real brain networks. Arguing against more global analyses of the current data, GMPVs explained similar proportions of variance of both local/self-inhibiting and between nodes EC across models, while the CCA suggested only two dimensions. Therefore, increasing model-complexity by adding nodes and connections within the established networks (CEN and DMN) might help to better understand the underlying processes.

Future Directions

There are wide possibilities for collecting data, with the best solution being to introduce the same protocols to multiple labs allowing for large-scale data accumulations. Recording additional variables such as respiration and heart rate during scanning, indicators

of cardiovascular health, sleep, eating (and drinking) and activity habits, and scanning at

different (especially longer) intervals, to allow for short-term to long-term ICCs, can be a

starting point for future fMRI studies on ageing. Integrating task- and rs-fMRI, can help to

better capturing the connectivity changes as an in relationship to age-related processes

(Geerligs & Tsvetanov, 2017; Millar, Ances, et al., 2020). Additionally, for richer data a

multimodal data collection could be recommended, for instance a combination of fMRI with

other methods such as EEG or MEG, might allow to infer causal links between observed

changes and age (Jafarian et al., 2020). For both, existing and future data, explorative

analyses, including machine learning can add to predicting age, disease, or certain

behaviours.

Analyses of the brain structure-function relationships will still need to be expanded

and grey matter properties considered more on this equation. Also generally, there is more

research needed on the structure-function relationship, especially considering effective

connectivity. Adding grey matter properties to structural models predicting functional

properties seems promising in advancing our understanding of the relationships between

structure and function of the human brain (Jamalabadi et al., 2021).

Conclusion

Common findings from the literature suggesting i) biological age to be a better

predictor of connectivity than chronological age and ii) resting state networks organised as

DMN and CEN containing structure-function relationship could be replicated. The

relationships between both non-lateralised and lateralised GMPVs and EC was weak,

suggesting that, amongst structural features, grey matter might not be the best predictor of

EC in asymmetrically thinning areas. Combining grey matter with other structural features might be a solution to reach better predictions of connectivity, or to generally observe relationships between brain structure and function. Furthermore, the evidence for age and ageing differences in EC was weak. For a better understanding of brain structure-function relationships during ageing, further research is needed observing EC and the relationship between EC and grey matter during healthy and pathological ageing, as well as contributing and underlying mechanisms, such as plasticity.

References

Abdallah, C. G., Averill, C. L., Ramage, A. E., Averill, L. A., Goktas, S., Nemati, S.,

Krystal, J. H., Roache, J. D., Resick, P. A., Young-McCaughan, S., Peterson, A. L., &

Fox, P. (2019). Salience Network Disruption in U.S. Army Soldiers With Posttraumatic

Stress Disorder. *Chronic Stress*, *3*, 247054701985046.

https://doi.org/10.1177/2470547019850467

Abdelkarim, D., Zhao, Y., Turner, M. P., Sivakolundu, D. K., Lu, H., & Rypma, B. (2019).

A neural-vascular complex of age-related changes in the human brain: Anatomy,

physiology, and implications for neurocognitive aging. In *Neuroscience and

Biobehavioral Reviews* (Vol. 107, pp. 927–944). Elsevier Ltd.

https://doi.org/10.1016/j.neubiorev.2019.09.005

Addis, D. R., Leclerc, C. M., Muscatell, K. A., & Kensinger, E. A. (2010). There are age-

related changes in neural connectivity during the encoding of positive, but not negative,

information. *Cortex*, *46*(4), 425–433. https://doi.org/10.1016/j.cortex.2009.04.011

Agcaoglu, O., Miller, R., Mayer, A. R., Hugdahl, K., & Calhoun, V. D. (2015).

Lateralization of resting state networks and relationship to age and gender.

NeuroImage, *104*, 310–325. https://doi.org/10.1016/j.neuroimage.2014.09.001

Allen, E. A., Erhardt, E. B., Damaraju, E., Gruner, W., Segall, J. M., Silva, R. F., Havlicek,

M., Rachakonda, S., Fries, J., Kalyanam, R., Michael, A. M., Caprihan, A., Turner, J.

A., Eichele, T., Adelsheim, S., Bryan, A. D., Bustillo, J., Clark, V. P., Ewing, S. W. F.,

… Calhoun, V. D. (2011). A baseline for the multivariate comparison of resting-state

networks. *Frontiers in Systems Neuroscience*, *5*, 2.

https://doi.org/10.3389/fnsys.2011.00002

Anand, A., Li, Y., Wang, Y., Wu, J., Gao, S., Bukhari, L., Mathews, V. P., Kalnin, A., & Lowe, M. J. (2005). Antidepressant effect on connectivity of the mood-regulating circuit: An fMRI study. *Neuropsychopharmacology, 30*(7), 1334–1344. https://doi.org/10.1038/sj.npp.1300725

Andrews-Hanna, J. R., Snyder, A. Z., Vincent, J. L., Lustig, C., Head, D., Raichle, M. E. E., & Buckner, R. L. (2007). Disruption of Large-Scale Brain Systems in Advanced Aging. *Neuron, 56*(5), 924–935. https://doi.org/10.1016/j.neuron.2007.10.038

Attwell, D., Buchan, A. M., Charpak, S., Lauritzen, M., MacVicar, B. A., & Newman, E. A. (2010). Glial and neuronal control of brain blood flow. In *Nature* (Vol. 468, Issue 7321, pp. 232–243). Nature Publishing Group. https://doi.org/10.1038/nature09613

Aycheh, H. M., Seong, J. K., Shin, J. H., Na, D. L., Kang, B., Seo, S. W., & Sohn, K. A. (2018). Biological brain age prediction using cortical thickness data: A large scale cohort study. *Frontiers in Aging Neuroscience.* https://doi.org/10.3389/fnagi.2018.00252

Bagarinao, E., Watanabe, H., Maesawa, S., Mori, D., Hara, K., Kawabata, K., Yoneyama, N., Ohdake, R., Imai, K., Masuda, M., Yokoi, T., Ogura, A., Taoka, T., Koyama, S., Tanabe, H. C., Katsuno, M., Wakabayashi, T., Kuzuya, M., Hoshiyama, M., … Sobue, G. (2020). Aging Impacts the Overall Connectivity Strength of Regions Critical for Information Transfer Among Brain Networks. *Frontiers in Aging Neuroscience, 12*, 1– 14. https://doi.org/10.3389/fnagi.2020.592469

Bagarinao, E., Watanabe, H., Maesawa, S., Mori, D., Hara, K., Kawabata, K., Yoneyama,

N., Ohdake, R., Imai, K., Masuda, M., Yokoi, T., Ogura, A., Taoka, T., Koyama, S., Tanabe, H. C., Katsuno, M., Wakabayashi, T., Kuzuya, M., Ozaki, N., … Sobue, G. (2019). Reorganization of brain networks and its association with general cognitive performance over the adult lifespan. *Scientific Reports*, *9*(1), 1–15. https://doi.org/10.1038/s41598-019-47922-x

Baker, D. A., Ware, J. M., Schweitzer, N. J., & Risko, E. F. (2017). Making sense of research on the neuroimage bias. *Public Understanding of Science*, *26*(2), 251–258. https://doi.org/10.1177/0963662515604975

Banks, S. J., Zhuang, X., Bayram, E., Bird, C., Cordes, D., Caldwell, J. Z. K., Cummings, J. L., & Initiative, for the A. D. N. (2018). Default Mode Network Lateralization and Memory in Healthy Aging and Alzheimer's Disease. *Journal of Alzheimer's Disease*, *66*(3), 1223. https://doi.org/10.3233/JAD-180541

Barber, A. D., Hegarty, C. E., Lindquist, M., & Karlsgodt, K. H. (2021). Heritability of Functional Connectivity in Resting State: Assessment of the Dynamic Mean, Dynamic Variance, and Static Connectivity across Networks. *Cerebral Cortex*, *0*(0), 1–11. https://academic.oup.com/cercor/advance-article-abstract/doi/10.1093/cercor/bhaa391/6082827

Bashyam, V. M., Erus, G., Doshi, J., Habes, M., Nasralah, I., Truelove-Hill, M., Srinivasan, D., Mamourian, L., Pomponio, R., Fan, Y., Launer, L. J., Masters, C. L., Maruff, P., Zhuo, C., Völzke, H., Johnson, S. C., Fripp, J., Koutsouleris, N., Satterthwaite, T. D., … Davatzikos, C. (2020). MRI signatures of brain age and disease over the lifespan based on a deep brain network and 14 468 individuals worldwide. *Brain*, *143*(7), 2312–

2324. https://doi.org/10.1093/brain/awaa160

Bastin, C., Yakushev, I., Bahri, M. A., Fellgiebel, A., Eustache, F., Landeau, B., Scheurich, A., Feyers, D., Collette, F., Chételat, G., & Salmon, E. (2012). Cognitive reserve impacts on inter-individual variability in resting-state cerebral metabolism in normal aging. *NeuroImage*, *63*(2), 713–722. https://doi.org/10.1016/j.neuroimage.2012.06.074

Batista-García-Ramó, K., & Fernández-Verdecia, C. I. (2018). What We Know About the Brain Structure–Function Relationship. *Behavioral Sciences*, *8*(4). https://doi.org/10.3390/BS8040039

Beaty, R. E., Benedek, M., Barry Kaufman, S., & Silvia, P. J. (2015). Default and Executive Network Coupling Supports Creative Idea Production. *Scientific Reports*, *5*(1), 1–14. https://doi.org/10.1038/srep10964

Bennett, C., Baird, A. A., Miller, M., & Wolford, G. (2009). Neural correlates of interspecies perspective taking in the post-mortem Atlantic Salmon: an argument for multiple comparisons correction. *NeuroImage*, *47*(Suppl 1), 125. https://doi.org/10.1016/s1053-8119(09)71202-9

Bennett, C. M., & Miller, M. B. (2013). FMRI reliability: Influences of task and experimental design. *Cognitive, Affective and Behavioral Neuroscience*, *13*(4), 690–702. https://doi.org/10.3758/s13415-013-0195-1

Bethlehem, R. A. I., Paquola, C., Seidlitz, J., Ronan, L., Bernhardt, B., Consortium, C. C. A. N., & Tsvetanov, K. A. (2020). Dispersion of functional gradients across the adult lifespan. *NeuroImage*, *222*, 117299. https://doi.org/10.1016/j.neuroimage.2020.117299

Beul, S. F., Barbas, H., & Hilgetag, C. C. (2017). A Predictive Structural Model of the

Primate Connectome. *Scientific Reports*, *7*, 43176. https://doi.org/10.1038/srep43176

Biswal, B. B., Mennes, M., Zuo, X. N., Gohel, S., Kelly, C., Smith, S. M., Beckmann, C. F.,

   Adelstein, J. S., Buckner, R. L., Colcombe, S., Dogonowski, A. M., Ernst, M., Fair, D.,

   Hampson, M., Hoptman, M. J., Hyde, J. S., Kiviniemi, V. J., Kötter, R., Li, S. J., …

   Milham, M. P. (2010). Toward discovery science of human brain function. *Proceedings

   of the National Academy of Sciences of the United States of America*, *107*(10), 4734–

   4739. https://doi.org/10.1073/pnas.0911855107

Biswal, B. B., Zerrin Yetkin, F., Haughton, V. M., & Hyde, J. S. (1995). Functional

   connectivity in the motor cortex of resting human brain using echo-planar mri.

   Magnetic Resonance in Medicine, *34*(4), 537–541.

   https://doi.org/10.1002/mrm.1910340409

Bittencourt-Villalpando, M., van der Horn, H. J., Maurits, N. M., & van der Naalt, J.

   (2021). Disentangling the effects of age and mild traumatic brain injury on brain

   network connectivity: A resting state fMRI study. *NeuroImage: Clinical*, *29*, 102534.

   https://doi.org/10.1016/j.nicl.2020.102534

Boekel, W., Wagenmakers, E. J., Belay, L., Verhagen, J., Brown, S., & Forstmann, B. U.

   (2015). A purely confirmatory replication study of structural brain-behavior

   correlations. *Cortex*, *66*, 115–133. https://doi.org/10.1016/j.cortex.2014.11.019

Boraxbekk, C. J., Salami, A., Wåhlin, A., & Nyberg, L. (2016). Physical activity over a

   decade modifies age-related decline in perfusion, gray matter volume, and functional

   connectivity of the posterior default-mode network-A multimodal approach.

   NeuroImage. https://doi.org/10.1016/j.neuroimage.2015.12.010

Botvinik-Nezer, R., Holzmeister, F., Camerer, C. F., Dreber, A., Huber, J., Johannesson, M.,

Kirchler, M., Iwanir, R., Mumford, J. A., Adcock, R. A., Avesani, P., Baczkowski, B.

M., Bajracharya, A., Bakst, L., Ball, S., Barilari, M., Bault, N., Beaton, D., Beitner, J.,

… Schonberg, T. (2020). Variability in the analysis of a single neuroimaging dataset by

many teams. *Nature*, *582*(7810), 84–88. https://doi.org/10.1038/s41586-020-2314-9

Bressler, S. L., & Menon, V. (2010). Large-scale brain networks in cognition: emerging

methods and principles. *Trends in Cognitive Sciences*, *14*(6), 277–290.

https://doi.org/10.1016/j.tics.2010.04.004

Bu, L., Huo, C., Xu, G., Liu, Y., Li, Z., Fan, Y., & Li, J. (2018). Alteration in Brain

Functional and Effective Connectivity in Subjects With Hypertension. *Frontiers in

Physiology*, *9*(MAY), 669. https://doi.org/10.3389/fphys.2018.00669

Caldwell, A., Lakens, D., DeBruine, L., Love, J., & Aust, F. (2021). *Superpower: Simulation-

Based Power Analysis for Factorial Designs* (0.1.2).

https://doi.org/10.1177/2515245920951503

Campbell, K. L., & Schacter, D. L. (2017). Ageing and the resting state: is cognition

obsolete? In *Language, Cognition and Neuroscience* (Vol. 32, Issue 6, pp. 661–668).

Routledge. https://doi.org/10.1080/23273798.2016.1227858

Canario, E., Chen, D., & Biswal, B. (2021). A review of resting-state fMRI and its use to

examine psychiatric disorders. *Psychoradiology*, *1*(1), 42–53.

https://doi.org/10.1093/psyrad/kkab003

Cao, W., Cao, X., Hou, C., Li, T., Cheng, Y., Jiang, L., Luo, C., Li, C., & Yao, D. (2016).

Effects of Cognitive Training on Resting-State Functional Connectivity of Default

Mode, Salience, and Central Executive Networks. *Frontiers in Aging Neuroscience*,

8(APR), 70. https://doi.org/10.3389/fnagi.2016.00070

Cao, W., Luo, C., Zhu, B., Zhang, D., Dong, L., Gong, J., Gong, D., He, H., Tu, S., Yin,

W., Li, J., Chen, H., & Yao, D. (2014). Resting-state functional connectivity in anterior

cingulate cortex in normal aging. *Frontiers in Aging Neuroscience*, *6*(OCT), 280.

https://doi.org/10.3389/fnagi.2014.00280

Carnevale, L., Maffei, A., Landolfi, A., Grillea, G., Carnevale, D., & Lembo, G. (2020).

Brain functional magnetic resonance imaging highlights altered connections and

functional networks in patients with hypertension. *Hypertension*, *76*(5), 1480–1490.

https://doi.org/10.1161/HYPERTENSIONAHA.120.15296

Carp, J., Park, J., Hebrank, A., Park, D. C., & Polk, T. A. (2011). Age-Related Neural

Dedifferentiation in the Motor System. *PLoS ONE*, *6*(12), e29411.

https://doi.org/10.1371/journal.pone.0029411

Champely, S., Ekstrom, C., Dalgaard, P., Gill, J., Weibelzahl, S., Anandkumar, A., Ford,

C., Volcic, R., & Rosario, H. De. (2020). *Package 'pwr'* (1.3-0). https://cran.r-

project.org/web/packages/pwr/pwr.pdf

Chand, G. B., & Dhamala, M. (2017). Interactions between the anterior cingulate-insula

network and the fronto-parietal network during perceptual decision-making.

NeuroImage, *152*, 381–389. https://doi.org/10.1016/j.neuroimage.2017.03.014

Chand, G. B., Wu, J., Hajjar, I., & Qiu, D. (2017). Interactions of the Salience Network and

Its Subsystems with the Default-Mode and the Central-Executive Networks in Normal

Aging and Mild Cognitive Impairment. *Brain Connectivity*, *7*(7), 401–412.

https://doi.org/10.1089/brain.2017.0509

Chang, C., Metzger, C. D., Glover, G. H., Duyn, J. H., Heinze, H. J., & Walter, M. (2013).

Association between heart rate variability and fluctuations in resting-state functional

connectivity. *NeuroImage*, *68*, 93–104.

https://doi.org/10.1016/j.neuroimage.2012.11.038

Chang, Y. (2014). Reorganization and plastic changes of the human brain associated with

skill learning and expertise. In *Frontiers in Human Neuroscience* (Vol. 8, Issue 1 FEB).

Frontiers Media S. A. https://doi.org/10.3389/fnhum.2014.00035

Chen, A. C., Oathes, D. J., Chang, C., Bradley, T., Zhou, Z. W., Williamsa, L. M., Glover,

G. H., Deisseroth, K., & Etkin, A. (2013). Causal interactions between fronto-parietal

central executive and default-mode networks in humans. *Proceedings of the National

Academy of Sciences of the United States of America*, *110*(49), 19944–19949.

https://doi.org/10.1073/pnas.1311772110

Chen, Y., Meng, X., Hu, Q., Cui, H., Ding, Y., Kang, L., Juhás, M., Greenshaw, A. J., Zhao,

A., Wang, Y., Cui, G., & Li, P. (2016). Altered resting-state functional organization

within the central executive network in obsessive–compulsive disorder. *Psychiatry and

Clinical Neurosciences*, *70*(10), 448–456. https://doi.org/10.1111/pcn.12419

Chiarello, C., Vazquez, D., Felton, A., & McDowell, A. (2016). Structural asymmetry of the

human cerebral cortex: Regional and between-subject variability of surface area, cortical

thickness, and local gyrification. *Neuropsychologia*, *93*.

https://doi.org/10.1016/j.neuropsychologia.2016.01.012

Choe, A. S., Jones, C. K., Joel, S. E., Muschelli, J., Belegu, V., Caffo, B. S., Lindquist, M.

A., van Zijl, P. C. M., & Pekar, J. J. (2015). Reproducibility and Temporal Structure

in Weekly Resting-State fMRI over a Period of 3.5 Years. *PLOS ONE*, *10*(10),

e0140134. https://doi.org/10.1371/journal.pone.0140134

Clarke, D., & Sokoloff, L. (1999). Circulation and Energy Metabolism of the Brain. In *Basic

Neurochemistry: Molecular, Cellular and Medical Aspects.*

Cohen, J. (1992). Statistical Power Analysis. *Current Directions in Psychological Science*,

1(3), 98–101. https://doi.org/10.1111/1467-8721.ep10768783

Cole, J. H. (2020). Multimodality neuroimaging brain-age in UK biobank: relationship to

biomedical, lifestyle, and cognitive factors. *Neurobiology of Aging.*

https://doi.org/10.1016/j.neurobiolaging.2020.03.014

Cole, J. H., Franke, K., & Cherbuin, N. (2019). *Quantification of the Biological Age of the

Brain Using Neuroimaging.* 293–328. https://doi.org/10.1007/978-3-030-24970-0_19

Corps, J., & Rekik, I. (2019). Morphological Brain Age Prediction using Multi-View Brain

Networks Derived from Cortical Morphology in Healthy and Disordered Participants.

Scientific Reports, *9*(1), 1–10. https://doi.org/10.1038/s41598-019-46145-4

Curtis, B. J., Williams, P. G., Jones, C. R., & Anderson, J. S. (2016). Sleep duration and

resting fMRI functional connectivity: examination of short sleepers with and without

perceived daytime dysfunction. *Brain and Behavior*, *6*(12), e00576.

https://doi.org/10.1002/brb3.576

D'Esposito, M., Deouell, L. Y., & Gazzaley, A. (2003). Alterations in the BOLD fMRI signal

with ageing and disease: A challenge for neuroimaging. *Nature Reviews Neuroscience*,

4(11), 863–872. https://doi.org/10.1038/nrn1246

D'Esposito, M., Zarahn, E., Aguirre, G. K., & Rypma, B. (1999). The effect of normal aging

on the coupling of neural activity to the bold hemodynamic response. *NeuroImage*,

10(1), 6–14. https://doi.org/10.1006/nimg.1999.0444

Dafflon, J., Pinaya, W. H. L., Turkheimer, F., Cole, J. H., Leech, R., Harris, M. A., Cox, S.

R., Whalley, H. C., McIntosh, A. M., & Hellyer, P. J. (2020). An automated machine

learning approach to predict brain age from cortical anatomical measures. *Human Brain

Mapping*, *41*(13), 3555–3566. https://doi.org/10.1002/hbm.25028

Dai, X. J., Gong, H. H., Wang, Y. X., Zhou, F. Q., Min, Y. J., Zhao, F., Wang, S. Y., Liu,

B. X., & Xiao, X. Z. (2012). Gender differences in brain regional homogeneity of

healthy subjects after normal sleep and after sleep deprivation: A resting-state fMRI

study. *Sleep Medicine*, *13*(6), 720–727. https://doi.org/10.1016/j.sleep.2011.09.019

Damoiseaux, J. S. (2017). Effects of aging on functional and structural brain connectivity.

NeuroImage, *160*, 32–40. https://doi.org/10.1016/j.neuroimage.2017.01.077

Damoiseaux, J. S., Beckmann, C. F., Sanz Arigita, E. J., Barkhof, F., Scheltens, P., Stam,

C. J., Smith, S. M., & Rombouts, S. A. R. B. (2008). Reduced resting-state brain

activity in the "default network" in normal aging. *Cerebral Cortex*, *18*(8), 1856–1864.

https://doi.org/10.1093/cercor/bhm207

Damoiseaux, J. S., & Greicius, M. D. (2009). Greater than the sum of its parts: a review of

studies combining structural connectivity and resting-state functional connectivity.

Brain Structure and Function 2009 213:6, *213*(6), 525–533.

https://doi.org/10.1007/S00429-009-0208-6

Damoiseaux, J. S., Rombouts, S. A. R. B., Barkhof, F., Scheltens, P., Stam, C. J., Smith, S.

M., & Beckmann, C. F. (2006). Consistent resting-state networks across healthy

subjects. *Proceedings of the National Academy of Sciences of the United States of*

America, 103(37), 13848–13853. https://doi.org/10.1073/pnas.0601417103

De Boeck, P., & Jeon, M. (2018). Perceived crisis and reforms: Issues, explanations, and

remedies. *Psychological Bulletin.* https://doi.org/10.1037/bul0000154

Diamond, A. (2013). Executive functions. *Annual Review of Psychology, 64*, 135–168.

https://doi.org/10.1146/annurev-psych-113011-143750

Dickerson, B. C., & Wolk, D. A. (2012). MRI cortical thickness biomarker predicts AD-like

CSF and cognitive decline in normal adults. *Neurology, 78*(2), 84–90.

https://doi.org/10.1212/WNL.0b013e31823efc6c

Dinga, R., Schmaal, L., Penninx, B. W. J. H., van Tol, M. J., Veltman, D. J., van Velzen,

L., Mennes, M., van der Wee, N. J. A., & Marquand, A. F. (2019). Evaluating the

evidence for biotypes of depression: Methodological replication and extension of

Drysdale et al. (2017). *NeuroImage: Clinical, 22*, 101796.

https://doi.org/10.1016/j.nicl.2019.101796

Dohmatob, E., Richard, H., Pinho, A. L., & Thirion, B. (2021). Brain topography beyond

parcellations: Local gradients of functional maps. *NeuroImage, 229*, 117706.

https://doi.org/10.1016/j.neuroimage.2020.117706

Doll, A., Sorg, C., Manoliu, A., Wöller, A., Meng, C., Förstl, H., Zimmer, C., Wohlschläger,

A. M., & Riedl, V. (2013). Shifted intrinsic connectivity of central executive and

salience network in borderline personality disorder. *Frontiers in Human Neuroscience,*

7, 1–13. https://doi.org/10.3389/fnhum.2013.00727

Donahue, M. J., Lu, H., Jones, C. K., Edden, R. A. E., Pekar, J. J., & Van Zijl, P. C. M.

(2006). Theoretical and experimental investigation of the VASO contrast mechanism.

Magnetic Resonance in Medicine, *56*(6), 1261–1273.

https://doi.org/10.1002/mrm.21072

DuPre, E., Hanke, M., & Poline, J. B. (2020). Nature abhors a paywall: How open science

can realize the potential of naturalistic stimuli. *NeuroImage*, *216*, 116330.

https://doi.org/10.1016/j.neuroimage.2019.116330

Eickhoff, S., Nichols, T. E., Van Horn, J. D., & Turner, J. A. (2016). Sharing the wealth:

Neuroimaging data repositories. In *NeuroImage* (Vol. 124, Issue Pt B, pp. 1065–1068).

Academic Press Inc. https://doi.org/10.1016/j.neuroimage.2015.10.079

Eklund, A., Nichols, T. E., & Knutsson, H. (2016). Cluster failure: Why fMRI inferences for

spatial extent have inflated false-positive rates. *Proceedings of the National Academy of

Sciences of the United States of America*, *113*(28), 7900–7905.

https://doi.org/10.1073/pnas.1602413113

Elbau, I. G., Brücklmeier, B., Uhr, M., Arloth, J., Czamara, D., Spoormaker, V. I., Czisch,

M., Stephan, K. E., Binder, E. B., & Sämann, P. G. (2018). The brain's hemodynamic

response function rapidly changes under acute psychosocial stress in association with

genetic and endocrine stress response markers. *Proceedings of the National Academy of

Sciences of the United States of America*, *115*(43), E10206–E10215.

https://doi.org/10.1073/pnas.1804340115

Elliott, M. L., Knodt, A. R., Ireland, D., Morris, M. L., Poulton, R., Ramrakha, S., Sison,

M. L., Moffitt, T. E., Caspi, A., & Hariri, A. R. (2020). What Is the Test-Retest

Reliability of Common Task-Functional MRI Measures? New Empirical Evidence and a

Meta-Analysis. *Psychological Science.* https://doi.org/10.1177/0956797620916786

Eslami, T., Mirjalili, V., Fong, A., Laird, A. R., & Saeed, F. (2019). ASD-DiagNet: A Hybrid

Learning Approach for Detection of Autism Spectrum Disorder Using fMRI Data.

Frontiers in Neuroinformatics, *13*, 70. https://doi.org/10.3389/fninf.2019.00070

Esposito, R., Cieri, F., Chiacchiaretta, P., Cera, N., Lauriola, M., Di Giannantonio, M.,

Tartaro, A., & Ferretti, A. (2018). Modifications in resting state functional

anticorrelation between default mode network and dorsal attention network: comparison

among young adults, healthy elders and mild cognitive impairment patients. *Brain

Imaging and Behavior*, *12*(1), 127–141. https://doi.org/10.1007/s11682-017-9686-y

Esteves, M., Marques, P., Magalhães, R., Castanho, T. C., Soares, J. M., Almeida, A.,

Santos, N. C., Sousa, N., & Leite-Almeida, H. (2017). Structural laterality is associated

with cognitive and mood outcomes: An assessment of 105 healthy aged volunteers.

NeuroImage, *153*, 86–96. https://doi.org/10.1016/j.neuroimage.2017.03.040

Farras-Permanyer, L., Mancho-Fora, N., Montalà-Flaquer, M., Bartrés-Faz, D., Vaqué-

Alcázar, L., Peró-Cebollero, M., & Guàrdia-Olmos, J. (2019). Age-related changes in

resting-state functional connectivity in older adults. *Neural Regeneration Research*,

14(9), 1544–1555. https://doi.org/10.4103/1673-5374.255976

Ferreira, L. K., & Busatto, G. F. (2013). Resting-state functional connectivity in normal

brain aging. *Neuroscience and Biobehavioral Reviews*, *37*(3), 384–400.

https://doi.org/10.1016/j.neubiorev.2013.01.017

Fiedler, K. (2011). Voodoo Correlations Are Everywhere-Not Only in Neuroscience.

Perspectives on Psychological Science : A Journal of the Association for Psychological Science, *6*(2), 163–171. https://doi.org/10.1177/1745691611400237

Filippi, M., Valsasina, P., Misci, P., Falini, A., Comi, G., & Rocca, M. A. (2013). The organization of intrinsic brain activity differs between genders: A resting-state fMRI study in a large cohort of young healthy subjects. *Human Brain Mapping*, *34*(6), 1330–1343. https://doi.org/10.1002/hbm.21514

Fischl, B. (2012). FreeSurfer. In *NeuroImage* (Vol. 62, Issue 2, pp. 774–781). Academic Press. https://doi.org/10.1016/j.neuroimage.2012.01.021

Fjell, A. M., Sneve, M. H., Grydeland, H., Storsve, A. B., Amlien, I. K., Yendiki, A., & Walhovd, K. B. (2017). Relationship between structural and functional connectivity change across the adult lifespan: A longitudinal investigation. *Human Brain Mapping*, *38*(1), 561–573. https://doi.org/10.1002/hbm.23403

Fox, M. D., Corbetta, M., Snyder, A. Z., Vincent, J. L., & Raichle, M. E. (2006). Spontaneous neuronal activity distinguishes human dorsal and ventral attention systems. *Proceedings of the National Academy of Sciences of the United States of America*, *103*(26), 10046–10051. https://doi.org/10.1073/pnas.0604187103

Francis, G. (2013). Replication, statistical consistency, and publication bias. *Journal of Mathematical Psychology*, *57*(5), 153–169. https://doi.org/10.1016/j.jmp.2013.02.003

Frässle, S., & Stephan, K. E. (2021). Test-retest reliability of regression dynamic causal modeling. *BioRxiv.* https://doi.org/https://doi.org/10.1101/2021.06.01.446526

Frégnac, Y., & Laurent, G. (2014). Neuroscience: Where is the brain in the Human Brain Project? *Nature*, *513*, 27–29. https://doi.org/10.1038/513027a

Friese, M., & Frankenbach, J. (2020). p-hacking and publication bias interact to distort

    meta-analytic effect size estimates. *Psychological Methods*, *25*(4), 456–471.

    https://doi.org/10.1037/met0000246

Friston, K. J. (2002). Beyond Phrenology: What Can Neuroimaging Tell Us About

    Distributed Circuitry? *Annual Review of Neuroscience*, *25*(1), 221–250.

    https://doi.org/10.1146/annurev.neuro.25.112701.142846

Friston, K. J., Harrison, L., & Penny, W. (2003). Dynamic causal modelling. *NeuroImage*,

    19(4), 1273–1302. https://doi.org/10.1016/S1053-8119(03)00202-7

Friston, K. J., Kahan, J., Biswal, B., & Razi, A. (2014). A DCM for resting state fMRI.

    NeuroImage, *94*, 396–407. https://doi.org/10.1016/J.NEUROIMAGE.2013.12.009

Furl, N. (2015). Structural and effective connectivity reveals potential network-based

    influences on category-sensitive visual areas. *Frontiers in Human Neuroscience*,

    0(MAY), 253. https://doi.org/10.3389/FNHUM.2015.00253

Garrett, D. D., Kovacevic, N., McIntosh, A. R., & Grady, C. L. (2010). Blood oxygen level-

    dependent signal variability is more than just noise. *Journal of Neuroscience*, *30*(14),

    4914–4921. https://doi.org/10.1523/JNEUROSCI.5166-09.2010

Garrett, D. D., Lindenberger, U., Hoge, R. D., & Gauthier, C. J. (2017). Age differences in

    brain signal variability are robust to multiple vascular controls. *Scientific Reports*, *7*(1),

    1–13. https://doi.org/10.1038/s41598-017-09752-7

Gaut, G., Li, X., Lu, Z., & Steyvers, M. (2019). Experimental design modulates variance in

    BOLD activation: The variance design general linear model. *Human Brain Mapping*,

    40(13), hbm.24677. https://doi.org/10.1002/hbm.24677

Geerligs, L., & Tsvetanov, K. A. (2017). The use of resting state data in an integrative

approach to studying neurocognitive ageing–commentary on Campbell and Schacter

(2016). In *Language, Cognition and Neuroscience* (Vol. 32, Issue 6, pp. 684–691).

Routledge. https://doi.org/10.1080/23273798.2016.1251600

Geerligs, L., Tsvetanov, K. A., Cam-CAN, & Henson, R. N. (2017). Challenges in measuring

individual differences in functional connectivity using fMRI: The case of healthy aging.

Human Brain Mapping, *38*(8), 4125–4156. https://doi.org/10.1002/hbm.23653

Gelman, A., & Loken, E. (2013). *The garden of forking paths: Why multiple comparisons*

can be a problem, even when there is no "fishing expedition" or "p-hacking."

Unpublished Draft.

http://www.stat.columbia.edu/~gelman/research/unpublished/p_hacking.pdf

Glover, G. H. (2011). Overview of functional magnetic resonance imaging. In *Neurosurgery*

Clinics of North America (Vol. 22, Issue 2, pp. 133–139). NIH Public Access.

https://doi.org/10.1016/j.nec.2010.11.001

Goh, J. O. S. (2011). Functional dedifferentiation and altered connectivity in older adults:

Neural accounts of cognitive aging. *Aging and Disease*, *2*(1), 30–48.

Goldstone, A., Mayhew, S. D., Przezdzik, I., Wilson, R. S., Hale, J. R., & Bagshaw, A. P.

(2016). Gender specific re-organization of resting-state networks in older age. *Frontiers*

in Aging Neuroscience, *8*(NOV), 285. https://doi.org/10.3389/fnagi.2016.00285

Gong, J. Y., Chen, G., Jia, Y., Zhong, S., Zhao, L., Luo, X., Qiu, S., Lai, S., Qi, Z., Huang,

L., & Wang, Y. (2019). Disrupted functional connectivity within the default mode

network and salience network in unmedicated bipolar II disorder. *Progress in Neuro-*

Psychopharmacology and Biological Psychiatry, *88*, 11–18.

https://doi.org/10.1016/j.pnpbp.2018.06.012

Gorbach, T., Lundquist, A., De Luna, X., Nyberg, L., & Salami, A. (2020). A Hierarchical

Bayesian Mixture Model Approach for Analysis of Resting-State Functional Brain

Connectivity: An Alternative to Thresholding. *Brain Connectivity*, *10*(5), 202–211.

https://doi.org/10.1089/brain.2020.0740

Gordon, E. M., Laumann, T. O., Gilmore, A. W., Newbold, D. J., Greene, D. J., Berg, J. J.,

Ortega, M., Hoyt-Drazen, C., Gratton, C., Sun, H., Hampton, J. M., Coalson, R. S.,

Nguyen, A. L., McDermott, K. B., Shimony, J. S., Snyder, A. Z., Schlaggar, B. L.,

Petersen, S. E., Nelson, S. M., & Dosenbach, N. U. F. (2017). Precision Functional

Mapping of Individual Human Brains. *Neuron*, *95*(4), 791-807.e7.

https://doi.org/10.1016/j.neuron.2017.07.011

Gorgolewski, K. J., & Poldrack, R. A. (2016). A Practical Guide for Improving

Transparency and Reproducibility in Neuroimaging Research. *PLOS Biology*, *14*(7),

e1002506. https://doi.org/10.1371/journal.pbio.1002506

Göttlich, M., Münte, T. F., Heldmann, M., Kasten, M., Hagenah, J., & Krämer, U. M.

(2013). Altered Resting State Brain Networks in Parkinson's Disease. *PLoS ONE*,

8(10). https://doi.org/10.1371/journal.pone.0077336

Goulden, N., Khusnulina, A., Davis, N. J., Bracewell, R. M., Bokde, A. L., McNulty, J. P.,

& Mullins, P. G. (2014). The salience network is responsible for switching between the

default mode network and the central executive network: Replication from DCM.

NeuroImage, *99*, 180–190. https://doi.org/10.1016/j.neuroimage.2014.05.052

Gountouna, V. E., Job, D. E., McIntosh, A. M., Moorhead, T. W. J., Lymer, G. K. L.,

Whalley, H. C., Hall, J., Waiter, G. D., Brennan, D., McGonigle, D. J., Ahearn, T. S.,

Cavanagh, J., Condon, B., Hadley, D. M., Marshall, I., Murray, A. D., Steele, J. D.,

Wardlaw, J. M., & Lawrie, S. M. (2010). Functional Magnetic Resonance Imaging

(fMRI) reproducibility and variance components across visits and scanning sites with a

finger tapping task. *NeuroImage*, *49*(1), 552–560.

https://doi.org/10.1016/j.neuroimage.2009.07.026

Grady, C. L. (2012). The cognitive neuroscience of ageing. *Nature Reviews Neuroscience*,

13(7), 491–505. https://doi.org/10.1038/nrn3256

Grady, C. L., & Garrett, D. D. (2014). Understanding variability in the BOLD signal and

why it matters for aging. *Brain Imaging and Behavior*, *8*(2), 274–283.

https://doi.org/10.1007/s11682-013-9253-0

Grady, C. L., Sarraf, S., Saverino, C., & Campbell, K. (2016). Age differences in the

functional interactions among the default, frontoparietal control, and dorsal attention

networks. *Neurobiology of Aging*, *41*, 159–172.

https://doi.org/10.1016/j.neurobiolaging.2016.02.020

Gratton, C., Laumann, T. O., Nielsen, A. N., Schlaggar, B. L., Dosenbach, N. U. F., &

Petersen Correspondence, S. E. (2018). Functional Brain Networks Are Dominated by

Stable Group and Individual Factors, Not Cognitive or Daily Variation. *Neuron*, *98*,

439-452.e5. https://doi.org/10.1016/j.neuron.2018.03.035

Greene, D. J., Marek, S., Gordon, E. M., Siegel, J. S., Gratton, C., Laumann, T. O.,

Gilmore, A. W., Berg, J. J., Nguyen, A. L., Dierker, D., Van, A. N., Ortega, M.,

Newbold, D. J., Hampton, J. M., Nielsen, A. N., McDermott, K. B., Roland, J. L.,

Norris, S. A., Nelson, S. M., … Dosenbach, N. U. F. (2020). Integrative and Network-

Specific Connectivity of the Basal Ganglia and Thalamus Defined in Individuals.

Neuron, *105*(4), 742-758.e6. https://doi.org/10.1016/j.neuron.2019.11.012

Greenwood, P. M. (2007). Functional plasticity in cognitive aging: Review and hypothesis.

Neuropsychology, *21*(6), 657. https://doi.org/10.1037/0894-4105.21.6.657

Greicius, M. (2008). Resting-state functional connectivity in neuropsychiatric disorders.

Current Opinion in Neurology, *21*(4), 424–430.

https://doi.org/10.1097/wco.0b013e328306f2c5

Hacker, C. D., Laumann, T. O., Szrama, N. P., Baldassarre, A., Snyder, A. Z., Leuthardt, E.

C., & Corbetta, M. (2013). Resting state network estimation in individual subjects.

NeuroImage, *82*, 616–633. https://doi.org/10.1016/j.neuroimage.2013.05.108

Hahn, G., Skeide, M. A., Mantini, D., Ganzetti, M., Destexhe, A., Friederici, A. D., & Deco,

G. (2019). A new computational approach to estimate whole-brain effective connectivity

from functional and structural MRI, applied to language development. *Scientific

Reports 2019 9:1*, *9*(1), 1–13. https://doi.org/10.1038/s41598-019-44909-6

Hamilton, J. P., Chen, G., Thomason, M. E., Schwartz, M. E., & Gotlib, I. H. (2011).

Investigating neural primacy in Major Depressive Disorder: Multivariate Granger

causality analysis of resting-state fMRI time-series data. *Molecular Psychiatry*, *16*(7),

763–772. https://doi.org/10.1038/mp.2010.46

Harms, M. P., Somerville, L. H., Ances, B. M., Andersson, J., Barch, D. M., Bastiani, M.,

Bookheimer, S. Y., Brown, T. B., Buckner, R. L., Burgess, G. C., Coalson, T. S.,

Chappell, M. A., Dapretto, M., Douaud, G., Fischl, B., Glasser, M. F., Greve, D. N.,

Hodge, C., Jamison, K. W., … Yacoub, E. (2018). Extending the Human Connectome

Project across ages: Imaging protocols for the Lifespan Development and Aging

projects. *NeuroImage*, *183*, 972–984. https://doi.org/10.1016/j.neuroimage.2018.09.060

Harrison, B. J., Pujol, J., Ortiz, H., Fornito, A., Pantelis, C., & Yücel, M. (2008).

Modulation of Brain Resting-State Networks by Sad Mood Induction. *PLoS ONE*, *3*(3),

e1794. https://doi.org/10.1371/journal.pone.0001794

Hawkins, D. M. (2004). The Problem of Overfitting. In *Journal of Chemical Information and

Computer Sciences* (Vol. 44, Issue 1, pp. 1–12). American Chemical Society.

https://doi.org/10.1021/ci0342472

He, X., Qin, W., Liu, Y., Zhang, X., Duan, Y., Song, J., Li, K., Jiang, T., & Yu, C. (2013).

Age-related decrease in functional connectivity of the right fronto-insular cortex with

the central executive and default-mode networks in adults from young to middle age.

Neuroscience Letters, *544*, 74–79. https://doi.org/10.1016/j.neulet.2013.03.044

He, X., Qin, W., Liu, Y., Zhang, X., Duan, Y., Song, J., Li, K., Jiang, T., & Yu, C. (2014).

Abnormal salience network in normal aging and in amnestic mild cognitive impairment

and Alzheimer's disease. *Human Brain Mapping*, *35*(7), 3446–3464.

https://doi.org/10.1002/hbm.22414

Holiga, Š., Sambataro, F., Luzy, C., Greig, G., Sarkar, N., Renken, R. J., Marsman, J. B. C.,

Schobel, S. A., Bertolino, A., & Dukart, J. (2018). Test-retest reliability of task-based

and resting-state blood oxygen level dependence and cerebral blood flow measures.

PLoS ONE, *13*(11), e0206583. https://doi.org/10.1371/journal.pone.0206583

Honey, C. J., Sporns, O., Cammoun, L., Gigandet, X., Thiran, J. P., Meuli, R., & Hagmann, P. (2009). Predicting human resting-state functional connectivity from structural connectivity. *Proceedings of the National Academy of Sciences*, *106*(6), 2035–2040. https://doi.org/10.1073/PNAS.0811168106

Hotelling, H. (1936). Relations Between Two Sets Of Variates. *Biometrika*, *28*(3–4), 321–377. https://doi.org/10.1093/biomet/28.3-4.321

Hua, J., Donahue, M. J., Zhao, J. M., Grgac, K., Huang, A. J., Zhou, J., & Van Zijl, P. C. M. (2009). Magnetization transfer enhanced Vascular-space-occupancy (MT-VASO) functional MRI. *Magnetic Resonance in Medicine*, *61*(4), 944–951. https://doi.org/10.1002/mrm.21911

Huber, D. E., Potter, K. W., & Huszar, L. D. (2019). Less "story" and more "reliability" in cognitive neuroscience. *Cortex*, *113*, 347–349. https://doi.org/10.1016/j.cortex.2018.10.030

Huber, L., Finn, E. S., Chai, Y., Goebel, R., Stirnberg, R., Stöcker, T., Marrett, S., Uludag, K., Kim, S. G., Han, S. H., Bandettini, P. A., & Poser, B. A. (2020). Layer-dependent functional connectivity methods. In *Progress in Neurobiology* (p. 101835). Elsevier Ltd. https://doi.org/10.1016/j.pneurobio.2020.101835

Huber, L., Handwerker, D. A., Jangraw, D. C., Chen, G., Hall, A., Stüber, C., Gonzalez-Castillo, J., Ivanov, D., Marrett, S., Guidi, M., Goense, J., Poser, B. A., & Bandettini, P. A. (2017). High-Resolution CBV-fMRI Allows Mapping of Laminar Activity and Connectivity of Cortical Input and Output in Human M1. *Neuron*, *96*(6), 1253-1263.e7. https://doi.org/10.1016/j.neuron.2017.11.005

Huber, L., Ivanov, D., Krieger, S. N., Streicher, M. N., Mildner, T., Poser, B. A., Möller, H.

E., & Turner, R. (2014). Slab-selective, BOLD-corrected VASO at 7 Tesla provides

measures of cerebral blood volume reactivity with high signal-to-noise ratio. *Magnetic*

Resonance in Medicine, *72*(1), 137–148. https://doi.org/10.1002/mrm.24916

Huber, L., Poser, B., Kaas, A., Fear, E., Desbach, S., Berwick, J., Goebel, R., Turner, R., &

Kennerley, A. (2020). Validating layer-specific VASO across species. *BioRxiv*,

2020.07.24.219378. https://doi.org/10.1101/2020.07.24.219378

Huber, L., Uludağ, K., & Möller, H. E. (2019). Non-BOLD contrast for laminar fMRI in

humans: CBF, CBV, and CMRO2. In *NeuroImage* (Vol. 197, pp. 742–760). Academic

Press Inc. https://doi.org/10.1016/j.neuroimage.2017.07.041

Hugdahl, K. (2005). Symmetry and asymmetry in the human brain. *European Review*,

13(S2), 119–133. https://doi.org/10.1017/S1062798705000700

Hugdahl, K. (2018). A life in academia: My career in brief. *Scandinavian Journal of*

Psychology, *59*(1), 3–25. https://doi.org/10.1111/sjop.12406

Hugdahl, K., Raichle, M. E., Mitra, A., & Specht, K. (2015). On the existence of a

generalized non-specific task-dependent network. *Frontiers in Human Neuroscience*,

0(AUGUST), 430. https://doi.org/10.3389/FNHUM.2015.00430

Hughes, C., Faskowitz, J., Cassidy, B. S., Sporns, O., & Krendl, A. C. (2020). Aging relates

to a disproportionately weaker functional architecture of brain networks during rest and

task states. *NeuroImage*, *209*, 116521.

https://doi.org/10.1016/j.neuroimage.2020.116521

Huntenburg, J. M., Bazin, P. L., Goulas, A., Tardif, C. L., Villringer, A., & Margulies, D. S.

(2017). A Systematic Relationship Between Functional Connectivity and Intracortical

Myelin in the Human Cerebral Cortex. *Cerebral Cortex*, *27*(2), 981–997.

https://doi.org/10.1093/cercor/bhx030

Hutchison, R. M., Womelsdorf, T., Allen, E. A., Bandettini, P. A., Calhoun, V. D.,

Corbetta, M., Della Penna, S., Duyn, J. H., Glover, G. H., Gonzalez-Castillo, J.,

Handwerker, D. A., Keilholz, S., Kiviniemi, V., Leopold, D. A., de Pasquale, F., Sporns,

O., Walter, M., & Chang, C. (2013). Dynamic functional connectivity: Promise, issues,

and interpretations. *NeuroImage*, *80*, 360–378.

https://doi.org/10.1016/j.neuroimage.2013.05.079

Hyder, F., Rothman, D. L., & Bennett, M. R. (2013). Cortical energy demands of signaling

and nonsignaling components in brain are conserved across mammalian species and

activity levels. *Proceedings of the National Academy of Sciences*, *110*(9), 3549–3554.

https://doi.org/10.1073/PNAS.1214912110

Ioannidis, J. P. A. (2018). Why most published research findings are false. In *Getting to

Good: Research Integrity in the Biomedical Sciences* (pp. 2–8). Springer International

Publishing. https://doi.org/10.1371/journal.pmed.0020124

Jafarian, A., Litvak, V., Cagnan, H., Friston, K. J., & Zeidman, P. (2020). Comparing

dynamic causal models of neurovascular coupling with fMRI and EEG/MEG.

NeuroImage, *216*, 116734. https://doi.org/10.1016/j.neuroimage.2020.116734

Jamadar, S. D., Sforazzini, F., Raniga, P., Ferris, N. J., Paton, B., Bailey, M. J.,

Brodtmann, A., Yates, P. A., Donnan, G. A., Ward, S. A., Woods, R. L., Storey, E.,

McNeil, J. J., & Egan, G. F. (2019). Sexual Dimorphism of Resting-State Network

Connectivity in Healthy Ageing. *Journals of Gerontology - Series B Psychological Sciences and Social Sciences*, *74*(7), 1121–1131. https://doi.org/10.1093/geronb/gby004

Jamalabadi, H., Zuberer, A., Kumar, V. J., Li, M., Alizadeh, S., Amani, A. M., Gaser, C., Esterman, M., & Walter, M. (2021). The missing role of gray matter in studying brain controllability. *Network Neuroscience*, *5*(1), 198–210. https://doi.org/10.1162/NETN_A_00174

Jin, T., & Kim, S. G. (2008). Improved cortical-layer specificity of vascular space occupancy fMRI with slab inversion relative to spin-echo BOLD at 9.4 T. *NeuroImage*, *40*(1), 59–67. https://doi.org/10.1016/j.neuroimage.2007.11.045

Joo, S. H., Lim, H. K., & Lee, C. U. (2016). Three large-scale functional brain networks from resting-state functional MRI in subjects with different levels of cognitive impairment. In *Psychiatry Investigation* (Vol. 13, Issue 1, p. 1). Korean Neuropsychiatric Association. https://doi.org/10.4306/pi.2016.13.1.1

Kaiser, R. H., Whitfield-Gabrieli, S., Dillon, D. G., Goer, F., Beltzer, M., Minkel, J., Smoski, M., Dichter, G., & Pizzagalli, D. A. (2016). Dynamic Resting-State Functional Connectivity in Major Depression. *Neuropsychopharmacology*, *41*(7), 1822–1830. https://doi.org/10.1038/npp.2015.352

Kalpouzos, G., Persson, J., & Nyberg, L. (2012). Local brain atrophy accounts for functional activity differences in normal aging. *Neurobiology of Aging*, *33*(3), 623.e1–623.e13. https://doi.org/10.1016/j.neurobiolaging.2011.02.021

Kampa, M., Schick, A., Sebastian, A., Wessa, M., Tüscher, O., Kalisch, R., & Yuen, K. (2020). Replication of fMRI group activations in the neuroimaging battery for the

Mainz Resilience Project (MARP). *NeuroImage*, *204*, 116223.

https://doi.org/10.1016/j.neuroimage.2019.116223

Karolis, V. R., Corbetta, M., & Thiebaut de Schotten, M. (2019). The architecture of

functional lateralisation and its relationship to callosal connectivity in the human brain.

Nature Communications, *10*(1), 1–9. https://doi.org/10.1038/s41467-019-09344-1

Khundrakpam, B. S., Tohka, J., Evans, A. C., Ball, W. S., Byars, A. W., Schapiro, M.,

Bommer, W., Carr, A., German, A., Dunn, S., Rivkin, M. J., Waber, D., Mulkern, R.,

Vajapeyam, S., Chiverton, A., Davis, P., Koo, J., Marmor, J., Mrakotsky, C., … O'Neill,

J. (2015). Prediction of brain maturity based on cortical thickness at different spatial

resolutions. *NeuroImage*, *11*, 350–359. https://doi.org/10.1016/j.neuroimage.2015.02.046

King, R. D., George, A. T., Jeon, T., Hynan, L. S., Youn, T. S., Kennedy, D. N., &

Dickerson, B. (2009). Characterization of atrophic changes in the cerebral cortex using

fractal dimensional analysis. *Brain Imaging and Behavior*, *3*(2), 154–166.

https://doi.org/10.1007/s11682-008-9057-9

Kirilina, E., Lutti, A., Poser, B. A., Blankenburg, F., & Weiskopf, N. (2016). The quest for

the best: The impact of different EPI sequences on the sensitivity of random effect

fMRI group analyses. *NeuroImage*, *126*, 49–59.

https://doi.org/10.1016/j.neuroimage.2015.10.071

Kong, X. Z., Mathias, S. R., Guadalupe, T., Abé, C., Agartz, I., Akudjedu, T. N., Aleman,

A., Alhusaini, S., Allen, N. B., Ames, D., Andreassen, O. A., Vasquez, A. A.,

Armstrong, N. J., Bergo, F., Bastin, M. E., Batalla, A., Bauer, J., Baune, B. T., Baur-

Streubel, R., … Orhan, F. (2018). Mapping cortical brain asymmetry in 17,141 healthy

individuals worldwide via the ENIGMA Consortium. *Proceedings of the National Academy of Sciences of the United States of America, 115*(22), E5154–E5163. https://doi.org/10.1073/pnas.1718418115

Kumral, D., Şansal, F., Cesnaite, E., Mahjoory, K., Al, E., Gaebler, M., Nikulin, V. V., & Villringer, A. (2020). BOLD and EEG signal variability at rest differently relate to aging in the human brain. *NeuroImage.* https://doi.org/10.1016/j.neuroimage.2019.116373

Kumral, D., Schaare, H. L., Beyer, F., Reinelt, J., Uhlig, M., Liem, F., Lampe, L., Babayan, A., Reiter, A., Erbey, M., Roebbig, J., Loeffler, M., Schroeter, M. L., Husser, D., Witte, A. V., Villringer, A., & Gaebler, M. (2019). The age-dependent relationship between resting heart rate variability and functional brain connectivity. *NeuroImage, 185*, 521–533. https://doi.org/10.1016/j.neuroimage.2018.10.027

Labrenz, F., Wrede, K., Forsting, M., Engler, H., Schedlowski, M., Elsenbruch, S., & Benson, S. (2016). Alterations in functional connectivity of resting state networks during experimental endotoxemia - An exploratory study in healthy men. *Brain, Behavior, and Immunity, 54*, 17–26. https://doi.org/10.1016/j.bbi.2015.11.010

Lau, W. K. W., Leung, M. K., Lee, T. M. C., & Law, A. C. K. (2016). Resting-state abnormalities in amnestic mild cognitive impairment: A meta-analysis. *Translational Psychiatry, 6*(4), 790. https://doi.org/10.1038/tp.2016.55

Lee, M. H., Smyser, C. D., & Shimony, J. S. (2013). Resting-state fMRI: A review of methods and clinical applications. *American Journal of Neuroradiology, 34*(10), 1866–1872. https://doi.org/10.3174/ajnr.A3263

Lehmann, B. C. L., Henson, R. N., Geerligs, L., Cam-CAN, & White, S. R. (2020).

Characterising group-level brain connectivity: a framework using Bayesian exponential

random graph models. *NeuroImage*, 117480.

https://doi.org/10.1016/j.neuroimage.2020.117480

Lekander, M., Karshikoff, B., Johansson, E., Soop, A., Fransson, P., Lundström, J. N.,

Andreasson, A., Ingvar, M., Petrovic, P., Axelsson, J., & Nilsonne, G. (2016). Intrinsic

functional connectivity of insular cortex and symptoms of sickness during acute

experimental inflammation. *Brain, Behavior, and Immunity*, *56*, 34–41.

https://doi.org/10.1016/j.bbi.2015.12.018

Lemaitre, H., Goldman, A. L., Sambataro, F., Verchinski, B. A., Meyer-Lindenberg, A.,

Weinberger, D. R., & Mattay, V. S. (2012). Normal age-related brain morphometric

changes: Nonuniformity across cortical thickness, surface area and gray matter volume?

Neurobiology of Aging. https://doi.org/10.1016/j.neurobiolaging.2010.07.013

Levakov, G., Faskowitz, J., Avidan, G., Sporns, O., & Levakov, G. (2021). Mapping

structure to function and behavior with individual-level connectome embedding.

BioRxiv. https://doi.org/10.1101/2021.01.13.426513

Li, M., Chen, H., Wang, J., Liu, F., Wang, Y., Lu, F., Yu, C., & Chen, H. (2015). Increased

cortical thickness and altered functional connectivity of the right superior temporal

gyrus in left-handers. *Neuropsychologia*, *67*, 27–34.

https://doi.org/10.1016/j.neuropsychologia.2014.11.033

Li, Z., Zang, Y. F., Ding, J., & Wang, Z. (2017). Assessing the mean strength and variations

of the time-to-time fluctuations of resting-state brain activity. *Medical and Biological*

Engineering and Computing, *55*(4), 631–640. https://doi.org/10.1007/s11517-016-1544-3

Lilienfeld, S. O. (2017). Psychology's Replication Crisis and the Grant Culture: Righting the

Ship. *Perspectives on Psychological Science*, *12*(4), 660–664.

https://doi.org/10.1177/1745691616687745

Lindquist, M. A., Meng Loh, J., Atlas, L. Y., & Wager, T. D. (2009). Modeling the

hemodynamic response function in fMRI: efficiency, bias and mis-modeling.

NeuroImage, *45*(1), 187–198. https://doi.org/10.1016/j.neuroimage.2008.10.065

Liu, T. T. (2016). Noise contributions to the fMRI signal: An overview. *NeuroImage*, *143*,

141–151. https://doi.org/10.1016/j.neuroimage.2016.09.008

Liu, W., Wei, D., Chen, Q., Yang, W., Meng, J., Wu, G., Bi, T., Zhang, Q., Zuo, X. N., &

Qiu, J. (2017). Longitudinal test-retest neuroimaging data from healthy young adults in

southwest China. *Scientific Data*, *4*(1), 1–9. https://doi.org/10.1038/sdata.2017.17

Liu, X., Gerraty, R. T., Grinband, J., Parker, D., & Razlighi, Q. R. (2017). Brain atrophy

can introduce age-related differences in BOLD response. *Human Brain Mapping*, *38*(7),

3402–3414. https://doi.org/10.1002/hbm.23597

Lo, S. K., Li, I. T., Tsou, T. S., & See, L. (1995). Non-significant in univariate but

significant in multivariate analysis: a discussion with examples. *Changgeng Yi Xue Za

Zhi / Changgeng Ji Nian Yi Yuan = Chang Gung Medical Journal / Chang Gung

Memorial Hospital*, *18*(2), 95–101. https://pubmed.ncbi.nlm.nih.gov/7641117/

Loken, E., & Gelman, A. (2017). Measurement error and the replication crisis. *Science*,

355(6325), 582–584. https://doi.org/10.1126/science.aam5409

Lombardo, M. V., Auyeung, B., Holt, R. J., Waldman, J., Ruigrok, A. N. V., Mooney, N.,

Bullmore, E. T., Baron-Cohen, S., & Kundu, P. (2016). Improving effect size estimation and statistical power with multi-echo fMRI and its impact on understanding the neural systems supporting mentalizing. *NeuroImage*, *142*, 55–66. https://doi.org/10.1016/j.neuroimage.2016.07.022

Loring, D. W., Meador, K. J., Allison, J. D., Pillai, J. J., Lavin, T., Lee, G. P., Balan, A., & Dave, V. (2002). Now you see it, now you don't: Statistical and methodological considerations in fMRI. *Epilepsy and Behavior*, *3*(6), 539–547. https://doi.org/10.1016/S1525-5050(02)00558-9

Lu, H., Hua, J., & van Zijl, P. C. M. (2013). Noninvasive functional imaging of cerebral blood volume with vascular-space-occupancy (VASO) MRI. *NMR in Biomedicine*, *26*(8), 932–948. https://doi.org/10.1002/nbm.2905

Luo, C., Zhang, X., Cao, X., Gan, Y., Li, T., Cheng, Y., Cao, W., Jiang, L., Yao, D., & Li, C. (2016). The Lateralization of Intrinsic Networks in the Aging Brain Implicates the Effects of Cognitive Training. *Frontiers in Aging Neuroscience*, *0*(MAR), 32. https://doi.org/10.3389/FNAGI.2016.00032

Luo, N., Sui, J., Abrol, A., Lin, D., Chen, J., Vergara, V. M., Fu, Z., Du, Y., Damaraju, E., Xu, Y., Turner, J. A., & Calhoun, V. D. (2020). Age-related structural and functional variations in 5,967 individuals across the adult lifespan. *Human Brain Mapping*, *41*(7), 1725–1737. https://doi.org/10.1002/hbm.24905

Luo, X., Chen, G., Jia, Y., Gong, J., Qiu, S., Zhong, S., Zhao, L., Chen, F., Lai, S., Qi, Z., Huang, L., & Wang, Y. (2018). Disrupted Cerebellar Connectivity With the Central Executive Network and the Default-Mode Network in Unmedicated Bipolar II Disorder.

Frontiers in Psychiatry, *9*, 705. https://doi.org/10.3389/fpsyt.2018.00705

Lynch, C. J., Power, J. D., Scult, M. A., Dubin, M., Gunning, F. M., Correspondence, L., & Liston, C. (2020). Rapid Precision Functional Mapping of Individuals Using Multi-Echo fMRI ll Rapid Precision Functional Mapping of Individuals Using Multi-Echo fMRI. *CellReports*, *33*, 108540. https://doi.org/10.1016/j.celrep.2020.108540

Madan, C. R. (2017). Advances in studying brain morphology: The benefits of open-access data. *Frontiers in Human Neuroscience*, *11*, 405. https://doi.org/10.3389/fnhum.2017.00405

Madan, C. R., & Kensinger, E. A. (2018). Predicting age from cortical structure across the lifespan. *European Journal of Neuroscience*, *47*(5), 399–416. https://doi.org/10.1111/ejn.13835

Mak, L. E., Minuzzi, L., MacQueen, G., Hall, G., Kennedy, S. H., & Milev, R. (2017). The Default Mode Network in Healthy Individuals: A Systematic Review and Meta-Analysis. *Brain Connectivity*, *7*(1), 25–33. https://doi.org/10.1089/brain.2016.0438

Malagurski, B., Liem, F., Oschwald, J., Mérillat, S., & Jäncke, L. (2020). Longitudinal functional brain network reconfiguration in healthy aging. *Human Brain Mapping*, *41*(17), 4829–4845. https://doi.org/10.1002/hbm.25161

Manoliu, A., Riedl, V., Zherdin, A., Mühlau, M., Schwerthöffer, D., Scherr, M., Peters, H., Zimmer, C., Förstl, H., Bäuml, J., Wohlschläger, A. M., & Sorg, C. (2014). Aberrant dependence of default mode/central executive network interactions on anterior insular salience network activity in schizophrenia. *Schizophrenia Bulletin*, *40*(2), 428–437. https://doi.org/10.1093/schbul/sbt037

Mantini, D., Perrucci, M. G., Del Gratta, C., Romani, G. L., & Corbetta, M. (2007).

Electrophysiological signatures of resting state networks in the human brain.

Proceedings of the National Academy of Sciences of the United States of America,

104(32), 13170–13175. https://doi.org/10.1073/pnas.0700668104

Marinsek, N. (2017). *30 years of trends in the MRI and fMRI literatures.*

https://nikkimarinsek.com/blog/fmri-bursts

Marstaller, L., Williams, M., Rich, A., Savage, G., & Burianová, H. (2015). Aging and large-

scale functional networks: White matter integrity, gray matter volume, and functional

connectivity in the resting state. *Neuroscience, 290,* 369–378.

https://doi.org/10.1016/j.neuroscience.2015.01.049

Martin, J. B. (1999). Molecular Basis of the Neurodegenerative Disorders. *New England*

Journal of Medicine, 340(25), 1970–1980.

https://doi.org/10.1056/nejm199906243402507

Martuzzi, R., Ramani, R., Qiu, M., Rajeevan, N., & Constable, R. T. (2010). Functional

connectivity and alterations in baseline brain state in humans. *NeuroImage, 49*(1), 823–

834. https://doi.org/10.1016/j.neuroimage.2009.07.028

Messé, A., Rudrauf, D., Giron, A., & Marrelec, G. (2015). Predicting functional connectivity

from structural connectivity via computational models using MRI: An extensive

comparison study. *NeuroImage, 111,* 65–75.

https://doi.org/10.1016/j.neuroimage.2015.02.001

Millar, P. R., Ances, B. M., Gordon, B. A., Benzinger, T. L. S., Morris, J. C., & Balota, D.

A. (2020). Evaluating Cognitive Relationships with Resting-State and Task-driven

Blood Oxygen Level-Dependent Variability. *Journal of Cognitive Neuroscience*, 1–24.

https://doi.org/10.1162/jocn_a_01645

Millar, P. R., Petersen, S. E., Ances, B. M., Gordon, B. A., Benzinger, T. L. S., Morris, J.

C., & Balota, D. A. (2020). Evaluating the Sensitivity of Resting-State BOLD

Variability to Age and Cognition after Controlling for Motion and Cardiovascular

Influences: A Network-Based Approach. *Cerebral Cortex*, *30*(11), 5686–5701.

https://doi.org/10.1093/cercor/bhaa138

Mowinckel, A. M., Espeseth, T., & Westlye, L. T. (2012). Network-specific effects of age and

in-scanner subject motion: A resting-state fMRI study of 238 healthy adults.

NeuroImage, *63*(3), 1364–1373. https://doi.org/10.1016/j.neuroimage.2012.08.004

Mueller, S., Wang, D., Fox, M. D., Yeo, B. T. T., Sepulcre, J., Sabuncu, M. R., Shafee, R.,

Lu, J., & Liu, H. (2013). Individual Variability in Functional Connectivity Architecture

of the Human Brain. *Neuron*, *77*(3), 586–595.

https://doi.org/10.1016/j.neuron.2012.12.028

Mulders, P. C., van Eijndhoven, P. F., Schene, A. H., Beckmann, C. F., & Tendolkar, I.

(2015). Resting-state functional connectivity in major depressive disorder: A review.

Neuroscience and Biobehavioral Reviews, *56*(9), 330–344.

https://doi.org/10.1016/j.neubiorev.2015.07.014

Müller, V. I., Cieslik, E. C., Laird, A. R., Fox, P. T., Radua, J., Mataix-Cols, D., Tench, C.

R., Yarkoni, T., Nichols, T. E., Turkeltaub, P. E., Wager, T. D., & Eickhoff, S. B.

(2018). Ten simple rules for neuroimaging meta-analysis. In *Neuroscience and*

Biobehavioral Reviews (Vol. 84, pp. 151–161). Elsevier Ltd.

https://doi.org/10.1016/j.neubiorev.2017.11.012

Narr, K. L., Bilder, R. M., Toga, A. W., Woods, R. P., Rex, D. E., Szeszko, P. R.,

Robinson, D., Sevy, S., Gunduz-Bruce, H., Wang, Y.-P., DeLuca, H., & Thompson, P.

M. (2005). Mapping Cortical Thickness and Gray Matter Concentration in First

Episode Schizophrenia. *Cerebral Cortex*, *15*(6), 708–719.

https://doi.org/10.1093/CERCOR/BHH172

Nichols, T. E., Das, S., Eickhoff, S. B., Evans, A. C., Glatard, T., Hanke, M., Kriegeskorte,

N., Milham, M. P., Poldrack, R. A., Poline, J. B., Proal, E., Thirion, B., Van Essen, D.

C., White, T., & Yeo, B. T. T. (2017). Best practices in data analysis and sharing in

neuroimaging using MRI. *Nature Neuroscience*, *20*(3), 299–303.

https://doi.org/10.1038/nn.4500

Niendam, T. A., Laird, A. R., Ray, K. L., Dean, Y. M., Glahn, D. C., & Carter, C. S.

(2012). Meta-analytic evidence for a superordinate cognitive control network subserving

diverse executive functions. *Cognitive, Affective and Behavioral Neuroscience*, *12*(2),

241–268. https://doi.org/10.3758/s13415-011-0083-5

Nieuwenhuis, S., Forstmann, B. U., & Wagenmakers, E. J. (2011). Erroneous analyses of

interactions in neuroscience: A problem of significance. In *Nature Neuroscience* (Vol.

14, Issue 9, pp. 1105–1107). Nature Publishing Group. https://doi.org/10.1038/nn.2886

Nilsson, L. G., Adolfsson, R., Bäckman, L., De Frias, C. M., Molander, B., & Nyberg, L.

(2004). Betula: A prospective cohort study on memory, health and aging. *Aging,*

Neuropsychology, and Cognition, *11*(2–3), 134–148.

https://doi.org/10.1080/13825580490511026

Nilsson, L. G., Bäckman, L., Erngrund, K., Nyberg, L., Adolfsson, R., Bucht, G., Karlsson, S., Widing, M., & Winblad, B. (1997). The betula prospective cohort study: Memory, health, and aging. *Aging, Neuropsychology, and Cognition*, *4*(1), 1–32. https://doi.org/10.1080/13825589708256633

Noble, S., Scheinost, D., & Constable, R. T. (2019). A decade of test-retest reliability of functional connectivity: A systematic review and meta-analysis. *NeuroImage*, *203*, 116157. https://doi.org/10.1016/j.neuroimage.2019.116157

Nomi, J. S., Bolt, T. S., Chiemeka Ezie, C. E., Uddin, L. Q., & Heller, A. S. (2017). Moment-to-moment BOLD signal variability reflects regional changes in neural flexibility across the lifespan. *Journal of Neuroscience*, *37*(22), 5539–5548. https://doi.org/10.1523/JNEUROSCI.3408-16.2017

Nuzzo, R. (2015). How scientists fool themselves - And how they can stop. *Nature*, *526*(7572), 182–185. https://doi.org/10.1038/526182a

O'Connor, E. E., & Zeffiro, T. A. (2019). Why is Clinical fMRI in a Resting State? *Frontiers in Neurology*, *10*(APR), 420. https://doi.org/10.3389/fneur.2019.00420

Ogawa, S., Lee, T. -M, Nayak, A. S., & Glynn, P. (1990). Oxygenation-sensitive contrast in magnetic resonance image of rodent brain at high magnetic fields. *Magnetic Resonance in Medicine*, *14*(1), 68–78. https://doi.org/10.1002/mrm.1910140108

Oi, H., Hashimoto, T., Nozawa, T., Kanno, A., Kawata, N., Hirano, K., Yamamoto, Y., Sugiura, M., & Kawashima, R. (2017). Neural correlates of ambient thermal sensation: An fMRI study. *Scientific Reports*, *7*(1), 1–11. https://doi.org/10.1038/s41598-017-11802-z

Onoda, K., Ishihara, M., & Yamaguchi, S. (2012). Decreased functional connectivity by

aging is associated with cognitive decline. *Journal of Cognitive Neuroscience*, *24*(11),

2186–2198. https://doi.org/10.1162/jocn_a_00269

Orban, C., Kong, R., Li, J., Chee, M. W. L., & Yeo, B. T. T. (2020). Time of day is

associated with paradoxical reductions in global signal fluctuation and functional

connectivity. *PLoS Biology*, *18*(2), e3000602.

https://doi.org/10.1371/journal.pbio.3000602

Pan, P., Zhang, Y., Liu, Y., Zhang, H., Guan, D., & Xu, Y. (2017). Abnormalities of

regional brain function in Parkinson's disease: A meta-analysis of resting state

functional magnetic resonance imaging studies. *Scientific Reports*, *7*(1), 1–10.

https://doi.org/10.1038/srep40469

Park, D. C., Polk, T. A., Park, R., Minear, M., Savage, A., & Smith, M. R. (2004). Aging

reduces neural specialization in ventral visual cortex. *Proceedings of the National

Academy of Sciences of the United States of America*, *101*(35), 13091–13095.

https://doi.org/10.1073/pnas.0405148101

Pashler, H., & Harris, C. R. (2012). Is the Replicability Crisis Overblown? Three Arguments

Examined. *Perspectives on Psychological Science.*

https://doi.org/10.1177/1745691612463401

Peel, N., Bartlett, H., & McClure, R. (2004). Healthy ageing: how is it defined and

measured? *Australasian Journal on Ageing*, *23*(3), 115–119.

https://doi.org/10.1111/j.1741-6612.2004.00035.x

Pinto, M. S., dos Santos, A. C., & Salmon, C. E. G. (2020). Age-related assessment of

diffusion parameters in specific brain tracts correlated with cortical thinning.
Neurological Sciences, 1–11. https://doi.org/10.1007/s10072-020-04688-9

Poldrack, R. A. (2011). Inferring mental states from neuroimaging data: From reverse
inference to large-scale decoding. *Neuron, 72*(5), 692–697.
https://doi.org/10.1016/j.neuron.2011.11.001

Poldrack, R. A. (2018). *The new mind readers: What neuroimaging can and cannot reveal
about our thoughts.*
https://books.google.com/books?hl=en&lr=&id=E3OYDwAAQBAJ&oi=fnd&pg=PP1
3&dq=the+new+mind+readers&ots=YsJHWBqVkT&sig=wUDfMJOM1ZMNVkvj40Y
7T--1H-s

Poldrack, R. A., Baker, C. I., Durnez, J., Gorgolewski, K. J., Matthews, P. M., Munafò, M.
R., Nichols, T. E., Poline, J. B., Vul, E., & Yarkoni, T. (2017). Scanning the horizon:
Towards transparent and reproducible neuroimaging research. *Nature Reviews
Neuroscience, 18*(2), 115–126. https://doi.org/10.1038/nrn.2016.167

Poldrack, R. A., & Gorgolewski, K. J. (2014). Making big data open: Data sharing in
neuroimaging. *Nature Neuroscience, 17*(11), 1510–1517.
https://doi.org/10.1038/nn.3818

Poldrack, R. A., Laumann, T. O., Koyejo, O., Gregory, B., Hover, A., Chen, M. Y.,
Gorgolewski, K. J., Luci, J., Joo, S. J., Boyd, R. L., Hunicke-Smith, S., Simpson, Z. B.,
Caven, T., Sochat, V., Shine, J. M., Gordon, E., Snyder, A. Z., Adeyemo, B., Petersen,
S. E., … Mumford, J. A. (2015). Long-term neural and physiological phenotyping of a
single human. *Nature Communications, 6*(1), 1–15.

https://doi.org/10.1038/ncomms9885

Pritschet, L., Santander, T., Taylor, C. M., Layher, E., Yu, S., Miller, M. B., Grafton, S. T., & Jacobs, E. G. (2020). Functional reorganization of brain networks across the human menstrual cycle. *NeuroImage*, *220*, 117091. https://doi.org/10.1016/j.neuroimage.2020.117091

Provenzano, J., Verduyn, P., Daniels, N., Fossati, P., & Kuppens, P. (2019). Mood congruency effects are mediated by shifts in salience and central executive network efficiency. *Social Cognitive and Affective Neuroscience*, *14*(9), 987–995. https://doi.org/10.1093/scan/nsz065

Pur, D. R., Eagleson, R. A., de Ribaupierre, A., Mella, N., & de Ribaupierre, S. (2019). Moderating Effect of Cortical Thickness on BOLD Signal Variability Age-Related Changes. *Frontiers in Aging Neuroscience.* https://doi.org/10.3389/fnagi.2019.00046

Purves, D., Cabeza, R., Huettel, S. A., LaBar, K. S., Platt, M. L., Woldorff, M. G., & Brannon, E. M. (2013). *Cognitive neuroscience.* Sunderland: Sinauer Associates, Inc.

R Core Team. (2017). *R: A language and environment for statistical computing.* R Foundation for Statistical Computing. https://www.r-project.org/

Raichle, M. E. (2015). The Brain's Default Mode Network. *Annual Review of Neuroscience*, *38*, 433–447. https://doi.org/10.1146/annurev-neuro-071013-014030

Raichle, M. E., MacLeod, A. M., Snyder, A. Z., Powers, W. J., Gusnard, D. A., & Shulman, G. L. (2001). A default mode of brain function. *Proceedings of the National Academy of Sciences of the United States of America*, *98*(2), 676–682. https://doi.org/10.1073/pnas.98.2.676

Rakić, M., Cabezas, M., Kushibar, K., Oliver, A., & Lladó, X. (2020). Improving the

detection of autism spectrum disorder by combining structural and functional MRI

information. *NeuroImage: Clinical*, *25*, 102181.

https://doi.org/10.1016/j.nicl.2020.102181

Reineberg, A. E., Gustavson, D. E., Benca, C., Banich, M. T., & Friedman, N. P. (2018).

The relationship between resting state network connectivity and individual differences

in executive functions. *Frontiers in Psychology*, *9*, 1–14.

https://doi.org/10.3389/fpsyg.2018.01600

Reishofer, G., Studencnik, F., Koschutnig, K., Deutschmann, H., Ahammer, H., & Wood, G.

(2018). Age is reflected in the Fractal Dimensionality of MRI Diffusion Based

Tractography. *Scientific Reports*, *8*(1), 1–9. https://doi.org/10.1038/s41598-018-23769-6

Rieck, J. R., Baracchini, G., & Grady, C. L. (2021). Contributions of Brain Function and

Structure to Three Different Domains of Cognitive Control in Normal Aging. *Journal of

Cognitive Neuroscience*, 1–22. https://doi.org/10.1162/jocn_a_01685

Riemer, F., Grüner, R., Beresniewicz, J., Kazimierczak, K., Ersland, L., & Hugdahl, K.

(2020). Dynamic switching between intrinsic and extrinsic mode networks as demands

change from passive to active processing. *Scientific Reports 2020 10:1*, *10*(1), 1–10.

https://doi.org/10.1038/s41598-020-78579-6

Roe, J. M., Vidal-Piñeiro, D., Sørensen, Ø., Brandmaier, A. M., Düzel, S., Gonzalez, H. A.,

Kievit, R. A., Knights, E., Kühn, S., Lindenberger, U., Mowinckel, A. M., Nyberg, L.,

Park, D. C., Pudas, S., Rundle, M. M., Walhovd, K. B., Fjell, A. M., & Westerhausen,

R. (2021). Asymmetric thinning of the cerebral cortex across the adult lifespan is

accelerated in Alzheimer's disease. *Nature Communications*, *12*(1), 721.

https://doi.org/10.1038/s41467-021-21057-y

Romero-Garcia, R., Atienza, M., & Cantero, J. L. (2014). Predictors of coupling between

structural and functional cortical networks in normal aging. *Human Brain Mapping*,

35(6), 2724–2740. https://doi.org/10.1002/hbm.22362

Rosenthal, G., Váša, F., Griffa, A., Hagmann, P., Amico, E., Goñi, J., Avidan, G., &

Sporns, O. (2018). Mapping higher-order relations between brain structure and function

with embedded vector representations of connectomes. *Nature Communications*, *9*(1),

1–12. https://doi.org/10.1038/s41467-018-04614-w

Rowe, J. B., Hughes, L. E., Barker, R. A., & Owen, A. M. (2010). Dynamic causal modelling

of effective connectivity from fMRI: Are results reproducible and sensitive to

Parkinson's disease and its treatment? *NeuroImage*, *52*(3), 1015–1026.

https://doi.org/10.1016/J.NEUROIMAGE.2009.12.080

Saenger, V. M., Barrios, F. A., Martínez-Gudiño, M. L., & Alcauter, S. (2012). Hemispheric

asymmetries of functional connectivity and grey matter volume in the default mode

network. *Neuropsychologia*, *50*(7), 1308–1315.

https://doi.org/10.1016/J.NEUROPSYCHOLOGIA.2012.02.014

Sala-Llonch, R., Bartrés-Faz, D., & Junqué, C. (2015). Reorganization of brain networks in

aging: a review of functional connectivity studies. *Frontiers in Psychology*, *6*.

https://doi.org/10.3389/fpsyg.2015.00663

Salami, A., Pudas, S., & Nyberg, L. (2014). Elevated hippocampal resting-state connectivity

underlies deficient neurocognitive function in aging. *Proceedings of the National*

Academy of Sciences of the United States of America.

https://doi.org/10.1073/pnas.1410233111

Sang, L., Zhang, J., Wang, L., Zhang, J., Zhang, Y., Li, P., Wang, J., & Qiu, M. (2015).

Alteration of brain functional networks in early-stage Parkinson's disease: A resting-

state fMRI study. *PLoS ONE*, *10*(10). https://doi.org/10.1371/journal.pone.0141815

Sanz-Arigita, E. J., Schoonheim, M. M., Damoiseaux, J. S., Rombouts, S. A. R. B., Maris,

E., Barkhof, F., Scheltens, P., & Stam, C. J. (2010). Loss of "Small-World" Networks in

Alzheimer's Disease: Graph Analysis of fMRI Resting-State Functional Connectivity.

PLoS ONE, *5*(11). https://doi.org/10.1371/journal.pone.0013788

Scouten, A., & Constable, R. T. (2007). Applications and limitations of whole-brain MAGIC

VASO functional imaging. *Magnetic Resonance in Medicine*, *58*(2), 306–315.

https://doi.org/10.1002/mrm.21273

Seghier, M. L. (2008). Laterality index in functional MRI: methodological issues. *Magnetic

Resonance Imaging*, *26*(5), 594. https://doi.org/10.1016/J.MRI.2007.10.010

Seitzman, B. A., Gratton, C., Laumann, T. O., Gordon, E. M., Adeyemo, B., Dworetsky, A.,

Kraus, B. T., Gilmore, A. W., Berg, J. J., Ortega, M., Nguyen, A., Greene, D. J.,

McDermott, K. B., Nelson, S. M., Lessov-Schlaggar, C. N., Schlaggar, B. L.,

Dosenbach, N. U. F., & Petersen, S. E. (2019). Trait-like variants in human functional

brain networks. *Proceedings of the National Academy of Sciences of the United States

of America*, *116*(45), 22851–22861. https://doi.org/10.1073/pnas.1902932116

Serra, L., Cercignani, M., Mastropasqua, C., Torso, M., Spanò, B., Makovac, E., Viola, V.,

Giulietti, G., Marra, C., Caltagirone, C., & Bozzali, M. (2016). Longitudinal changes in

functional brain connectivity predicts conversion to Alzheimer's disease. *Journal of Alzheimer's Disease*, *51*(2), 377–389. https://doi.org/10.3233/JAD-150961

Shaw, M. E., Abhayaratna, W. P., Sachdev, P. S., Anstey, K. J., & Cherbuin, N. (2016). Cortical Thinning at Midlife: The PATH Through Life Study. *Brain Topography*, *29*, 875–884. https://doi.org/10.1007/s10548-016-0509-z

Shulman, G. L., Fiez, J. A., Corbetta, M., Buckner, R. L., Miezin, F. M., Raichle, M. E., & Petersen, S. E. (1997). Common blood flow changes across visual tasks: II. Decreases in cerebral cortex. *Journal of Cognitive Neuroscience*, *9*, 648–663. https://doi.org/10.1162/jocn.1997.9.5.648

Simmons, J. P., Nelson, L. D., & Simonsohn, U. (2011). False-positive psychology: Undisclosed flexibility in data collection and analysis allows presenting anything as significant. *Psychological Science*, *22*(11), 1359–1366. https://doi.org/10.1177/0956797611417632

Šimundić, A.-M. (2009). Measures of Diagnostic Accuracy: Basic Definitions. *EJIFCC*, *19*(4), 203–211. http://www.ncbi.nlm.nih.gov/pubmed/27683318

Skouras, S., Gray, M., Critchley, H., & Koelsch, S. (2013). fMRI Scanner Noise Interaction with Affective Neural Processes. *PLoS ONE*, *8*(11), e80564. https://doi.org/10.1371/journal.pone.0080564

Skouras, S., & Scharnowski, F. (2019). The effects of psychiatric history and age on self-regulation of the default mode network. *NeuroImage*, *198*, 150–159. https://doi.org/10.1016/j.neuroimage.2019.05.008

Smith, S. M., Vidaurre, D., Beckmann, C. F., Glasser, M. F., Jenkinson, M., Miller, K. L.,

Nichols, T. E., Robinson, E. C., Salimi-Khorshidi, G., Woolrich, M. W., Barch, D. M., Uğurbil, K., & Van Essen, D. C. (2013). Functional connectomics from resting-state fMRI. In *Trends in Cognitive Sciences* (Vol. 17, Issue 12, pp. 666–682). Elsevier Current Trends. https://doi.org/10.1016/j.tics.2013.09.016

Snyder, A. Z. (2016). Intrinsic Brain Activity and Resting State Networks. *Neuroscience in the 21st Century: From Basic to Clinical, Second Edition*, 1625–1676. https://doi.org/10.1007/978-1-4939-3474-4_133

Sokolov, A. A., Zeidman, P., Erb, M., Ryvlin, P., Pavlova, M. A., & Friston, K. J. (2018). Linking structural and effective brain connectivity: structurally informed Parametric Empirical Bayes (si-PEB). *Brain Structure and Function 2018 224:1*, *224*(1), 205–217. https://doi.org/10.1007/S00429-018-1760-8

Somandepalli, K., Kelly, C., Reiss, P. T., Zuo, X. N., Craddock, R. C., Yan, C. G., Petkova, E., Castellanos, F. X., Milham, M. P., & Di Martino, A. (2015). Short-term test–retest reliability of resting state fMRI metrics in children with and without attention-deficit/hyperactivity disorder. *Developmental Cognitive Neuroscience*, *15*, 83–93. https://doi.org/10.1016/J.DCN.2015.08.003

Specht, K. (2020). Current Challenges in Translational and Clinical fMRI and Future Directions. In *Frontiers in Psychiatry.* https://doi.org/10.3389/fpsyt.2019.00924

Spreng, R. N., Stevens, W. D., Viviano, J. D., & Schacter, D. L. (2016). Attenuated anticorrelation between the default and dorsal attention networks with aging: evidence from task and rest. *Neurobiology of Aging*, *45*, 149–160. https://doi.org/10.1016/j.neurobiolaging.2016.05.020

Sridharan, D., Levitin, D. J., & Menon, V. (2008). A critical role for the right fronto-insular cortex in switching between central-executive and default-mode networks. *Proceedings of the National Academy of Sciences of the United States of America*, *105*(34), 12569–12574. https://doi.org/10.1073/pnas.0800005105

Stumme, J., Jockwitz, C., Hoffstaedter, F., Amunts, K., & Caspers, S. (2020). Functional network reorganization in older adults: Graph-theoretical analyses of age, cognition and sex. *NeuroImage*, *214*, 116756. https://doi.org/10.1016/j.neuroimage.2020.116756

Sun, G., Qian, S., Jiang, Q., Liu, K., Li, B., Li, M., Zhao, L., Zhou, Z., von Deneen, K. M., & Liu, Y. (2013). Hyperthermia-Induced Disruption of Functional Connectivity in the Human Brain Network. *PLoS ONE*, *8*(4), e61157. https://doi.org/10.1371/journal.pone.0061157

Tardif, C. L., Schäfer, A., Trampel, R., Villringer, A., Turner, R., & Bazin, P. L. (2016). Open Science CBS Neuroimaging Repository: Sharing ultra-high-field MR images of the brain. *NeuroImage*, *124*(Part B), 1143–1148. https://doi.org/10.1016/j.neuroimage.2015.08.042

Thomas, R. M., Gallo, S., Cerliani, L., Zhutovsky, P., El-Gazzar, A., & van Wingen, G. (2020). Classifying Autism Spectrum Disorder Using the Temporal Statistics of Resting-State Functional MRI Data With 3D Convolutional Neural Networks. *Frontiers in Psychiatry*, *11*, 1. https://doi.org/10.3389/fpsyt.2020.00440

Tian, L., Wang, J., Yan, C., & He, Y. (2011). Hemisphere- and gender-related differences in small-world brain networks: A resting-state functional MRI study. *NeuroImage*, *54*(1), 191–202. https://doi.org/10.1016/j.neuroimage.2010.07.066

Toga, A. W., & Thompson, P. M. (2003). Mapping brain asymmetry. *Nature Reviews*

   Neuroscience, 4(1), 37–48. https://doi.org/10.1038/nrn1009

Tomasi, D., & Volkow, N. D. (2012). Aging and functional brain networks. *Molecular*

   Psychiatry, 17(5), 549–558. https://doi.org/10.1038/mp.2011.81

Tsang, A., Lebel, C. A., Bray, S. L., Goodyear, B. G., Hafeez, M., Sotero, R. C., McCreary,

   C. R., & Frayne, R. (2017). White Matter Structural Connectivity Is Not Correlated to

   Cortical Resting-State Functional Connectivity over the Healthy Adult Lifespan.

   Frontiers in Aging Neuroscience, 9(MAY), 144.

   https://doi.org/10.3389/fnagi.2017.00144

Tsvetanov, K. A., Gazzina, S., Jones, S. P., Swieten, J. van, Borroni, B., Sanchez-Valle, R.,

   Moreno, F., Jr., R. L., Graff, C., Synofzik, M., Galimberti, D., Masellis, M., Tartaglia,

   M. C., Finger, E., Vandenberghe, R., Mendonça, A. de, Tagliavini, F., Santana, I.,

   Ducharme, S., … (GENFI), T. G. F. I. (2020). Brain functional network integrity

   sustains cognitive function despite atrophy in presymptomatic genetic frontotemporal

   dementia. *MedRxiv.* https://doi.org/https://doi.org/10.1101/19012203

Tsvetanov, K. A., Henson, R., Jones, P. S., Mutsaerts, H.-J., Fuhrmann, D., Tyler, L., &

   Rowe, J. (2019). The effects of age on resting-state BOLD signal variability is explained

   by cardiovascular and neurovascular factors. *BioRxiv.* https://doi.org/10.1101/836619

Tsvetanov, K. A., Henson, R. N. A., & Rowe, J. B. (2020). *Separating vascular and neuronal*

   effects of age on fMRI BOLD signals. 376(1815), 1–20.

   https://doi.org/https://doi.org/10.1098/rstb.2019.0631

Tsvetanov, K. A., Henson, R. N. A., Tyler, L. K., Davis, S. W., Shafto, M. A., Taylor, J. R.,

Williams, N., Cam-CAN, & Rowe, J. B. (2015). The effect of ageing on fMRI: Correction for the confounding effects of vascular reactivity evaluated by joint fMRI and MEG in 335 adults. *Human Brain Mapping*, *36*(6), 2248–2269. https://doi.org/10.1002/hbm.22768

Tsvetanov, K. A., Henson, R. N., Tyler, L. K., Razi, A., Geerligs, L., Ham, T. E., & Rowe, J. B. (2016). Extrinsic and intrinsic brain network connectivity maintains cognition across the lifespan despite accelerated decay of regional brain activation. *Journal of Neuroscience*, *36*(11), 3115–3126. https://doi.org/10.1523/JNEUROSCI.2733-15.2016

Turner, B. O., Paul, E. J., Miller, M. B., & Barbey, A. K. (2018). Small sample sizes reduce the replicability of task-based fMRI studies. *Communications Biology*, *1*(1), 1–10. https://doi.org/10.1038/s42003-018-0073-z

Uddin, L. Q. (2015). Salience processing and insular cortical function and dysfunction. *Nature Reviews Neuroscience*, *16*(1), 55–61. https://doi.org/10.1038/nrn3857

Uh, J., Lin, A. L., Lee, K., Liu, P., Fox, P., & Lu, H. (2011). Validation of VASO cerebral blood volume measurement with positron emission tomography. *Magnetic Resonance in Medicine*, *65*(3), 744–749. https://doi.org/10.1002/mrm.22667

United Nations. (2019). *World Population Ageing 2019: Highlights.* https://www.un.org/en/development/desa/population/publications/pdf/ageing/WorldPopulationAgeing2019-Highlights.pdf

Vaisvilaite, L., Hushagen, V., Grønli, J., & Specht, K. (2020). Time-of-day influence on resting-state fMRI: an overlooked factor contributing to the replication crisis? *BioRxiv*. https://doi.org/10.1101/2020.08.20.258517

van den Heuvel, M. P., & Hulshoff Pol, H. E. (2010). Exploring the brain network: A review

on resting-state fMRI functional connectivity. *European Neuropsychopharmacology*,

20(8), 519–534. https://doi.org/10.1016/j.euroneuro.2010.03.008

Van Horn, J. D., & Gazzaniga, M. S. (2013). Why share data? Lessons learned from the

fMRIDC. In *NeuroImage* (Vol. 82, pp. 677–682). Academic Press.

https://doi.org/10.1016/j.neuroimage.2012.11.010

Varangis, E., Habeck, C. G., Razlighi, Q. R., & Stern, Y. (2019). The Effect of Aging on

Resting State Connectivity of Predefined Networks in the Brain. *Frontiers in Aging*

Neuroscience, *11*(234). https://doi.org/10.3389/fnagi.2019.00234

Vieira, B. H., Rondinoni, C., & Garrido Salmon, C. E. (2020). Evidence of regional

associations between age-related inter-individual differences in resting-state functional

connectivity and cortical thinning revealed through a multi-level analysis. *NeuroImage*,

211, 116662. https://doi.org/10.1016/j.neuroimage.2020.116662

Voss, M. W., Erickson, K. I., Chaddock, L., Prakash, R. S., Colcombe, S. J., Morris, K. S.,

Doerksen, S., Hu, L., McAuley, E., & Kramer, A. F. (2008). Dedifferentiation in the

visual cortex: An fMRI investigation of individual differences in older adults. *Brain*

Research, *1244*, 121–131. https://doi.org/10.1016/j.brainres.2008.09.051

Voss, M. W., Erickson, K. I., Prakash, R. S., Chaddock, L., Malkowski, E., Alves, H., Kim,

J. S., Morris, K. S., White, S. M., Wójcicki, T. R., Hu, L., Szabo, A., Klamm, E.,

McAuley, E., & Kramer, A. F. (2010). Functional connectivity: A source of variance in

the association between cardiorespiratory fitness and cognition? *Neuropsychologia*.

https://doi.org/10.1016/j.neuropsychologia.2010.01.005

Vul, E., Harris, C., Winkielman, P., & Pashler, H. (2009). Puzzlingly High Correlations in

fMRI Studies of Emotion, Personality, and Social Cognition. *Perspectives on

Psychological Science : A Journal of the Association for Psychological Science*, *4*(3),

274–290. https://doi.org/10.1111/j.1745-6924.2009.01125.x

Wang, J., Li, W., Miao, W., Dai, D., Hua, J., & He, H. (2014). Age estimation using cortical

surface pattern combining thickness with curvatures. *Medical and Biological

Engineering and Computing*, *52*(4), 331–341. https://doi.org/10.1007/s11517-013-1131-9

Wang, L., Zhang, Y., Zhang, J., Sang, L., Li, P., Yan, R., Qiu, M., & Liu, C. (2019). Aging

Changes Effective Connectivity of Motor Networks During Motor Execution and Motor

Imagery. *Frontiers in Aging Neuroscience*, *11*. https://doi.org/10.3389/fnagi.2019.00312

Wang, Zhijiang, Dai, Z., Gong, G., Zhou, C., & He, Y. (2014). Understanding Structural-

Functional Relationships in the Human Brain: A Large-Scale Network Perspective.

Http://Dx.Doi.Org.Pva.Uib.No/10.1177/1073858414537560, *21*(3), 290–305.

https://doi.org/10.1177/1073858414537560

Wang, Zhiqun, Wang, J., Zhang, H., Mchugh, R., Sun, X., Li, K., & Yang, Q. X. (2015).

Interhemispheric functional and structural disconnection in Alzheimer's disease: A

combined resting-state fMRI and DTI study. *PLoS ONE*, *10*(5).

https://doi.org/10.1371/journal.pone.0126310

Waring, J. D., Addis, D. R., & Kensinger, E. A. (2013). Effects of aging on neural

connectivity underlying selective memory for emotional scenes. *Neurobiology of Aging*,

34(2), 451–467. https://doi.org/10.1016/j.neurobiolaging.2012.03.011

Wei, L., Zhang, J., Long, Z., Wu, G. R., Hu, X., Zhang, Y., & Wang, J. (2014). Reduced

topological efficiency in cortical-basal ganglia motor network of parkinson's disease: A

resting state fMRI Study. *PLoS ONE*, *9*(10).

https://doi.org/10.1371/journal.pone.0108124

West, K. L., Zuppichini, M. D., Turner, M. P., Sivakolundu, D. K., Zhao, Y., Abdelkarim,

D., Spence, J. S., & Rypma, B. (2019). BOLD hemodynamic response function changes

significantly with healthy aging. *NeuroImage*, *188*, 198–207.

https://doi.org/10.1016/j.neuroimage.2018.12.012

WHO. (2020). *Healthy ageing and functional ability.* Healthy Ageing and Functional Ability.

https://www.who.int/westernpacific/news/q-a-detail/ageing-healthy-ageing-and-

functional-ability#:~:text=WHO defines healthy ageing as,they have reason to value.

Wicherts, J. (2017). File Drawer Problem. In *Encyclopedia of Personality and Individual

Differences* (pp. 1–3). https://doi.org/10.1007/978-3-319-28099-8_1307-1

Wicherts, J., Veldkamp, C. L. S., Augusteijn, H. E. M., Bakker, M., van Aert, R. C. M., &

van Assen, M. A. L. M. (2016). Degrees of freedom in planning, running, analyzing, and

reporting psychological studies: A checklist to avoid P-hacking. In *Frontiers in

Psychology.* https://doi.org/10.3389/fpsyg.2016.01832

Wink, A. M. (2019). Eigenvector centrality dynamics from resting-state fMRI: Gender and

age differences in healthy subjects. *Frontiers in Neuroscience*, *13*(JUN).

https://doi.org/10.3389/fnins.2019.00648

Woo, C. W., Krishnan, A., & Wager, T. D. (2014). Cluster-extent based thresholding in

fMRI analyses: Pitfalls and recommendations. *NeuroImage*, *91*, 412–419.

https://doi.org/10.1016/j.neuroimage.2013.12.058

Wu, C. W., Liu, H. L., Chen, J. H., & Yang, Y. (2010). Effects of CBV, CBF, and blood-brain barrier permeability on accuracy of PASL and VASO measurement. *Magnetic Resonance in Medicine*, *63*(3), 601–608. https://doi.org/10.1002/mrm.22165

Xu, C., Li, C., Wu, H., Wu, Y., Hu, S., Zhu, Y., Zhang, W., Wang, L., Zhu, S., Liu, J., Zhang, Q., Yang, J., & Zhang, X. (2015). Gender differences in cerebral regional homogeneity of adult healthy volunteers: A resting-state fMRI study. *BioMed Research International*, *2015*. https://doi.org/10.1155/2015/183074

Xu, M., Wang, Z., Zhang, H., Pantazis, D., Wang, H., & Li, Q. (2020). A new Graph Gaussian embedding method for analyzing the effects of cognitive training. *PLOS Computational Biology*, *16*(9), e1008186. https://doi.org/10.1371/journal.pcbi.1008186

Yao, D., Sui, J., Wang, M., Yang, E., Jiaerken, Y., Luo, N., Yap, P. T., Liu, M., & Shen, Di. (2021). A Mutual Multi-Scale Triplet Graph Convolutional Network for Classification of Brain Disorders Using Functional or Structural Connectivity. *IEEE Transactions on Medical Imaging*, *40*(4), 1279–1289. https://doi.org/10.1109/TMI.2021.3051604

Yarkoni, T. (2019). *The Generalizability Crisis*. PsyArXiv. https://doi.org/10.31234/OSF.IO/JQW35

Yassin, W., Nakatani, H., Zhu, Y., Kojima, M., Owada, K., Kuwabara, H., Gonoi, W., Aoki, Y., Takao, H., Natsubori, T., Iwashiro, N., Kasai, K., Kano, Y., Abe, O., Yamasue, H., & Koike, S. (2020). Machine-learning classification using neuroimaging data in schizophrenia, autism, ultra-high risk and first-episode psychosis. *Translational Psychiatry*, *10*(1), 1–11. https://doi.org/10.1038/s41398-020-00965-5

Yau, Y., Zeighami, Y., Baker, T. E., Larcher, K., Vainik, U., Dadar, M., Fonov, V. S., Hagmann, P., Griffa, A., Mišić, B., Collins, D. L., & Dagher, A. (2018). Network connectivity determines cortical thinning in early Parkinson's disease progression. *Nature Communications*, *9*(1), 1–10. https://doi.org/10.1038/s41467-017-02416-0

Yeo, B. T., Krienen, F. M., Sepulcre, J., Sabuncu, M. R., Lashkari, D., Hollinshead, M., Roffman, J. L., Smoller, J. W., Zöllei, L., Polimeni, J. R., Fisch, B., Liu, H., & Buckner, R. L. (2011). The organization of the human cerebral cortex estimated by intrinsic functional connectivity. *Journal of Neurophysiology*, *106*(3), 1125–1165. https://doi.org/10.1152/jn.00338.2011

Ystad, M., Hodneland, E., Adolfsdottir, S., Haász, J., Lundervold, A. J., Eichele, T., & Lundervold, A. (2011). Cortico-striatal connectivity and cognition in normal aging: A combined DTI and resting state fMRI study. *NeuroImage*, *55*(1), 24–31. https://doi.org/10.1016/j.neuroimage.2010.11.016

Zeidman, P., Jafarian, A., Corbin, N., Seghier, M. L., Razi, A., Price, C. J., & Friston, K. J. (2019). A guide to group effective connectivity analysis, part 1: First level analysis with DCM for fMRI. *NeuroImage*, *200*, 174–190. https://doi.org/10.1016/j.neuroimage.2019.06.031

Zeidman, P., Jafarian, A., Seghier, M., Litvak, V., NeuroImage, H. C.-, & 2019, U. (2019). A guide to group effective connectivity analysis, part 2: Second level analysis with PEB. *Elsevier*, *200*, 12–25. https://www.sciencedirect.com/science/article/pii/S1053811919305233

Zhang, C., Baum, S. A., Adduru, V. R., Biswal, B. B., & Michael, A. M. (2018). Test-retest

reliability of dynamic functional connectivity in resting state fMRI. *NeuroImage*, *183*, 907–918. https://doi.org/10.1016/j.neuroimage.2018.08.021

Zhang, C., Dougherty, C. C., Baum, S. A., White, T., & Michael, A. M. (2018). Functional connectivity predicts gender: Evidence for gender differences in resting brain connectivity. *Human Brain Mapping*, *39*(4), 1765–1776. https://doi.org/10.1002/hbm.23950

Zhang, Y., Zhang, H., Chen, X., Lee, S. W., & Shen, D. (2017). Hybrid High-order Functional Connectivity Networks Using Resting-state Functional MRI for Mild Cognitive Impairment Diagnosis. *Scientific Reports*, *7*(1), 1–15. https://doi.org/10.1038/s41598-017-06509-0

Zhao, X., Liu, Y., Wang, X., Liu, B., Xi, Q., Guo, Q., Jiang, H., Jiang, T., & Wang, P. (2012). Disrupted small-world brain networks in moderate Alzheimer's disease: A resting-state fMRI study. *PLoS ONE*, *7*(3), e33540. https://doi.org/10.1371/journal.pone.0033540

Zhou, B., Liu, Y., Zhang, Z., An, N., Yao, H., Wang, P., Wang, L., Zhang, X., & Jiang, T. (2013). Impaired Functional Connectivity of the Thalamus in Alzheimer’ s Disease and Mild Cognitive Impairment: A Resting-State fMRI Study. *Current Alzheimer Research*, *10*(7), 754–766. https://doi.org/10.2174/15672050113109990146

Zimmermann, J., Ritter, P., Shen, K., Rothmeier, S., Schirner, M., & McIntosh, A. R. (2016). Structural architecture supports functional organization in the human aging brain at a regionwise and network level. *Human Brain Mapping*, *37*(7), 2645–2661. https://doi.org/10.1002/hbm.23200

Zuo, N., Hu, T., Liu, H., Sui, J., Liu, Y., & Jiang, T. (2020). Gray Matter-Based Age

Prediction Characterizes Different Regional Patterns. In *Neuroscience Bulletin* (pp. 1–

5). Springer. https://doi.org/10.1007/s12264-020-00558-8

Zuo, X. N., & Xing, X. X. (2014). Test-retest reliabilities of resting-state FMRI

measurements in human brain functional connectomics: A systems neuroscience

perspective. In *Neuroscience and Biobehavioral Reviews* (Vol. 45, pp. 100–118).

https://doi.org/10.1016/j.neubiorev.2014.05.009

Zuo, X. N., Xu, T., & Milham, M. P. (2019). Harnessing reliability for neuroscience research.

Nature Human Behaviour, *3*(8), 768–771. https://doi.org/10.1038/s41562-019-0655-x

Appendices

Appendix A

Regions of Interest in the anterior Central Executive Network (for Dynamic Causal

Modelling)

Hemisphere	F Statistic	Cluster Size (mm²)	MNI Coordinates			Short Name
			x	y	z	
left	17.93	233.32	-40.2	47.2	3.7	Frontal_Mid_L
right	17.93	210.73	40.1	46	5.7	Frontal_Mid_R
right	4.755	198.48	6	10.7	29.8	Cingulum_Ant_R
left	4.755	170.32	-6.6	12.7	26.4	Cingulum_Ant_L
right	11.354	133.41	39.8	37.4	26.2	Frontal_Mid_R
left	16.916	117.43	-30.4	47.7	9.9	Frontal_Mid_L
left	11.354	116.7	-40.8	38.4	25.1	Frontal_Inf_Tri_L
right	16.916	91.96	29.4	46.7	13	Frontal_Mid_R
left	11.192	77.31	-38.3	41.9	-3.8	Frontal_Inf_Orb_L
left	6.535	67.68	-23.5	37.3	-10.8	Frontal_Mid_Orb_L
right	4.333	61.9	21.2	13.6	55.7	Frontal_Sup_R
left	4.333	59.96	-20	13.4	57.5	Frontal_Sup_L
right	11.192	58.34	38.6	43.2	0.7	Frontal_Inf_Tri_R
left	2.949	56.62	-10.1	14.2	50.7	Supp_Motor_Area_L
right	6.535	54.99	24.6	38	-12.2	Frontal_Sup_Orb_R
left	20.02	50.07	-35.9	29.8	33.9	Frontal_Mid_L
right	7.763	49.8	45.5	24.2	32.2	Frontal_Inf_Tri_R
right	2.949	46.94	10.3	14.5	49.1	Supp_Motor_Area_R
left	7.763	41.24	-45.4	26.8	28.9	Frontal_Inf_Tri_L
left	4.443	39.77	-28.9	10.2	47.6	Frontal_Mid_L
left	15.676	39.43	-25.8	35.3	32.2	Frontal_Mid_L
right	4.797	35.02	43.5	31.4	20.9	Frontal_Mid_R
right	20.02	34.87	34.3	28.4	34	Frontal_Mid_R
left	5.395	33.75	-23.6	44.1	18.3	Frontal_Mid_L
right	15.676	32.4	26.8	33.3	32.6	Frontal_Mid_R
right	4.443	31.4	27.7	13.6	44.2	Frontal_Mid_R
left	1.86	28.58	-30.5	43.3	-13	Frontal_Mid_Orb_L
left	4.797	26.3	-43.4	31.1	20.5	Frontal_Inf_Tri_L
left	1.185	23.68	-9.1	32.8	39.9	Frontal_Sup_Medial_L
right	1.86	23.31	32.6	48.8	-10.8	Frontal_Mid_Orb_R
right	5.395	21.93	23.8	41.7	22.6	Frontal_Sup_R

CONTINUATION APPENDIX A

Hemisphere	F Statistic	Cluster Size (mm²)	MNI Coordinates			Short Name
			x	y	z	
left	1.085	20.79	-28	6.5	53.9	Frontal_Mid_L
right	1.185	20.66	8.6	34.1	39.3	Frontal_Sup_Medial_R
right	14.073	19.38	8.8	24.3	38.4	Cingulum_Mid_R
left	14.073	16.52	-9.5	22.8	39.1	Cingulum_Mid_L
right	1.085	16.24	29	8.2	48.3	Frontal_Mid_R
left	1.638	12.52	-23.8	38.7	27.8	Frontal_Mid_L
left	1.607	12.18	-28.6	45.8	16.8	Frontal_Mid_L
right	1.638	11.5	27.4	39.3	30.3	Frontal_Mid_R
left	2.59	9.76	-12.6	32.5	27.2	Cingulum_Ant_L
right	2.59	8.91	14.6	32.6	26	Cingulum_Ant_R
right	1.607	7.5	27.3	41.1	18.6	Frontal_Mid_R

Appendix B

Regions of Interest in the posterior Central Executive Network (for Dynamic Causal

Modelling)

Hemisphere	F Statistic	Cluster Size (mm²)	MNI Coordinates			Short Name
			x	y	z	
left	9.348	87.11	-42.9	-54.5	36.5	Angular_L
right	9.348	85.06	41.4	-51.9	40.8	Parietal_Inf_R
right	4.779	83.6	54.6	-39.7	39.9	SupraMarginal_R
left	4.779	75.88	-56.2	-41.3	40.3	Parietal_Inf_L
left	11.682	69.37	-34.7	-66.1	42.7	Parietal_Inf_L
right	11.682	62.54	37.1	-62.9	45.1	Angular_R
right	14.281	10.07	15.3	-62.7	31.9	Precuneus_R
left	14.281	9.49	-15.2	-64.5	30.6	Precuneus_L
right	4.56	7.04	32.5	-55	39.5	Angular_R
left	4.56	5.63	-30.2	-55	35.7	Angular_L

Appendix C

Regions of Interest in the anterior Default Mode Network (for Dynamic Causal Modelling)

Hemisphere	F Statistic	Cluster Size (mm²)	MNI Coordinates			Short Name
			x	y	z	
left	21.269	1742.43	-7.1	54.2	30.3	Frontal_Sup_Medial_L
right	21.269	1678.16	6.8	52.2	31.6	Frontal_Sup_Medial_R
left	13.151	257.18	-23.5	21.1	35.7	Frontal_Mid_L
right	13.151	216.36	25.2	23.5	39.5	Frontal_Mid_R
right	5.985	153.71	19.8	61.4	-1.3	Frontal_Sup_Orb_R
left	5.985	146.01	-17.7	61.7	-4.5	Frontal_Sup_Orb_L
left	1.858	124.19	-6.6	35.6	17.1	Cingulum_Ant_L
right	1.858	107.65	7	34.3	17.8	Cingulum_Ant_R
left	5.264	97.72	-22.6	49.9	20.5	Frontal_Mid_L
left	12.548	88.21	-19.4	29.1	51.4	Frontal_Sup_L
right	12.548	82.53	18.5	28.5	53	Frontal_Sup_R
right	5.264	62.97	23	47.7	22.8	Frontal_Sup_R
left	5.17	53.11	-32	12.9	47.7	Frontal_Mid_L
left	6.768	51.02	-4.5	25.1	-4.1	Olfactory_L
right	6.768	48.12	5.5	31.2	-6.1	Cingulum_Ant_R
left	6.231	44.55	-14.4	20.3	56.7	Frontal_Sup_L
right	5.17	44.31	31.3	17.6	45.8	Frontal_Mid_R
right	6.231	39.05	16.5	21.3	54.4	Frontal_Sup_R
left	2.876	33.9	-8.1	37.4	39.3	Frontal_Sup_Medial_L
right	2.876	29.19	8.6	36.8	37.2	Frontal_Sup_Medial_R
right	2.257	28.79	10.4	31.2	53.2	Frontal_Sup_Medial_R
right	0.497	26.32	8.5	49.2	-14.3	Rectus_R
left	2.257	23.86	-9.6	34.5	51.6	Frontal_Sup_Medial_L
left	0.497	23.39	-4.5	46.6	-20.5	Rectus_L
right	5.45	22.22	28.8	48.7	0.2	Frontal_Mid_R
left	5.45	22.02	-29	50.8	-2.5	Frontal_Sup_Orb_L
left	5.617	21.97	-43.8	37.6	-4.5	Frontal_Inf_Orb_L
right	5.617	16.57	41.6	39.2	-1.7	Frontal_Inf_Orb_R
left	0.43	14.49	-28.7	57.1	-8.6	Frontal_Mid_Orb_L
right	0.43	13.71	31.7	55.1	-7.3	Frontal_Mid_Orb_R
right	4.913	8.95	45.5	23.5	8.2	Frontal_Inf_Tri_R
right	0.188	8.91	10.6	11.8	63.1	Supp_Motor_Area_R
left	4.913	7.86	-43.6	23.9	7.5	Frontal_Inf_Tri_L
left	0.188	7.3	-10	8.7	64.6	Supp_Motor_Area_L

Appendix D

Regions of Interest in the posterior Default Mode Network (for Dynamic Causal Modelling)

Hemisphere	*F* Statistic	Cluster Size (mm²)	MNI Coordinates			Short Name
			x	*y*	*z*	
right	27.711	857.31	62.4	-16.3	-15.4	Temporal_Mid_R
left	11.305	383.78	-41.7	-63.7	33.8	Angular_L
right	11.305	368.03	47.1	-59.9	31.5	Angular_R
left	21.509	341.52	-49.2	-41.7	0.2	Temporal_Mid_L
right	21.509	277.09	45.8	-41.5	0.1	Temporal_Mid_R
left	8.713	95.39	-55.1	-28.4	-12.4	Temporal_Mid_L
right	2.506	89.98	50.8	-52.9	31.9	Angular_R
right	8.713	85.62	55.3	-27.2	-12.5	Temporal_Mid_R
left	2.506	69.33	-51.6	-60.1	30.9	Angular_L
right	5.998	53.69	39.8	-64.7	46.9	Angular_R
left	5.998	50.36	-36.7	-68	46.1	Angular_L
left	5.284	49.82	-56.5	-11.9	-8	Temporal_Mid_L
right	0.98	46.56	4.3	-15.4	36.6	Cingulum_Mid_R
left	2.868	44.76	-5.3	-33.3	35.8	Cingulum_Mid_L
left	0.98	44.33	-3.8	-12.1	37.5	Cingulum_Mid_L
right	2.868	42.47	6.3	-37.2	32.8	Cingulum_Mid_R
right	5.284	41.94	56.7	-12.1	-5.1	Temporal_Sup_R
right	14.885	39.91	12	-63.8	31.2	Precuneus_R
left	3.21	39.65	-38	-56.9	22.3	Angular_L
right	8.147	38.78	57.6	-42.6	25.7	SupraMarginal_R
right	3.21	35.63	46.1	-55.9	20.9	Temporal_Mid_R
left	14.885	34.83	-12.3	-63.8	29.6	Cuneus_L
left	2.404	34.12	-51	-52.5	19.8	Temporal_Mid_L
left	8.147	27.67	-60	-49.8	27.6	SupraMarginal_L
right	2.404	25.1	47	-46.5	19.3	Temporal_Mid_R
right	3.506	22.04	48.1	-59.9	40	Angular_R
left	3.506	19.44	-44.3	-65.1	42.8	Angular_L
left	2.516	15.63	-51.6	-56.4	27.2	Angular_L
right	2.516	15.46	52.3	-51.3	28.5	Angular_R
left	0.789	11.94	-3.9	-9.5	33.4	Cingulum_Mid_L
right	0.789	10.19	3.8	-14.6	34	Cingulum_Mid_R
left	3.306	9.42	-17.1	-58.9	12.3	Calcarine_L
right	4.201	8.38	7.6	-44.7	45.5	Precuneus_R
left	4.201	7.6	-7.6	-44.2	45.6	Precuneus_L

CONTINUATION APPENDIX D

Hemisphere	F Statistic	Cluster Size (mm²)	MNI Coordinates			Short Name
			x	y	z	
left	1.565	7.52	-52.4	-50.1	32.3	SupraMarginal_L
right	1.194	7.24	55.9	-42.5	16.5	Temporal_Sup_R
right	1.565	6.57	53.9	-47.8	32.4	Angular_R
right	3.306	6.05	21.1	-57	16.9	Calcarine_R
left	1.194	5.56	-61.2	-49.8	17.2	Temporal_Mid_L

Appendix E

Repeated measures correlations of Grey Matter Probability Values (GMPV) for the 8 nodes
(overview of nodes in Table 1).

Correlations	r-value	95% CI lower bound	95% CI higher bound	Uncorrected p-value	Corrected p-value
ldPFC x lmTG	0.300	0.177	0.414	<.001	<.001
ldPFC x lPFC	0.214	0.086	0.335	.001	.024
ldPFC x rPC	0.134	0.003	0.260	.044	.920
ldPFC x rdPFC	0.395	0.278	0.499	<.001	<.001
ldPFC x rmTG	0.287	0.163	0.403	<.001	<.001
ldPFC x rPFC	0.281	0.156	0.397	<.001	<.001
lmTG x lPFC	0.271	0.145	0.387	<.001	.001
lmTG x rPC	0.203	0.075	0.325	.002	.043
lmTG x rdPFC	0.181	0.052	0.305	.006	.127
lmTG x rmTG	0.311	0.188	0.424	<.001	<.001
lmTG x rPFC	0.397	0.282	0.502	<.001	<.001
lPFC x rPC	0.237	0.110	0.357	<.001	.006
lPFC x rdPFC	0.142	0.012	0.268	.032	.664
lPFC x rmTG	0.217	0.089	0.338	.001	.021
lPFC x rPFC	0.586	0.493	0.666	<.001	<.001
rPC x rdPFC	0.132	0.001	0.258	.047	.990
rPC x rmTG	0.188	0.059	0.311	.004	.092
rPC x rPFC	0.198	0.069	0.320	.003	.058
rdPFC x rmTG	0.136	0.005	0.262	.041	.854
rdPFC x rPFC	0.253	0.127	0.372	<.001	.002
rmTG x rPFC	0.227	0.100	0.347	.001	.012

Note: The table shows a clear relationship of GMPVs across the ROIs. Corrections refer to Bonferroni
corrections, in this case, calculated by multiplying the p-values by the number of tests (21).

Appendix F

Full Canonical Correlation Coefficient Tables

Appendix F.1

Standardized Canonical Coefficients for Effective Connectivity for the significant Dimensions

1 and 2 for all within-DMN Connections

DMN nodes and Connections	Dimension 1	Dimension 2
ldPFC	**-0.27**	0.00
raPFC_2_ldPFC	0.05	**-0.14**
rPC_2_ldPFC	**0.16**	0.04
lPC_2_ldPFC	-0.04	**-0.19**
lmTG_2_ldPFC	0.04	**-0.07**
rmTG_2_ldPFC	0.12	**-0.27**
ldPFC_2_raPFC	-0.08	**0.15**
raPFC	0.02	**-0.21**
rPC_2_raPFC	-0.05	**0.11**
lPC_2_raPFC	0.03	**-0.05**
ldPFC_2_rPC	**-0.20**	0.09
raPFC_2_rPC	0.04	**0.09**
rPC	**0.27**	-0.09
lPC_2_rPC	**-0.12**	0.02
ldPFC_2_lPC	**0.26**	0.13
raPFC_2_lPC	**0.06**	-0.02
rPC_2_lPC	**-0.24**	0.06
lPC	**0.23**	0.17

Note: Larger loadings on one dimension are marked big.

Appendix F.2

Standardized Canonical Coefficients for Effective Connectivity for the significant Dimensions

1 and 2 for all within-CEN Connections

CEN nodes and Connections	Dimension 1	Dimension 2
lPFC	0.05	**-0.45**
rPFC_2_lPFC	-0.11	**0.30**
lmTG_2_lPFC	-0.08	**0.16**
rmTG_2_lPFC	-0.02	**-0.16**
ldPFC_2_rPFC	0.06	**-0.29**
raPFC_2_rPFC	**-0.02**	0.01
lPFC_2_rPFC	0.03	**-0.22**
rPFC	-0.29	**0.37**
lmTG_2_rPFC	**0.15**	-0.09
rmTG_2_rPFC	**0.12**	-0.03
lPFC_2_lmTG	**0.29**	0.05
rPFC_2_lmTG	0.02	**-0.09**
lmTG	**-0.22**	-0.10
rmTG_2_lmTG	0.13	**0.15**
lPFC_2_rmTG	**-0.24**	0.05
rPFC_2_rmTG	0.15	**-0.24**
lmTG_2_rmTG	-0.18	**-0.25**
rmTG	**0.24**	0.04

Appendix F.3

Standardized Canonical Coefficients for Effective Connectivity for the significant Dimensions

1 and 2 for all between-CEN-DMN Connections

Between CEN and DMN Connections	Dimension 1	Dimension 2
lPFC_2_raPFC	**-0.15**	-0.02
rPFC_2_raPFC	**-0.07**	0.05
lmTG_2_raPFC	**-0.12**	0.05
rmTG_2_raPFC	0.01	**0.04**
lPFC_2_rPC	**0.37**	0.28
rPFC_2_rPC	**0.20**	0.09
lmTG_2_rPC	0.13	**0.19**
rmTG_2_rPC	-0.02	**0.17**
lPFC_2_lPC	**-0.16**	-0.13
rPFC_2_lPC	**-0.13**	0.08
lmTG_2_lPC	**-0.23**	0.05
rmTG_2_lPC	**-0.18**	-0.02
ldPFC_2_lPFC	-0.02	**0.21**
raPFC_2_lPFC	-0.08	**0.37**
rPC_2_lPFC	**-0.36**	0.17
lPC_2_lPFC	**-0.15**	0.02
rPC_2_rPFC	**0.04**	0.02
lPC_2_rPFC	**0.07**	0.06
ldPFC_2_lmTG	-0.06	**0.20**
raPFC_2_lmTG	-0.12	**0.24**
rPC_2_lmTG	**-0.40**	0.19
lPC_2_lmTG	**-0.34**	-0.16
ldPFC_2_rmTG	**0.18**	0.00
raPFC_2_rmTG	0.08	**0.12**
rPC_2_rmTG	**0.11**	0.02
lPC_2_rmTG	-0.07	**-0.10**
lPFC_2_ldPFC	**-0.04**	0.03
rPFC_2_ldPFC	0.14	-0.14

Appendix G

Power Simulations

Four of the sixty-four EC values were randomly selected from a pool of self-inhibitory EC and between nodes EC values to simulate data simulations using the SuperPower package (Caldwell et al., 2021). Self-inhibitory EC values were ldPFC and rmTG EC and the two between nodes EC values were connections from ldPFC to raPFC and from rmTG to lPFC. Simulations indicated power $\beta < 80\%$ when using MANOVAs, especially for the between-nodes EC. Yet, it is difficult to predict the power when including variables which might be bundled in multivariate models as done here with semi-parametric MANOVAs and when considering strong variability between EC values at/between different locations. For specifics find the code on OSF under ANOVA_Power_EC.Rmd at https://osf.io/9bax3/.

Appendix H

Low fMRI Study Replicability

A high rate of false positives in neuroimaging has previously become known as 'voodoo correlations' (Fiedler, 2011; Vul et al., 2009). A popular example is the dead salmon study (C. Bennett et al., 2009). Bennett and colleagues (2009) presented allegedly significant BOLD contrasts – when not controlling for multiple comparison – in a dead fish's head. Ever since, reporting corrected results has somewhat become the standard in neuroimaging studies.

Additionally, different factors can contribute to reduced replicability in each study phase. Starting with the fMRI study design, it is crucial to make sure that the study design is sufficiently powered[8]. Translated to task-fMRI that would mean to increase samples significantly, as previous research suggests that even for current standards large samples of n = 100 participants have a rather satisfying than perfect replicability (Turner et al., 2018). Yet, replicability also depends on the task used (which will influence observable effects) and how the data are analysed (focussing on group level or region of interest activations) (Kampa et al., 2020). The central design-trade-off evolves hence around the number of subjects and how often to test each subject. Observing one (Poldrack et al., 2015) or few

---

[8] Statistical power (also β) is the probability of detecting a true effect, or in other words, detecting an effect when the null hypothesis is false (Cohen, 1992). Power is dependent on the choice of the alpha level (usually α =.05), sample size (N) and effect size.

individuals (Gordon et al., 2017) intensively can provide high quality data and unique

insights into the functioning of the observed individuals' brains when observed often and

long enough. However, the data generalisability of single or few subject studies is limited

(Lehmann et al., 2020). When examining fewer individuals, higher resolutions might be

desirable to improve data quality. However, when reaching higher resolutions, co-registration

procedures might become problematic. Vice versa, when using large datasets including

multiple subjects, group-averaged data might obscure precise activity or network mapping

(Gordon et al., 2017). Additionally, different sources of artifacts specific to MRI and fMRI

data can impact both effect size estimates and statistical power (Lombardo et al., 2016).

Beyond design choices, which usually affect artifacts, power and effect size, the choice

of pre-processing and analysis methods can lead to substantial variations in results

(Botvinik-Nezer et al., 2020; Eklund et al., 2016; Poldrack et al., 2017), which also applies to

rs-fMRI data use in order to estimate FC (Geerligs et al., 2017). This is nicely illustrated by

a study, which described 70 different labs' analyses of the same dataset to answer 9

hypotheses, resulting in different, and partly opposing conclusions based on different

analytical approaches (Botvinik-Nezer et al., 2020).

The described issues lead to low reliability in fMRI studies (Elliott et al., 2020;

Holiga et al., 2018; Noble et al., 2019; C. Zhang, Baum, et al., 2018; X. N. Zuo et al., 2019).

Without reliability, fMRI findings cannot be generalised and are hence unlikely to replicate.

Although study results on reliability in rs-fMRI are conflicting (Noble et al., 2019; C. Zhang,

Baum, et al., 2018), rs-fMRI reliability seems to be stronger than task-fMRI reliability

(Holiga et al., 2018). Additionally, recent large-scale analyses of task-fMRI show low test-

retest reliability (Elliott et al., 2020). However, the replicability on task-fMRI seems to be higher for group activations and lower for regions of interest (Kampa et al., 2020). Replicability differs between task – as can be expected, there seems to be a positive relationship between originally observed effect sizes / activation strength and replicability (Kampa et al., 2020). Although it is difficult to make general claims about task-fMRI replicability, as opposed to rs-fMRI, task-fMRI has the advantage of a control condition (Specht, 2020). Overall, fMRI study replicability is reduced by QRP usage, publication bias, problems with study design (including low power and data quality), data processing and statistical testing, and finally, misinterpreting results.

Appendix I

Examples of Factors influencing the BOLD Signal

	Factor	Study
Endogenous Factors	age(ing)	(Agcaoglu et al., 2015; Goldstone et al., 2016; Kumral et al., 2020; Millar, Petersen, et al., 2020; Mowinckel et al., 2012; Tsvetanov et al., 2019; Wink, 2019)
	genetic disposition	(Barber et al., 2021)
	neurovascular factors	(Millar, Petersen, et al., 2020; Tsvetanov et al., 2019; West et al., 2019)
	(cardio)vascular factors (e.g., cardiac pulsations)	(Hutchison et al., 2013; Tsvetanov et al., 2015)
	heart rate variability	(C. Chang et al., 2013)
	Age-dependent heart rate variability	(Kumral et al., 2019)
	hypertension	(Bu et al., 2018; Carnevale et al., 2020)
	Body temperature	(Sun et al., 2013)
	respiration	(Hutchison et al., 2013)
	movement in the scanner	(Hutchison et al., 2013)
	activity levels	(Boraxbekk et al., 2016)
	habitual sleep duration	(Curtis et al., 2016)
	sleep deprivation	(Dai et al., 2012)
	mood	(Harrison et al., 2008)
	neuropsychological disorders	(e.g. depression: Hamilton et al., 2011)
	antidepressants for de-pression	(Anand et al., 2005)
	anaesthesia	(Martuzzi et al., 2010)
	inflammation	(Labrenz et al., 2016; Lekander et al., 2016)
	laterality	(Tian et al., 2011)
	gender	(Dai et al., 2012; Filippi et al., 2013; Goldstone et al., 2016; Jamadar et al., 2019; Tian et al., 2011; Wink, 2019; C. Xu et al., 2015; C. Zhang, Dougherty, et al., 2018)
	menstrual cycle (oestrogen and progesterone changes)	(Pritschet et al., 2020)
Exogenous Factors	noise of the MR scanner	(Skouras et al., 2013)
	scanner drift	(Hutchison et al., 2013)
	time of year	(Choe et al., 2015)
	time of day	(Orban et al., 2020; Vaisvilaite et al., 2020)
	verbal intelligence and education	(Bastin et al., 2012)
	room temperature (fluctuations)	(Oi et al., 2017)

Appendix J

Exploring Grey Matter Probability Value Differences Between Age Groups Across

Measurement Timepoints

A 2 (age group) x 2 (timepoint) mixed semi-parametric MANOVA on GMPVs

testing whether there was atrophy of grey matter in the ROIs over time and differences in

GMPVs between age groups revealed that there a significant main effect of age $F(8, 227) =$

120.37, $p < .001$, but no significant effect of timepoint ($p = .20$) or the age-time interaction

($p = .57$).

To further examine the influence of age group on GMPVs, independent samples

Welch's t-tests were used to examine whether there are age-group differences for each of the

8 nodes with Bonferroni corrected $\alpha = 0.05/8$. In the anterior DMN, GMPV was higher in

ldPFC in younger ($M = 0.63$, $SD = 0.09$) compared to the older participants ($M = 0.61$, SD

$= 0.08$), $t(450.25) = 2.63$, $p = .004$, $d = 0.24$, 95% CI[-0.02; 0.51]. Also in raPFC, GMPV

was higher in younger ($M = 0.53$, $SD = 0.12$) compared to the older participants ($M = 0.49$,

$SD = 0.10$), $t(451.57) = 3.05$, $p = .001$, $d = 0.28$, 95% CI[0.02; 0.54] as well as in the

posterior DMN's rPC, with GMPV being higher in the younger group ($M = 0.58$, $SD =$

0.07) compared to the older group ($M = 0.55$, $SD = 0.08$) $t(452) = 3.03$, $p = .001$, $d = 0.29$,

95% CI[0.02; 0.55]. In the anterior CEN, rPFC GMPV was higher in the younger ($M = 0.52$,

$SD = 0.12$) compared to the older group ($M = 0.49$, $SD = 0.10$), $t(399.42) = 4.49$, $p < .001$,

$d = 0.30$, 95% CI[0.04; 0.56]. In the posterior CEN, lmTG GMPV was higher in the younger

($M = 0.52$, $SD = 0.12$) compared to the older group ($M = 0.49$, $SD = 0.10$), $t(414.62) =$

7.46, $p < .001$, $d = 0.71$, 95% CI[0.44; 0.98], rmTG GMPV for younger ($M = 0.67$, $SD =$

0.07) compared to the older group ($M = 0.64$, $SD = 0.06$), $t(449.1) = 3.95$, $p < .001$, $d = 0.37$, 95% CI[0.11; 0.63] (see Figure below). No other comparisons were significant.

Grey Matter Probability Values by Age Group
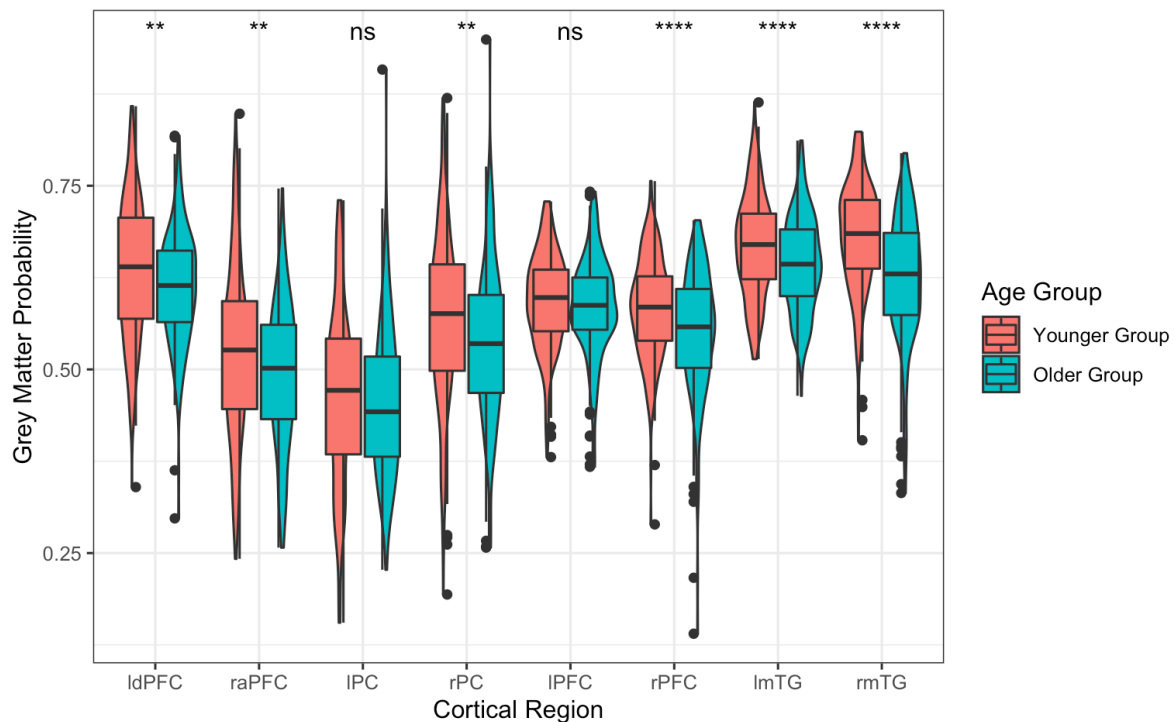
Note: Age groups were defined as "up to 45 years of age" (younger group) and older than 45 years of age (older group). Significance levels are based on uncorrected p-values indicating *$p < .05$, **$p < .01$, ***$p < .001$, ****$p < .0001$. ldPFC and raPFC are part of the anterior portion of the DMN, lPC and rPC of the posterior portion, respectively. lPFC and rPFC are part of the anterior portion of the CEN, lmTG and rmTG of the posterior portion, respectively. ldPFC = left dorsal Prefrontal Cortex, raPFC = right anterior Prefrontal Cortex, lPC = left Precuneus, rPC = right Precuneus, lPFC = left Prefrontal Cortex, rPFC = right Prefrontal Cortex, lmTG = left medial Temporal Gyrus, rmTG = right medial Temporal Gyrus.

Appendix K

Bilateral Correlations of GMPV and EC at the Eight Nodes

Region and Measure	Spearman's r	Statistic	p	p corrected
ant_DMN_GM	0.38	9625782.51	<.001	<.001
post_DMN_GM	0.41	9233754.76	<.001	<.001
ant_CEN_DMN_GM	0.32	10645439.4	<.001	<.001
post_CEN_DMN_GM	0.62	5877776.64	<.001	<.001
self_inhib_ant_DMN_EC	0.26	11524102	<.001	<.001
self_inhib_post_DMN_EC	0.00	15535658	.931	1
ant_DMN_EC	-0.31	20467546	<.001	<.001
Precuneus_Frontal_same_side_DMN_EC	-0.08	16881476	.081	1
Frontal_Precuneus_cross_DMN_EC	0.03	15107116	.511	1
post_DMN_EC	-0.51	23503302	<.001	<.001
Precuneus_Frontal_cross_DMN_EC	0.01	15395112	.781	1
Frontal_Precuneus_same_side_DMN_EC	0.06	14597374	.171	1
self_inhib_post_CEN_EC	-0.07	16639020	.151	1
self_inhib_ant_CEN_EC	0.08	14320944	.081	1
ant_CEN_EC	-0.39	21673586	<.001	<.001
Fronto_Temporal_same_side_CEN_EC	0.04	14902744	.341	1
Temporo_Fronto_same_side_CEN_EC	-0.04	16291296	.341	1
Fronto_Temporal_cross_CEN_EC	-0.01	15761968	.821	1
Temporo_Fronto_cross_CEN_EC	-0.01	15785712	.801	1
post_CEN_EC	-0.35	21035214	<.001	<.001

Spearman correlations were conducted due to non-normality of the data for anterior DMN in ldPFC and raPFC, posterior DMN in lPC and rPC, anterior CEN in lPFC and rPFC, and posterior CEN in lmTG and rmTG. The correlations above show a clear pattern of bi-lateral relationships for GMPVs, but not for EC values.

Appendix L

Intra Class Correlations of Effective Connectivity at T_5 and T_6

ICC Label	ICC
Frontal_Mid_L	0.04
Frontal_Mid_R_2_Frontal_Mid_L	0.01
Precuneus_R_2_Frontal_Mid_L	0.01
Precuneus_L_2_Frontal_Mid_L	<.01
Frontal_Sup_Medial_L_2_Frontal_Mid_L	0.09
Frontal_Sup_Medial_R_2_Frontal_Mid_L	0.19
Temporal_Mid_L_2_Frontal_Mid_L	0.15
Temporal_Mid_R_2_Frontal_Mid_L	<.01
Frontal_Mid_L_2_Frontal_Mid_R	<.01
Frontal_Mid_R	<.01
Precuneus_R_2_Frontal_Mid_R	<.01
Precuneus_L_2_Frontal_Mid_R	<.01
Frontal_Sup_Medial_L_2_Frontal_Mid_R	<.01
Frontal_Sup_Medial_R_2_Frontal_Mid_R	0.02
Temporal_Mid_L_2_Frontal_Mid_R	0.10
Temporal_Mid_R_2_Frontal_Mid_R	<.01
Frontal_Mid_L_2_Precuneus_R	<.01
Frontal_Mid_R_2_Precuneus_R	<.01
Precuneus_R	0.10
Precuneus_L_2_Precuneus_R	<.01
Frontal_Sup_Medial_L_2_Precuneus_R	<.01
Frontal_Sup_Medial_R_2_Precuneus_R	<.01
Temporal_Mid_L_2_Precuneus_R	0.13
Temporal_Mid_R_2_Precuneus_R	0.14
Frontal_Mid_L_2_Precuneus_L	<.01
Frontal_Mid_R_2_Precuneus_L	<.01
Precuneus_R_2_Precuneus_L	0.04
Precuneus_L	<.01
Frontal_Sup_Medial_L_2_Precuneus_L	0.10
Frontal_Sup_Medial_R_2_Precuneus_L	0.01
Temporal_Mid_L_2_Precuneus_L	0.04
Temporal_Mid_R_2_Precuneus_L	<.01
Frontal_Mid_L_2_Frontal_Sup_Medial_L	0.05
Frontal_Mid_R_2_Frontal_Sup_Medial_L	0.02
Precuneus_R_2_Frontal_Sup_Medial_L	<.01
Precuneus_L_2_Frontal_Sup_Medial_L	<.01

CONTINUATION APPENDIX L

ICC Label	ICC
Frontal_Sup_Medial_L	<.01
Frontal_Sup_Medial_R_2_Frontal_Sup_Medial_L	0.09
Temporal_Mid_L_2_Frontal_Sup_Medial_L	0.04
Temporal_Mid_R_2_Frontal_Sup_Medial_L	<.01
Frontal_Mid_L_2_Frontal_Sup_Medial_R	0.03
Frontal_Mid_R_2_Frontal_Sup_Medial_R	0.03
Precuneus_R_2_Frontal_Sup_Medial_R	0.02
Precuneus_L_2_Frontal_Sup_Medial_R	<.01
Frontal_Sup_Medial_L_2_Frontal_Sup_Medial_R	0.08
Frontal_Sup_Medial_R	0.11
Temporal_Mid_L_2_Frontal_Sup_Medial_R	<.01
Temporal_Mid_R_2_Frontal_Sup_Medial_R	0.01
Frontal_Mid_L_2_Temporal_Mid_L	<.01
Frontal_Mid_R_2_Temporal_Mid_L	0.06
Precuneus_R_2_Temporal_Mid_L	<.01
Precuneus_L_2_Temporal_Mid_L	0.05
Frontal_Sup_Medial_L_2_Temporal_Mid_L	<.01
Frontal_Sup_Medial_R_2_Temporal_Mid_L	<.01
Temporal_Mid_L	0.11
Temporal_Mid_R_2_Temporal_Mid_L	0.09
Frontal_Mid_L_2_Temporal_Mid_R	<.01
Frontal_Mid_R_2_Temporal_Mid_R	<.01
Precuneus_R_2_Temporal_Mid_R	0.05
Precuneus_L_2_Temporal_Mid_R	<.01
Frontal_Sup_Medial_L_2_Temporal_Mid_R	0.06
Frontal_Sup_Medial_R_2_Temporal_Mid_R	<.01
Temporal_Mid_L_2_Temporal_Mid_R	0.09
Temporal_Mid_R	<.01
Precuneus_L_GM	0.05
Frontal_Mid_L_GM	0.01
Temporal_Mid_L_GM	<.01
Frontal_Sup_Medial_L_GM	0.05
Precuneus_R_GM	<.01
Frontal_Mid_R_GM	0.04
Temporal_Mid_R_GM	<.01
Frontal_Sup_Medial_R_GM	0.02

Appendix M

Age and GMPVs Predicting EC

Appendix M.1

GAM Result Table

Best fitting models are marked **fat**.
Note: The best fitting model was determined based on the variance explained, the AIC, and its simplicity.

EC	Model 0		Model 1			Model 2			Model 3			Model 4	
	R^2_{adj}	AIC	R^2_{adj}	AIC	Change in deviance e1plained p-value	R^2_{adj}	AIC	Change in deviance e1plained p-value	R^2_{adj}	AIC	Change in deviance e1plained p-value	R^2_{adj}	AIC
Self-Inhibitory EC													
lPFC	0.014	236.64	0.039	225.93	<.001	**0.067**	**224.60**	**.056**	0.055	234.34	1.000	0.024	240.14
rPFC	0.003	202.93	0.004	203.51	.311	0.026	202.85	.093	**0.026**	**202.85**	**.002**	0.018	205.15
lmTG	-0.002	243.90	-0.002	244.24	.329	0.046	235.73	.003	**0.046**	**235.73**	**.019**	0.014	245.54
rmTG	0.009	277.43	0.014	278.20	1.000	**0.047**	**271.98**	**.013**	0.040	274.20	.063	0.019	281.53
ldPFC	0.005	213.76	0.020	210.66	.041	**0.048**	**209.56**	**.054**	0.042	209.12	.228	0.014	281.57
raPFC	0.011	250.79	**0.039**	**242.06**	**.004**	0.053	245.84	.243	0.025	255.80	.002	0.015	257.74
lPC	0.035	296.74	0.039	296.29	.134	0.087	287.19	.003	**0.085**	**287.10**	**.233**	0.056	296.04
rPC	0.004	292.61	0.010	291.16	1.000	0.036	293.84	.148	**0.029**	**289.74**	**.395**	0.026	291.33

CONTINUATION 1 APPENDIX M.1

EC	Model 0		Model 1			Model 2			Model 3			Model 4	
	R^2_{adj}	AIC	R^2_{adj}	AIC	Change in deviance e1plained p-value	R^2_{adj}	AIC	Change in deviance e1plained p-value	R^2_{adj}	AIC	Change in deviance e1plained p-value	R^2_{adj}	AIC
Within CEN EC													
rPFC 2 lPFC	0.008	281.19	0.008	282.13	.480	0.052	278.97	.015	**0.056**	**282.92**	**.473**	-0.004	295.50
lPFC 2 rPFC	-0.002	280.84	-0.002	280.85	.016	0.007	285.29	.404	**0.007**	**285.29**	**1.000**	-0.007	291.85
lPFC 2 lmTG	-0.002	180.30	-0.001	180.88	.308	0.023	181.61	.088	**0.023**	**180.65**	**.612**	-0.003	189.68
lmTG 2 lPFC	-0.002	180.30	-0.001	180.88	.308	0.023	181.61	.088	**0.023**	**180.65**	**.612**	-0.003	189.68
lPFC 2 rmTG	-0.001	158.35	-0.001	158.36	.002	0.039	153.92	.015	**0.039**	**153.92**	**.006**	0.012	161.01
rmTG 2 lPFC	< 0.001	319.48	0.004	320.67	.272	0.049	317.57	.020	**0.042**	**317.59**	**.185**	0.002	327.55
rPFC 2 lmTG	-0.001	185.67	< 0.001	187.33	.478	0.007	188.90	.314	**0.006**	**188.31**	**.288**	-0.006	196.86
lmTG 2 rPFC	< 0.001	445.01	0.001	445.71	.350	0.022	446.12	.122	**0.022**	**446.12**	**< .001**	0.008	450.29
rPFC 2 rmTG	< 0.001	218.17	< 0.001	218.17	.025	0.008	220.04	.302	**0.008**	**219.92**	**.171**	-0.003	228.50
rmTG 2 rPFC	0.002	321.48	0.025	318.61	.029	0.048	324.79	.256	**0.047**	**321.43**	**.592**	< 0.001	331.00
lmTG 2 rmTG	0.011	378.79	0.011	379.01	.270	0.026	377.80	.100	**0.026**	**377.80**	**.005**	0.010	388.02
rmTG 2 lmTG	-0.002	393.52	**0.012**	**393.60**	**.115**	0.018	396.42	.418	0.016	399.13	.933	-0.007	404.62
Within DMN EC													
ldPFC 2 raPFC	-0.001	146.41	-0.001	146.41	.002	0.007	155.80	.636	**0.007**	**155.80**	**1.000**	-0.011	159.78
raPFC 2 ldPFC	0.008	242.43	0.008	243.13	.345	0.049	239.86	.019	**0.049**	**239.27**	**.432**	0.014	248.27
ldPFC 2 lPC	0.001	253.74	0.011	250.32	.019	0.074	240.27	.002	**0.062**	**246.23**	**1.000**	0.048	240.70
lPC 2 ldPFC	-0.001	17.31	0.002	18.00	.292	0.031	23.70	.166	**0.028**	**21.39**	**.488**	0.008	22.26

CONTINUATION 2 APPENDIX M.1

EC	Model 0		Model 1			Model 2			Model 3			Model 4	
	R^2_{adj}	AIC	R^2_{adj}	AIC	Change in deviance e1plained p-value	R^2_{adj}	AIC	Change in deviance e1plained p-value	R^2_{adj}	AIC	Change in deviance e1plained p-value	R^2_{adj}	AIC
ldPFC 2 rPC	0.001	260.80	0.001	261.49	.447	0.055	254.61	.005	**0.055**	**254.61**	**.004**	0.017	262.17
rPC 2 ldPFC	-0.002	-48.24	0.002	-45.01	.391	0.040	-50.33	.014	**0.040**	**-50.33**	**< .001**	-0.012	-34.99
raPFC 2 lPC	0.028	285.87	0.033	285.02	.102	0.075	278.89	.009	**0.074**	**278.77**	**.204**	0.050	284.55
lPC 2 raPFC	-0.001	71.16	< 0.001	71.83	.342	0.023	74.57	.146	**0.022**	**74.09**	**.308**	-0.002	80.28
raPFC 2 rPC	< 0.001	279.00	< 0.001	279.00	.005	0.047	268.46	.002	**0.047**	**268.46**	**.002**	0.027	275.10
rPC 2 raPFC	-0.001	7.78	< 0.001	9.27	.480	0.035	8.55	.038	**0.032**	**8.55**	**.213**	-0.002	17.18
lPC 2 rPC	0.001	312.49	0.001	312.50	.025	0.030	314.34	.097	**0.029**	**313.47**	**.365**	0.017	314.22
rPC 2 lPC	-0.001	242.85	-0.001	242.85	.002	0.058	232.56	.002	**0.058**	**232.56**	**.009**	0.039	233.36
Between DMN and CEN EC													
raPFC 2 lPFC	0.001	277.65	0.043	264.01	<.001	**0.129**	**243.42**	**< .001**	0.107	248.04	.029	0.042	267.52
raPFC 2 rPFC	-0.002	285.81	0.004	284.14	.057	0.064	274.94	.003	**0.064**	**274.94**	**.002**	0.029	280.31
lPFC 2 ldPFC	-0.001	-13.42	-0.001	-12.66	.399	0.024	-16.56	.031	**0.024**	**-16.56**	**< .001**	0.003	-6.43
rPFC 2 raPFC	0.002	30.95	0.012	27.11	.017	0.030	28.39	.144	**0.031**	**34.57**	**.697**	0.010	35.81
raPFC 2 lmTG	-0.002	319.62	-0.002	319.62	.003	0.052	316.76	.013	**0.052**	**316.76**	**.001**	0.008	324.01
raPFC 2 rmTG	-0.001	288.42	**0.014**	**288.86**	**.109**	0.019	291.64	.415	0.024	293.74	.322	-0.004	298.62
lmTG 2 raPFC	-0.002	228.96	0.005	228.71	.156	0.029	228.90	.084	**0.022**	**224.34**	**.432**	0.009	232.89
rmTG 2 raPFC	0.001	72.57	0.006	74.34	.304	0.028	66.18	.003	**0.028**	**66.18**	**.002**	0.020	72.61

CONTINUATION 3 APPENDIX M.1

EC	Model 0		Model 1			Model 2			Model 3			Model 4	
	R^2_{adj}	AIC	R^2_{adj}	AIC	Change in deviance e1plained p-value	R^2_{adj}	AIC	Change in deviance e1plained p-value	R^2_{adj}	AIC	Change in deviance e1plained p-value	R^2_{adj}	AIC
ldPFC 2 lPFC	-0.002	206.89	0.020	202.27	.017	**0.072**	**196.52**	**.009**	0.051	198.56	.053	0.027	202.56
ldPFC 2 rPFC	-0.002	225.13	0.008	225.48	.139	0.049	224.37	.038	**0.035**	**223.39**	**.160**	0.012	227.49
lPFC 2 ldPFC	-0.002	-14.78	-0.002	-14.77	<.001	**0.011**	**-7.36**	**.461**	0.009	-10.60	.580	0.004	-8.58
rPFC 2 ldPFC	-0.002	86.63	-0.002	86.63	.001	0.014	92.16	.303	**0.013**	**90.47**	**.499**	0.001	93.89
ldPFC 2 lmTG	0.002	287.22	0.002	287.22	.005	0.048	282.50	.010	**0.048**	**282.50**	**.004**	0.017	289.39
ldPFC 2 rmTG	0.025	228.03	0.025	228.03	.007	0.061	229.44	.067	**0.059**	**227.69**	**.396**	0.039	230.51
lmTG 2 ldPFC	-0.001	199.78	0.002	200.78	.311	0.047	197.04	.015	**0.044**	**194.49**	**.475**	0.012	202.72
rmTG 2 ldPFC	< 0.001	93.54	0.018	89.60	.024	0.090	75.56	< .001	**0.077**	**75.87**	**.143**	0.020	93.46
lPC 2 lPFC	-0.001	194.11	0.025	187.09	.006	**0.083**	**178.48**	**.002**	0.057	187.70	.004	0.034	186.69
lPC 2 rPFC	-0.002	191.20	0.005	190.08	.116	0.046	182.88	.006	**0.045**	**182.28**	**.366**	0.024	188.28
lPFC 2 lPC	-0.002	53.00	-0.002	53.00	.001	0.059	49.45	.007	**0.044**	**50.99**	**.061**	0.015	54.06
rPFC 2 lPC	0.022	175.07	0.022	175.07	.004	0.039	174.40	.097	**0.039**	**175.71**	**.555**	0.031	179.50
lPC 2 lmTG	-0.002	189.44	0.005	188.64	.116	0.074	174.14	.001	**0.068**	**168.73**	**.543**	0.060	169.50
lPC 2 rmTG	0.007	170.76	0.012	169.36	.072	0.047	164.02	.016	**0.044**	**163.97**	**.220**	0.029	169.21
lmTG 2 lPC	0.003	268.96	0.020	262.20	.003	**0.036**	**262.51**	**.141**	0.028	265.92	.013	0.029	265.66
rmTG 2 lPC	0.005	229.45	0.010	229.97	.200	0.070	229.62	.011	**0.071**	**226.21**	**.797**	0.007	237.07
rPC 2 lPFC	-0.002	191.64	-0.002	191.87	.262	0.080	174.44	< .001	**0.080**	**173.90**	**.353**	0.040	181.41

CONTINUATION 4 APPENDIX M.1

EC	Model 0		Model 1			Model 2			Model 3			Model 4	
	R^2_{adj}	AIC	R^2_{adj}	AIC	Change in deviance e1plained p-value	R^2_{adj}	AIC	Change in deviance e1plained p-value	R^2_{adj}	AIC	Change in deviance e1plained p-value	R^2_{adj}	AIC
rPC 2 rPFC	-0.001	121.31	0.001	122.55	.364	**0.054**	**109.41**	**.001**	0.042	115.46	1.000	0.028	116.70
lPFC 2 rPC	-0.002	193.71	0.004	193.57	.159	**0.087**	**173.94**	**< .001**	0.080	177.53	1.000	0.046	180.42
rPFC 2 rPC	< 0.001	190.09	< 0.001	190.68	.405	0.030	187.35	.028	**0.030**	**185.34**	**.618**	0.008	195.45
rPC 2 lmTG	-0.002	204.81	0.004	203.32	.066	0.049	189.81	.001	**0.046**	**189.59**	**.257**	0.036	196.10
rPC 2 rmTG	0.001	129.72	0.001	129.72	.001	0.018	133.89	.248	**0.018**	**133.89**	**.001**	-0.011	143.97
lmTG 2 rPC	-0.002	355.13	0.006	356.89	.228	0.035	352.81	.026	**0.035**	**352.81**	**.003**	0.011	357.84
rmTG 2 rPC	-0.002	338.47	0.001	339.61	.315	0.033	340.92	.072	**0.026**	**341.58**	**.138**	0.010	341.95

Appendix M.2

Significant Predictors for the best fitting models

EC	Best Fitting Model	Best Fitting Model's Significant Predictors
		Self-Inhibitory EC
lPFC	2	rPFC GMPV $F(9, 454) = 1.57$, $p = .007$, age $F(9, 454) = 0.99$, $p = .002$, and timepoint (model coefficient) $t(454) = 2.71$, $p = .007$
rPFC	3	ldPFC GMPV $F(9, 454) = 0.95$, $p = .007$, lmTG GMPV $F(9, 454) = 0.37$, $p = .046$
lmTG	3	rPC GMPV $F(9, 454) = 0.62$, $p = .014$, lmTG GMPV $F(9, 454) = 1.54$, $p = .016$, and rmTG GMPV $F(9, 454) = 0.40$, $p = .04$
rmTG	2	rPC GMPV F(9, 454) = 1.28, p = .014, and age F(9, 454) = 0.67, p = .044, and timepoint (model coefficient) t(454) = -2.54, p = .012
ldPFC	2	lPC GMPV $F(9, 454) = 0.71$, $p = .047$
raPFC	1	age $F(9, 454) = 1.67$, $p = .002$, timepoint $t(454) = 2.45$, $p = .015$
lPC	3	ldPFC $F(9, 454) = 0.51$, $p = .024$, lPFC $F(9, 454) = 1.24$, $p = .005$
rPC	3	rPC GMPV $F(9, 454) = 0.997$, $p = .005$
		Within CEN EC
rPFC 2 lPFC	3	ldPFC GMPV $F(9, 454) = 1.36$, $p = .025$, timepoint $t(454) = 2.19$, $p = .029$
lPFC 2 rPFC	3	none
lPFC 2 lmTG	3	none
lmTG 2 lPFC	3	none
lPFC 2 rmTG	3	rPFC GMPV $F(9, 454) = 0.97$, $p = .002$, rmTG $F(9, 454) = 0.65$, $p = .044$
rmTG 2 lPFC	3	raPFC GMPV $F(9, 454) = 0.80$, $p = .0278$, rmTG $F(9, 454) = 0.69$, $p = .047$
rPFC 2 lmTG	3	none
lmTG 2 rPFC	3	none

CONTINUATION 1 APPENDIX M.2

rPFC 2 rmTG	3	none
rmTG 2 rPFC	3	lPC GMPV $F(9, 454) = 1.29$, $p = .0445$, lmTG $F(9, 454) = 0.67$, $p = .048$
lmTG 2 rmTG	3	laPFC GMPV $F(9, 454) = 1.70$, $p = .008$
rmTG 2 lmTG	1	none

Within DMN EC

ldPFC 2 raPFC	3	none
raPFC 2 ldPFC	3	ldPFC GMPV $F(9, 454) = 0.39$, $p = .047$, raPFC GMPV $F(9, 454) = 0.81$, $p = .027$, rPFC GMPV $F(9, 454) = 0.50$, $p = .022$, lmTG GMPV $F(9, 454) = 0.78$, $p = .025$
ldPFC 2 lPC	3	raPFC GMPV $F(9, 454) = 0.68$, $p = .009$, rPFC GMPV $F(9, 454) = 1.23$, $p = .04$
lPC 2 ldPFC	3	none
ldPFC 2 rPC	3	raPFC GMPV $F(9, 454) = 0.65$, $p = .011$, lPFC GMPV $F(9, 454) = 1.46$, $p = .003$
rPC 2 ldPFC	3	rPC GMPV $F(9, 454) = 1.73$, $p = .004$
raPFC 2 lPC	3	raPFC GMPV $F(9, 454) = 0.77$, $p = .035$, lPC GMPV $F(9, 454) = 0.41$, $p = .037$, lmTG GMPV $F(9, 454) = 1.16$, $p = .021$
lPC 2 raPFC	3	ldPFC GMPV $F(9, 454) = 0.72$, $p = .042$
raPFC 2 rPC	3	raPFC GMPV $F(9, 454) = 0.66$, $p = .011$, rPC GMPV $F(9, 454) = 0.41$, $p < 0.001$
rPC 2 raPFC	3	none
lPC 2 rPC	3	ldPFC GMPV $F(9, 454) = 0.84$, $p = .004$
rPC 2 lPC	3	ldPFC GMPV $F(9, 454) = 1.05$, $p = .001$, lPC GMPV $F(9, 454) = 1.53$, $p = .002$, rmTG GMPV $F(9, 454) = 0.51$, $p = .023$

Between DMN and CEN EC

raPFC 2 lPFC	2	ldPFC GMPV $F(9, 454) = 1.40$, $p = .024$, rmTG GMPV $F(9, 454) = 2.50$, $p < 0.001$, age $F(9, 454) = 1.66$, $p = .005$
raPFC 2 rPFC	3	rPC GMPV $F(9, 454) = 0.66$, $p = .011$, lmTG GMPV $F(9, 454) = 0.88$, $p = .014$, and rmTG GMPV $F(9, 454) = 1.06$, $p = .022$
lPFC 2 ldPFC	3	rPC GMPV $F(9, 454) = 0.43$, $p = .036$, rPFC GMPV $F(9, 454) = 0.66$, $p = .045$
rPFC 2 raPFC	3	lmTG GMPV $F(9, 454) = 0.71$, $p = .038$
raPFC 2 lmTG	3	laPFC GMPV $F(9, 454) = 0.93$ $p = .033$, rmTG GMPV $F(9, 454) = 1.28$ $p = .014$
raPFC 2 rmTG	1	none
lmTG 2 raPFC	3	lPFC GMPV $F(9, 454) = 0.59$ $p = .016$
rmTG 2 raPFC	3	ldPFC GMPV $F(9, 454) = 0.76$, $p = .006$, lPFC GMPV $F(9, 454) = 0.85$, $p = .004$

CONTINUATION 2 APPENDIX M.2

ldPFC 2 lPFC	2	ldPFC GMPV $F(9, 454) = 1.29$, $p = .004$, rPC GMPV $F(9, 454) = 0.98$, $p = .007$, age $F(9, 454) = 1.30$, $p = .020$
ldPFC 2 rPFC	3	ldPFC GMPV $F(9, 454) = 1.64$, $p = .004$, rPC GMPV $F(9, 454) = 0.55$, $p = .032$
lPFC 2 ldPFC	2	lPFC GMPV $F(9, 454) = 0.38$ $p = .037$
rPFC 2 ldPFC	3	none
ldPFC 2 lmTG	3	ldPFC GMPV $F(9, 454) = 0.94$, $p = .003$
ldPFC 2 rmTG	3	rmTG GMPV $F(9, 454) = 0.56$, $p = .039$
lmTG 2 ldPFC	3	none
rmTG 2 ldPFC	3	lPFC GMPV $F(9, 454) = 1.19$ $p = .003$, rmTG GMPV F$(9, 454) = 2.86$ p $< .001$
lPC 2 lPFC	1	lmTG GMPV $F(9, 454) = 1.63$, $p = .038$, age $F(9, 454) = 1.70$, $p < .001$
lPC 2 rPFC	3	lPC GMPV $F(9, 454) = 0.39$, $p = .045$, lmTG GMPV $F(9, 454) = 0.81$, $p = .016$, rmTG GMPV $F(9, 454) = 0.60$, $p = .015$
lPFC 2 lPC	3	lmTG GMPV $F(9, 454) = 0.88$, $p = .009$
rPFC 2 lPC	3	ldPFC GMPV $F(9, 454) = 0.37$, $p = .046$
lPC 2 lmTG	3	lPC GMPV $F(9, 454) = 2.34$, $p < .001$
lPC 2 rmTG	3	lPC GMPV $F(9, 454) = 0.52$, $p = .048$, rPFC GMPV $F(9, 454) = 0.43$, $p = .037$
lmTG 2 lPC	2	rmTG GMPV $F(9, 454) = 0.57$, $p = .036$, age $F(9, 454) = 0.63$, $p = .013$
rmTG 2 lPC	3	rPFC GMPV $F(9, 454) = 1.83$ $p = .010$
rPC 2 lPFC	3	rPC GMPV $F(9, 454) = 3.90$, $p < .001$, lPC GMPV $F(9, 454) = 0.54$, $p = .035$, lmTG GMPV $F(9, 454) = 0.73$, $p = .009$
rPC 2 rPFC	2	rPC GMPV $F(9, 454) = 2.02$, $p < .001$, lPC GMPV $F(9, 454) = 0.66$, $p = .011$, age $F(9, 454) = 0.81$, $p = .015$
lPFC 2 rPC	2	ldPFC GMPV $F(9, 454) = 0.63$, $p = .012$, lPC GMPV $F(9, 454) = 1.77$, $p = .008$, lPFC GMPV $F(9, 454) = 1.34$, $p < .001$, age $F(9, 454) = 0.56$, $p = .024$
rPFC 2 rPC	3	lPFC GMPV $F(9, 454) = 0.53$, $p = .021$, rPFC GMPV $F(9, 454) = 1.08$, $p = .034$
rPC 2 lmTG	3	rPC GMPV $F(9, 454) = 1.51$, $p < .001$, lPC GMPV $F(9, 454) = 1.36$, $p = .002$, lmTG GMPV $F(9, 454) = 0.77$, $p = .006$
rPC 2 rmTG	3	none
lmTG 2 rPC	3	rPC GMPV $F(9, 454) = 0.60$, $p = .015$
rmTG 2 rPC	3	none

Appendix N

GAMs with Lateralised GMPV Predicting EC

The four lateralised GMPVs were used in GAMs to model the eight self-inhibitory EC values and fifty-six between nodes ECs from the

lateralised GMPVs. That was done with the help of six models for each EC value: a null model (Equation 6), from which predictors were added

stepwise to a full GAM including all four GMPVs (Equations 7-10), and a linear model (Equation 11) to test for a better fit of the linear model,

using the AIC to compare all models' and AoD to compare the GAMs' fit.

$$\text{Model 0: EC} = \beta_0 + f(age) + T + \varepsilon, \; \varepsilon \sim N(0, \sigma^2) \tag{6}$$

$$\text{Model 1: EC} = \beta_0 + f(GM_1) + f(age) + T + \varepsilon, \; \varepsilon \sim N(0, \sigma^2) \tag{7}$$

$$\text{Model 2: EC} = \beta_0 + f(GM_1) + f(GM_2) + f(age) + T + \varepsilon, \; \varepsilon \sim N(0, \sigma^2) \tag{8}$$

$$\text{Model 3: EC} = \beta_0 + f(GM_1) + \ldots + f(GM_3) + f(age) + T + \varepsilon, \; \varepsilon \sim N(0, \sigma^2 \tag{9}$$

$$\text{Model 4: EC} = \beta_0 + f(GM_1) + \ldots + f(GM_4) + f(age) + T + \varepsilon, \; \varepsilon \sim N(0, \sigma^2) \tag{10}$$

$$\text{Model 5: EC} = \beta_0 + (GM_1)\beta_1 + \ldots + (GM_4)\beta_4 + (age)\beta_5 + T + \varepsilon, \; \varepsilon \sim N(0, \sigma^2) \tag{11}$$

GM_1: lateralized anterior DMN GMPV, GM_2: lateralized posterior DMN GMPV,

GM_3: lateralized anterior CEN GMPV, GM_4: lateralized posterior CEN GMPV, T: timepoint, age: cohort membership

EC	Model 0 (age + timepoint)		Model 1 (+ anterior CEN GMPV)			Model 2 (+ posterior CEN GMPV)			Model 3 (+ anterior DMN GMPV)			Model 4 (+ posterior DMN GMPV)			Model 5 (full linear model)	
	R^2_{adj}	AIC	R^2_{adj}	AIC	p var ex chg	R^2_{adj}	AIC	p var ex chg	R^2_{adj}	AIC	p var ex chg	R^2_{adj}	AIC	p var ex chg	R^2_{adj}	AIC
						Self-Inhibitory EC										
lPFC	**0.039**	**225.93**	0.039	226.17	.279	0.039	226.17	.000	0.040	227.72	.536	0.040	227.72	1.000	0.033	233.03
rPFC	**0.004**	**203.51**	0.008	202.89	.130	0.008	202.89	.003	0.008	202.89	.002	0.009	204.29	.427	0.002	208.38
lmTG	-0.002	244.24	0.006	243.29	.124	**0.011**	**241.44**	**.036**	0.011	241.44	.002	0.012	242.97	.537	0.006	245.30
rmTG	0.014	278.16	0.019	279.06	.255	0.019	279.06	.007	0.019	279.06	.001	**0.026**	**277.14**	**.065**	0.007	283.43
ldPFC	0.020	210.66	0.021	211.12	.280	0.038	210.14	.081	0.042	211.55	.312	**0.056**	**207.44**	**.027**	0.014	214.70
raPFC	0.039	242.06	**0.054**	**239.61**	**.060**	0.054	239.61	1.000	0.054	239.69	.136	0.054	249.67	.607	0.024	214.70
lPC	0.039	296.29	0.049	296.84	.150	0.051	297.21	.249	0.053	298.67	.383	**0.075**	**293.36**	**.021**	0.037	300.83
rPC	0.010	291.16	0.012	292.31	.371	0.012	292.31	.004	0.018	290.54	.058	**0.018**	**290.54**	**.003**	0.014	293.00
						Within CEN EC										
rPFC 2 lPFC	**0.008**	**282.13**	0.008	282.14	1.000	0.011	285.69	.456	0.011	285.69	.001	0.009	284.34	.305	-0.001	290.09
lPFC 2 rPFC	-0.002	280.85	**0.049**	**267.86**	**.001**	0.049	269.90	.787	0.049	269.90	.004	0.053	269.79	1.000	-0.002	285.97
lPFC 2 lmTG	**-0.001**	**180.88**	-0.001	180.88	.001	-0.001	180.88	.001	-0.001	180.88	.000	0.027	174.68	.012	-0.008	187.94
lmTG 2 lPFC	**0.032**	**446.13**	0.032	446.14	.025	0.032	446.14	.010	0.032	446.14	.011	0.032	446.14	.006	0.001	458.81
lPFC 2 rmTG	-0.001	158.36	-0.001	158.35	1.000	-0.001	158.36	.001	**0.008**	**155.35**	**.028**	0.015	156.36	.255	0.009	158.73
rmTG 2 lPFC	0.004	320.67	0.006	320.93	.235	0.008	322.52	.385	0.008	322.52	1.000	**0.027**	**317.39**	**.021**	0.000	324.18
rPFC 2 lmTG	**< 0.001**	**187.33**	0.001	187.95	.315	0.002	188.69	.378	0.002	188.69	.001	0.002	188.69	.002	-0.005	192.41
lmTG 2 rPFC	**0.001**	**445.71**	0.001	447.07	.498	0.003	447.24	.216	0.003	447.24	.006	0.004	447.83	.362	-0.001	450.26
rPFC 2 rmTG	**< 0.001**	**218.17**	< 0.001	218.17	.010	0.000	218.17	.004	0.002	220.37	.493	0.002	220.37	.001	-0.006	226.03

CONTINUATION 1 APPENDIX N TABLE

rmTG 2 rPFC	**0.025**	**318.61**	0.025	318.61	.008	0.029	319.69	.308	0.029	320.79	.548	0.035	319.04	.061	0.005	324.91
lmTG 2 rmTG	**0.011**	**379.01**	0.011	379.69	.452	0.011	380.15	.307	0.011	380.24	.151	0.011	380.23	.010	0.004	386.91
rmTG 2 lmTG	0.012	393.60	0.012	393.60	.009	0.012	393.46	.159	0.012	393.60	.157	**0.035**	**388.07**	.018	-0.008	401.14
Within DMN EC																
ldPFC 2 raPFC	-0.001	146.41	< 0.001	147.78	.417	< 0.001	147.78	< .001	**0.012**	**149.31**	.173	0.018	152.22	.343	-0.008	154.33
raPFC 2 ldPFC	0.008	243.13	0.011	244.58	.389	0.017	244.58	.169	0.024	240.72	1.000	**0.037**	**240.06**	.111	0.015	243.91
ldPFC 2 lPC	0.011	250.32	0.014	249.97	.151	0.016	251.60	.390	**0.034**	**251.02**	.079	0.034	251.02	1.000	0.008	255.33
lPC 2 ldPFC	**0.002**	**18.00**	0.002	18.00	.001	0.002	19.15	.543	0.002	19.15	< .001	0.002	19.15	< .001	-0.006	24.62
ldPFC 2 rPC	0.001	261.49	0.001	261.87	.284	**0.022**	**257.53**	.025	0.022	257.53	.002	0.022	257.64	-.006	<0.001	268.21
rPC 2 ldPFC	0.002	-45.01	0.006	-48.68	1.000	**0.023**	**-49.56**	.083	0.023	-49.56	1.000	0.023	-49.56	.001	-0.007	-41.26
raPFC 2 lPC	0.033	285.02	**0.039**	**284.62**	.169	0.039	284.62	1.000	0.039	285.99	.552	0.039	285.99	< .001	0.032	289.09
lPC 2 raPFC	< 0.001	71.83	**0.013**	**71.59**	.121	0.013	71.59	1.000	0.016	70.92	.153	0.017	72.60	.590	-0.006	78.23
raPFC 2 rPC	< 0.001	279.00	**0.011**	**275.10**	.017	0.013	276.59	.407	0.013	276.58	.002	0.017	276.93	.252	0.009	279.83
rPC 2 raPFC	< 0.001	9.27	0.013	7.81	.069	**0.061**	**-8.22**	< .001	0.061	-8.22	< .001	0.064	-2.45	.606	0.002	11.43
lPC 2 rPC	0.001	312.50	0.001	312.49	.021	0.006	312.31	.178	**0.011**	**314.16**	.333	0.017	315.16	.254	0.002	316.99
rPC 2 lPC	-0.001	242.85	0.013	241.62	.078	0.020	240.76	.131	0.030	240.81	.140	**0.055**	**235.92**	.022	0.011	242.61
Between DMN and CEN EC																
raPFC 2 lPFC	0.043	264.01	0.049	266.75	.340	0.049	267.52	.496	**0.062**	**265.59**	.080	0.064	265.40	.167	0.025	271.77
raPFC 2 rPFC	0.004	284.14	0.017	284.91	.133	0.019	285.46	.298	**0.033**	**283.68**	.081	0.035	284.17	.304	0.005	287.60
lPFC 2 ldPFC	**-0.001**	**-12.66**	-0.001	-12.66	1.000	< 0.001	-11.92	.346	0.009	-12.17	.154	0.009	-11.92	.285	-0.006	-6.10
rPFC 2 raPFC	0.012	27.11	0.029	27.08	.108	0.034	28.23	.269	**0.037**	**29.34**	.340	0.037	29.34	< .001	0.013	30.72
raPFC 2 lmTG	-0.002	319.62	-0.002	319.62	.004	-0.001	320.28	.336	-0.001	320.28	1.000	**0.019**	**317.25**	.042	-0.006	326.53
raPFC 2 rmTG	0.014	288.86	0.013	290.44	.631	0.014	290.48	.159	**0.018**	**289.40**	.082	0.009	290.87	.066	0.003	291.48
lmTG 2 raPFC	0.005	228.71	0.007	230.41	.428	0.011	231.76	.323	**0.020**	**231.01**	.135	0.020	231.01	1.000	-0.004	234.98
rmTG 2 raPFC	0.006	74.34	0.026	70.09	.028	0.026	70.09	.001	0.028	70.76	.339	**0.030**	**69.67**	.054	0.012	72.46

CONTINUATION 2 APPENDIX N TABLE

ldPFC 2 lPFC	0.020	202.27	0.020	202.27	.004	**0.049**	**196.09**	**.011**	0.053	197.22	.317	0.053	197.21	1.000	0.003	209.73
ldPFC 2 rPFC	0.008	225.48	**0.013**	**224.47**	**.098**	0.016	224.17	.164	0.016	224.18	.012	0.019	224.39	.226	0.007	226.02
lPFC 2 ldPFC	-0.002	-14.77	-0.001	-14.02	.407	-0.001	-14.02	.000	**0.003**	**-13.23**	**.281**	0.003	-13.23	< .001	-0.009	-6.50
rPFC 2 ldPFC	-0.002	86.63	-0.002	87.29	.419	**< 0.001**	88.48	.392	**0.006**	**89.30**	**.245**	0.006	89.30	< .001	-0.006	93.27
ldPFC 2 lmTG	**0.002**	**287.22**	0.003	287.87	.419	0.003	287.87	.001	0.003	289.34	.527	0.003	289.33	.006	-0.005	295.35
ldPFC 2 rmTG	0.025	228.03	0.026	229.31	.506	**0.039**	**226.67**	**.054**	0.044	228.72	.347	0.044	230.07	.514	0.018	236.39
lmTG 2 ldPFC	0.002	200.78	**0.027**	**197.06**	**.028**	0.027	197.06	.004	0.027	197.12	.115	0.027	197.12	.008	-0.006	207.21
rmTG 2 ldPFC	**0.018**	**89.60**	0.020	89.72	.208	0.020	89.73	.008	0.031	89.47	.134	0.032	90.25	.337	0.001	98.14
lPC 2 lPFC	0.025	187.09	0.032	188.71	.240	**0.051**	**182.68**	**.015**	0.051	182.69	.027	0.051	184.42	.784	0.017	190.63
lPC 2 rPFC	0.005	190.08	0.010	190.90	.251	**0.020**	**189.40**	**.095**	0.020	189.40	.003	0.020	189.40	.001	0.009	191.35
lPFC 2 lPC	-0.002	53.00	-0.002	53.65	.418	**0.003**	**54.90**	**.294**	0.003	54.90	< .001	0.007	55.18	.248	-0.003	58.67
rPFC 2 lPC	**0.022**	**175.07**	0.022	175.07	.002	0.023	176.64	.440	0.028	177.91	.321	0.029	178.77	.359	0.019	181.29
lPC 2 lmTG	0.005	188.64	0.012	188.26	.160	**0.025**	**183.27**	**.010**	0.028	184.32	.356	0.029	187.90	.621	0.023	183.05
lPC 2 rmTG	0.012	169.36	0.015	169.28	.181	0.033	167.21	.056	**0.046**	**165.58**	**.094**	0.046	165.58	< .001	0.018	170.63
lmTG 2 lPC	**0.020**	**262.20**	0.020	262.20	1.000	0.020	262.20	.003	0.020	263.37	.489	0.020	263.38	.002	0.014	268.64
rmTG 2 lPC	**0.010**	**229.97**	0.014	230.79	.297	0.018	231.73	.267	0.020	233.23	.467	0.020	233.23	.003	0.003	235.28
rPC 2 lPFC	-0.002	191.87	-0.002	191.86	.027	**0.022**	**181.79**	**< .001**	0.022	181.79	.003	0.027	181.29	.173	0.023	185.17
rPC 2 rPFC	0.001	122.55	0.001	122.55	.002	0.021	114.56	.002	**0.030**	**115.00**	**.185**	0.030	115.81	.448	0.015	118.87
lPFC 2 rPC	0.004	193.57	0.010	191.22	.022	0.012	192.11	.342	0.012	193.22	.534	**0.025**	**191.31**	**.070**	0.008	194.23
rPFC 2 rPC	< 0.001	190.68	0.003	191.71	.330	0.003	191.71	1.000	**0.021**	**194.43**	**.155**	0.023	194.37	.174	0.006	192.49
rPC 2 lmTG	0.004	203.32	0.004	203.32	.003	0.027	193.61	.001	0.029	193.77	.223	**0.039**	**191.44**	**.072**	0.035	192.46
rPC 2 rmTG	**0.001**	**129.72**	0.001	129.72	.001	0.001	130.02	.313	0.001	130.02	.008	0.001	131.58	.549	-0.007	138.00
lmTG 2 rPC	**0.006**	**356.89**	0.006	356.90	.007	0.006	356.89	.004	0.006	356.89	< .001	0.003	356.08	.246	-0.004	361.06
rmTG 2 rPC	0.001	339.61	0.006	340.32	.258	0.006	340.33	.011	**0.012**	**340.95**	**.230**	0.013	341.69	.350	-0.002	343.57

p var exp chg is the p-value for the change in variance explained when comparing models.

Note: The best fitting model was determined based on the variance explained, the AIC, and its simplicity. Significant predictors are not reported.

Appendix O

EC	Model 0		Model 1			Model 2			Model 3			Model 4			Model 5	
	R_{adj}^2	AIC	R_{adj}^2	AIC	dev expl chg p	R_{adj}^2	AIC	dev expl chg p	R_{adj}^2	AIC	dev expl chg p	R_{adj}^2	AIC	dev expl chg p	R_{adj}^2	AIC
CEN PFC	0.00	1071.17	0.00	1071.51	0.33	0.00	1071.51	1.00	0.00	1071.51	0.00	0.00	1071.51	0.01	-0.01	1078.56
mTG	0.00	1032.26	0.00	1032.51	0.24	0.01	1032.32	0.17	0.01	1032.33	0.01	0.01	1033.69	0.45	0.00	1035.16
DMN PFC	0.00	1006.95	0.00	1006.94	0.01	0.00	1007.47	0.40	0.04	998.92	0.00	0.05	998.50	0.12	-0.01	1014.61
PC	0.00	1070.86	0.00	1071.50	0.33	0.00	1072.26	0.39	0.00	1073.82	0.34	0.02	1072.23	0.06	0.00	1077.12
CEN PFC to mTG	0.00	1086.72	0.00	1086.73	1.00	0.00	1086.72	0.01	0.00	1086.72	0.00	0.01	1088.94	0.28	-0.01	1095.29
CEN mTG to PFC	0.01	1121.42	0.01	1122.80	0.49	0.01	1122.79	0.04	0.01	1122.80	0.04	0.01	1122.79	0.03	0.00	1130.09
DMN PFC to PC	0.00	1094.39	0.00	1094.90	0.39	0.00	1095.81	0.43	0.00	1095.80	0.18	0.01	1096.06	0.20	0.00	1094.94
DMN PC to PFC	0.00	1114.80	0.01	1112.04	0.05	0.04	1103.79	0.01	0.04	1107.11	0.78	0.04	1110.58	0.50	0.00	1119.78
DMN PFC to CEN PFC	0.01	1065.21	0.01	1066.80	0.49	0.01	1066.81	0.02	0.01	1066.88	0.11	0.01	1066.86	0.04	-0.01	1074.65
CEN PFC to DMN PFC	0.00	1101.98	0.00	1103.28	0.39	0.01	1104.28	0.36	0.01	1103.04	0.10	0.01	1103.04	0.02	0.00	1105.31

CONTINUATION APPENDIX O

DMN PFC to mTG	0.00	1072.00	**0.01**	**1072.74**	**0.26**	0.01	1072.74	0.01	0.01	1073.32	0.26	0.01	1075.07	0.40	0.00	1076.69
mTG DMN to PFC	0.00	1109.17	**0.03**	**1102.85**	**0.01**	0.03	1104.84	0.54	0.03	1105.25	0.34	0.03	1103.48	1.00	0.00	1113.30
PC to CEN PFC	0.00	1087.56	0.00	1088.93	0.30	**0.04**	**1074.11**	**0.00**	0.04	1075.56	0.45	0.04	1077.04	0.37	0.03	1075.40
CEN PFC to PC	**0.00**	**1096.88**	0.00	1096.88	0.01	0.00	1096.88	0.00	0.01	1097.30	0.24	0.01	1098.18	0.46	0.00	1100.78
PC to mTG	0.00	1095.88	0.00	1097.12	0.37	0.01	1097.85	0.28	0.02	1097.76	0.10	**0.03**	**1099.72**	**0.28**	0.00	1097.75
mTG to PC	0.00	1070.21	0.00	1070.21	**0.01**	**0.00**	**1070.21**	1.00	0.00	1070.21	1.00	0.00	1070.21	0.01	-0.01	1077.43

Model 0: Age and Cohort, Model 1: Model 0 + anterior DMN lateralized GMPV, Model 2: Model 1 + posterior DMN lateralized GMPV, Model 3: Model 2 + anterior CEN lateralized GMPV, Model 4: Model 3 + posterior DMN lateralized GMPV (full model), Model 5: Full linear model. dev expl chg p = deviance explained p-value

In half (eight of sixteen) of the EC connections models, the null model provided the best explanation of the data, compared with the other models. However, in those cases the variance explained by the model was $\geq 1\%$. Interestingly, adding more lateralized GMPVs to the models did add little to the variance explained and, in some models, decreased R_{adj}^2. In most of the models which were better in explaining the variance in lateralised EC than the null model, one specific lateralized GMPVs contributed most to explaining the variance. The location of such "explanatory nodes" did not necessarily match the exact location of the EC nodes, which might be an indication for a mix of local and global effects.